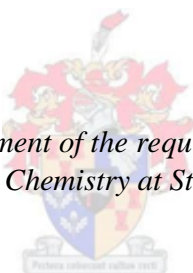# Novel Multinuclear complexes of Rh and Ru and their application in alkene hydroformylation

by

Jacquin October

Thesis presented in fulfilment of the requirements for the degree of
Master of Science in Chemistry at Stellenbosch University

Supervisor: Prof. Selwyn Frank Mapolie

Faculty of Science

December 2015

Declaration

By submitting this thesis/dissertation electronically, I declare that the entirety of the work contained therein is my own, original work, that I am the sole author thereof (save to the extent explicitly otherwise stated), that reproduction and publication thereof by Stellenbosch University will not infringe any third party rights and that I have not previously in its entirety or in part submitted it for obtaining any qualification.

December 2015

………………………

Dedication

This MSc thesis is dedicated to my grandparents (mamma and pappa) and my mother.

Dedication

Abstract

This project entailed the synthesis and characterization of mono- and multi-nuclear rhodium and ruthenium iminopyridyl complexes and their application in the hydroformylation of 1-octene. The multi-nuclear complexes were synthesized in order to investigate whether it could produce catalysts with higher activity than their mononuclear analogues.

Four novel iminopyridyl ligands, ranging from mono- to tetra-functional compounds, were synthesized. The synthesis was a two-step process initially involving a Schiff base condensation reaction between 2-pyridinecarboxaldehyde and 4-aminophenol to produce a hydroxy functionalized pyridine-imine. The latter was then subjected to a nucleophilic substitution reaction with an appropriate benzyl bromide derivative to yield the target ligands. All these ligands were isolated in moderate to good yields and characterized using a range of analytical techniques.

These ligands, together with the hydroxy functionalized pyridine imine, were then complexed to both Rh(I) and Ru(II) metal precursors, yielding ten novel metal complexes. The characterization of some of the complexes, especially the multi-nuclear complexes, were slightly more difficult due to their low solubility. However, all these complexes could be isolated in good to high yields as stable green-brown (in the case of Rh(I)) and yellow-orange (in the case of Ru(II)) solids.

Finally, these complexes were applied as catalyst precursors in the hydroformylation of 1-octene. In the case of the Rh(I) complexes, relatively high activities were observed, with conversions ranging between 50 – 90 % in all cases, when tested at 30 bar, 75 °C and a 0.05 mol% catalyst loading. The activity was found to increase when going from the mono- to the bi-nuclear catalyst. However, solubility in the reaction medium was a major issue for the tri-nuclear catalyst, as it contributed to the lower activity observed. High chemoselectivity towards aldehydes was observed for all catalysts, which increased with reaction times. During shorter reaction time, linear regioselectivity was also relatively high. This however, decreased with increasing reaction time as the internal octenes formed initially, were converted to branched aldehydes. When the Ru(II) complexes were tested under the same conditions as the Rh(I) complexes, very low activity was observed. Under more stringent conditions (45 bar, 120 °C, 0.5 mol%) the ruthenium catalysts performed relatively well, compared to other complexes in the literature. The same trend in terms of the chemo- and

regioselectivity for the Ru(II) complexes were observed. The Rh(I) complexes were far more active than the Ru(II) complexes.

Opsomming

Hierdie projek behels die sintese en karakterisering van mono- en multi-kernige rhodium en ruthenium iminopiridiel komplekse en hul toepassing in the hidroformulering van 1-okteen. Die multi-kernige komplekse is gesintetiseer met die doel om vas te stel of hulle katalisatore wat meer aktief is as hul monokernige eweknieë, kan produseer.

Vier nuwe iminopiridiel ligande, wat strek vanaf mono- tot tetra-funksionele verbindings, is gesintetiseer. Die sintese was 'n twee-stap proses wat aanvanklik 'n Schiff basis kondensasie reaksie tussen 2-piridienaldehied en 4-aminofenol behels, om 'n fenol gefunksioneerde piridien-imien te vorm. Die laasgenoemde was gevolglik aan 'n nukleofiliese substitusie reaksie met 'n gepaste bensiel bromied derivaat onderhewig. Al hierdie ligande is geisoleer in matige tot goeie opbrengste en gekarakteriseer met 'n reeks analitiese tegnieke.

Hierdie ligande, tesame met die fenol gefunksioneerde piridien imien, is dan met Rh(I) en Ru(II) metaal uitgangstowwe gekomplekseer, wat tien nuwe metaal komplekse tot gevolg gehad het. Die karakterisering van sommige van die kompekse, spesifiek die multi-kernige komplekse, was effens moeiliker as gevolg van hul swak oplosbaarheid. Al hierdie komplekse kon egter in goeie tot hoë opbrengste as stabiele groen-bruin (in die geval van Rh(I)) en geel-oranje (in die geval van Ru(II)) vastestowwe geisoleer word.

Laastens is die komplekse as katalisator-voorlopers in die hidroformulering van 1-okteen gebruik. In die geval van die Rh(I) komplekse is redelike hoë aktiwiteite waargeneem, met omsettings tussen 50 – 90 % in alle gevalle, wanneer hulle by 30 bar, 75 °C en 'n katalisator lading van 0.05 mol% getoets is. Die aktiwiteit neem toe vanaf die mono- na die bi-kernige katalisator. Oplosbaarheid in die reaksie medium was egter 'n probleem vir die tri-kernige katalisator, wat 'n laer aktiwiteit tot gevolg gehad het. Hoë chemoselektiwiteit na aldehiede is waargeneem vir al die katalisatore en dit neem toe met reaksietyd. Gedurende korter reaksietye was die liniêre regioselektiwiteit ook redelik hoog, maar neem af met toenemende reaksietyd soos die interne okteen wat aanvanklik vorm na vertakte aldehiede omgeskakel word. Toe die Ru(II) komplekse onder dieselfde toestande as die Rh(I) komplekse getoets is, was baie lae aktiwiteite waargeneem. Onder hoër temperatuur en druk (45 bar, 120 °C, 0.5 mol%) toon die ruthenium katalisatore redelik goeie aktiwiteite in vergelyking met ander komplekse wat in die literatuur gerapporteer is. Dieselfde tendense in terme van die chemo- en regioselektiwiteit is vir die Ru(II) komplekse waargeneem. Die Rh(I) kompleks was baie meer aktief as die Ru(II) komplekse.

Acknowledgements

A project of this magnitude would definitely not be possible without the valuable contribution and guidance of an exceptional supervisor. Therefore, I would like to extend my sincere gratitude towards Professor Selwyn Mapolie for fruitful discussions, availability, always being honest in terms of my work and progress and teaching me how to think critically about concepts and rationalizing why things are the way they are.

I would also like to thank my colleagues, the Organometallic Research Group, for useful discussions and just general conversations. They are not only my colleagues, but also became very good friends. Here, I would particularly like to thank Andrew, Hennie, Manana, Corli, Derik, Angelique, Ené, Annick and Laura. Also, a special thanks to Cassiem for always keeping the jokes coming, I haven't laughed so much before. The help of the RME-nano and Luckay research groups is also much appreciated.

Furthermore, you can't go through life without special friends. Thus, I would also like to thank Natasha (Tessa), Lyndall and Grant (Team Pullen) and my good friend Ryan (Riley) for giving a 'programmers' view on chemistry. I love you guys and keep the hikes coming (no snakes please).

What would your life be without family? First of all, a very special thanks to my mother for everything she did so far in my life, especially when I was still an undergraduate. To my grandparents (mamma and pappa), thank you for raising me to be the man I am today. Pappa, I know you're smiling with pride as you look down from heaven. To my broader family, thank you for loving me and keeping me humble.

Moreover, a project like this would not be successful without support staff. The help of Malcolm Taylor, Malcolm Mclean, Uncle Johnny and Jabu is much appreciated.

I would also like to thank the Central Analytical Facility (CAF), especially Elsa (NMR) and Fletcher (MS) for friendly service.

Financial support by c*change and the NRF is also very much appreciated, without which, this project would not have been possible.

Lastly, the biggest thanks goes to our Heavenly Father for blessing me with everything I have, especially the people in my life. Without Him I am nothing, and with Him I am capable of anything.

Conference Contributions

Poster Presentations

J. October and S.F. Mapolie

Synthesis and Characterization of Rh Metallodendrimers as Potential Catalyst Precursors for the Hydroformylation of Alkenes to Aldehydes. Catalysis Society of South Africa (CATSA) annual conference at Wild Coast Sun Hotel, Port Edward, 2013.

Ru(II) Metallodendrimers as Catalyst Precursors for the Hydroformylation of Alkenes. Catalysis Society of South Africa (CATSA) annual conference at St. Georges Hotel and Conference Centre, Johannesburg, 2014.

Novel Rh(I) and Ru(II) Metallodendrimers and their application as Hydroformylation Catalysts. C*change Syngas Convention at The Vineyard Hotel, Cape-Town, 2015.

Table of Contents

Chapter 1 : Literature Review of Dendrimers and Their Applications

Chapter 4 : Evaluation of Rh(I) and Ru(II) Catalyst Precursors in the
Hydroformylation of 1-Octene

List of Figures

List of Tables

List of Abbreviations and Symbols

Units

Å	Angstrom
J	coupling constant
°C/min	degrees celsius per minute
Hz	Hertz
m/z	mass to charge ratio
MHz	Megahertz
mg/kg	milligram per kilogram
mg/ml	milligram per millitre
ml/min	millilitre per minute
mmol	millimole
nm	nanometre
ppm	parts per million
cm^{-1}	wavenumber

Chemicals

NTf_2	bis(trifluoromethylsulfonyl)amide
COD	cyclooctadiene
Gx	dendrimer generation, where x = 0, 1, 2 …
DNA	deoxyribonucleic acid
DMSO-d_6	deuterated dimethyl sulfoxide
DAB	diaminobutane
DCM	dichloromethane
DMSO	dimethyl sulfoxide
EdU	5-ethynyl-2'-deoxyuridine
5FU	5-Fluorouracil
MeOH	methanol
MAO	methylaluminoxane
TPPMS	monosulfonated triphenylphosphine

PAMAM	poly(amidoamine)
Bis-MPA	poly(2,2-bis(hydroxymethyl)-propionic acid)
THF	tetrahydrofuran
bdppts	tetrasulfonated 2,4-bis(diphenylphosphino)pentane
dpppts	tetrasulfonated 1,3-bis(diphenylphosphino)propane
PTA	1,3,5-triaza-7-phosphaadamantane
TPP	triphenylphosphine
TPPTS	trisulfonated triphenylphosphine

Instrumentation

ATR	attenuated total reflectance
ESI-MS	electrospray ionisation mass spectrometry
FTIR	fourier transform infrared
GC-FID	gas chromatography flame ionization detector
HP-IR	high pressure infrared
HPLC	high pressure liquid chromatography
ICP-OES	inductively coupled plasma optical emission spectroscopy
NMR	nuclear magnetic resonance

NMR spectra peak description

bs	broad singlet
comp	complex
d	doublet
dd	doublet of doublets
dt	doublet of triplets
m	multiplet
s	singlet
t	triplet

xvii

Other

ALT	alanine transaminase
BUN	blood urea nitrogen
% ee	enantiomeric excess
EPR	enhanced permeability and retention
exp	experimental
TOF	turnover frequency
TON	turnover number

Chapter 1 : Literature Review of Dendrimers and Their Applications

1.1   Introduction

Catalysis is widely used to convert simple and cheap feedstocks to more complex value-added materials. Many known chemical reactions are mediated by some sort of catalyst. These catalysts include organic or inorganic compounds as well as salts of heavy metal ions. The metal ions are usually complexed to ligands which influence the stability, selectivity and activity of the catalyst. Catalysis using metal complexes can be divided into two categories, namely homogeneous and heterogeneous catalysis. Heterogeneous catalysis holds many advantages over homogeneous catalysis, of which the most important advantage is the ability to recover the catalyst easily from the reaction medium after completion of the reaction. This drawback of homogeneous catalysis can be overcome by immobilizing the catalyst on some sort of support. After the reaction, the catalyst can be recovered through precipitation or ultrafiltration. These types of catalysts are then regarded as "heterogenized" catalyst systems. Different types of supports are known and include resins[1], inorganic supports[2] and dendrimers[3]. Dendrimers are large macromolecules with well-defined structures. They are globular and monodispersive in shape and consist of a core, branching units and endgroups. Due to the unique properties of dendrimers, they find wide application in various fields. These include magnetic resonance imaging where they are used as contrast agents[4], as drug delivery agents[5], as carriers (vectors) in gene therapy[6], catalysis[7] and many more. Added to the fact that dendrimers allows recovery of the catalyst, they can enhance the rate of the reaction considerably. Dendrimers can act as multifunctional ligands allowing for multiple metal ions to coordinate to the ligand.

1.2   Dendrimers

1.2.1   History of dendrimers

Tomalia and co-workers[8] were one of the first research groups which reported the synthesis of dendrimers. They named these macromolecules "starburst polymers", because it appeared as if these macromolecules possessed "starburst" topology as can be seen in Figure 1-1. As will be discussed later, dendrimers can be classified according to their generations. The generation refers to the number of branching cycles emanating from the core. Figure 1-1

Chapter 1: Literature Review of Dendrimers and Their Applications

shows a generation 1 (G1) and generation 2 (G2) dendrimer prepared by this group with ammonia as core.
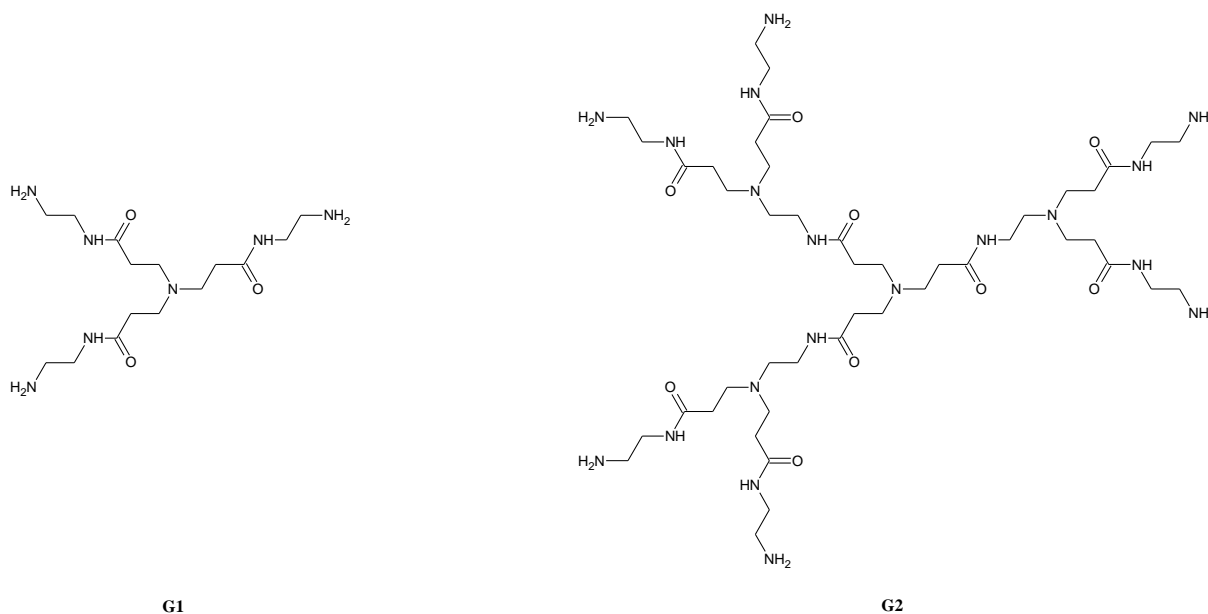
Figure 1-1: Starburst Polymers[8]

Also in 1985, Newkome and co-workers[9] reported the synthesis of dendrimers which they called arborols. They based their structures on the Leeuwenberg model. The Leeuwenberg model is an architectural model of trees. This can be seen in Figure 1-2. The short alkyl chain represents the stem and the rest of the structure the branches. The outer surface (branches) of the dendrimers consisted out of polar functional groups.

$R = CONHC(CH_2OH)_3$
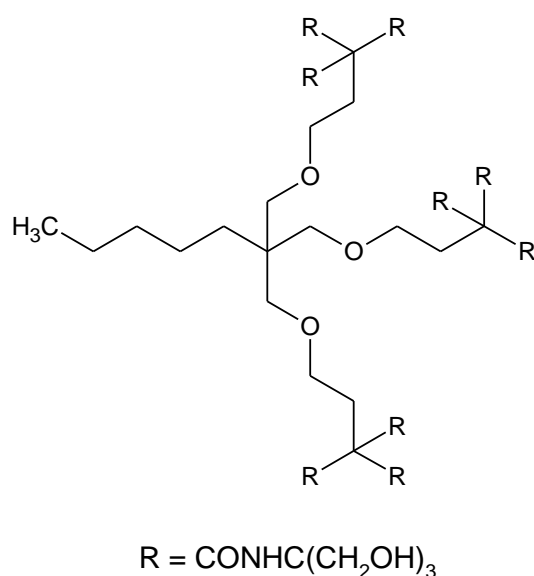
Figure 1-2: Arborol prepared by Newkome and co-workers[9]

2

Chapter 1: Literature Review of Dendrimers and Their Applications

This means that the inner surface was hydrophobic while the outer surface was hydrophilic. These types of molecules can also be classified as micelles. The groups of Tomalia[8] and Newkome[9] prepared the above mentioned dendrimers by a divergent synthesis approach. The divergent approach is where you start initially from the core and grow the dendrimer outwards. In 1990, Fréchet and co-workers[10] reported the first convergent approach for dendrimer preparation. In this approach, one starts from the dendrimer periphery and systematically progress inwards towards the core. This approach has a few advantages over the divergent approach which will be discussed later.

1.2.2   Synthesis of dendrimers

As previously mentioned, two approaches exist for the synthesis of dendrimers, namely the divergent and convergent approach. Tomalia[8] and Newkome[9] prepared the first dendrimers utilizing the divergent approach. The dendrimers made by Tomalia[8] had either ethylenediamine or ammonia as cores. From this core, the dendrimer was grown outwards by performing a series of Michael additions with methyl acrylate leading to ester functionalities on the dendrimer periphery. Lastly, the ester is reacted with ethylenediamine forming an amide to complete a generation. Doing sequential Michael addition and amidation reactions, expands the dendrimer to higher generations. For the amidation reaction, the esters are reacted with an excess of ethylenediamine in order to ensure that all of the ester groups are amidated. This reaction normally requires a few days to complete, especially in the case of higher generation dendrimers, and often involves difficult purification steps. The problem that can arise here is incomplete amidation reactions (not all the ester groups are amidated) and this is one drawback of the divergent approach. To circumvent this drawback, Fréchet[10] developed the convergent approach. In the convergent approach, as briefly discussed earlier, you start the synthesis of the dendrimer at the periphery and work inwards to the core. The dendrimer synthesized by Fréchet and co-workers[10] was prepared by reacting two moles of benzylic bromide with 3,5-dihydroxybenzylalcohol. The alcohol functionality that remains is then converted to the bromide which they labelled [G-1]-Br. Reacting [G-1]-Br with a suitable core, like 1,1,1-tris(4'-hydroxyphenyl)ethane, results in a generation 1 dendrimer. To expand this dendrimer to higher generations, [G-1]-Br can simply be reacted with 3,5-dihydroxybenzylalcohol forming [G-2]-OH which is converted to the bromide [G-2]-Br and this then is combined with the core. This way of building the dendrimer is much simpler and easier compared to the divergent approach for dendrimer synthesis.

1.2.3   Dendrimer Properties

Dendrimers consist of a core, branches and peripheral end-groups. Figure 1-3 shows a fourth generation dendrimer with the core, branching units and terminal groups denoted. The generation of the dendrimer refers to the number of branching cycles which emanates from the core. As can be seen from the figure, dendrimers are globular in shape. They are also monodispersive, meaning that they have uniform molecular weight. There are several factors that can influence the dispersity of the dendrimer, as discussed by Tomalia and co-workers.[8] These factors include dendrimer bridging, incomplete dendrimer growth and many others.
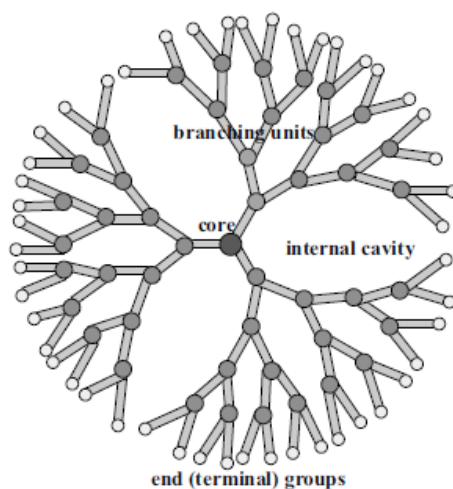
Figure 1-3: Representation of a Generation 4 dendrimer[11]

1.2.4   Dendrimer Applications

The properties of dendrimers can be exploited and these materials can be used in several applications. The fields in which dendrimers are mostly applied are in medicine and catalysis, and as such only applications in these two fields will be briefly overviewed here.

1.2.4.1 Application of Dendrimers in Medicine

Since the discovery of dendrimers, a large number of papers have been published on utilizing dendrimers for medicinal purposes. Haensler and Szoka[12] reported the use of PAMAM dendrimers to mediate the transfection of cells. Viruses have previously been utilized as gene transfer vehicles, but using dendrimers for this purpose could be a much safer option. Using agarose gel electrophoresis, the authors showed that these dendrimers are able to bind DNA successfully, making them ideal for transporting genes into cells. In order to accomplish maximum activity and efficiency, the dendrimer-DNA conjugate had to be optimized in terms of the diameter of the dendrimer used as well as the dendrimer content. Results showed

that the larger the diameter of the dendrimer, the better the transfection efficiencies. The best transfection efficiency was achieved with a conjugate consisting of a generation 6 PAMAM dendrimer with a diameter of 68 Å and primary amines/nucleotides of 10. Furthermore, the authors studied the cytotoxicity of the PAMAM dendrimer-DNA conjugate compared to that of a polylysine-DNA conjugate. They studied the toxicity in the presence and the absence of DNA and observed that in both cases the cytotoxicity of the PAMAM dendrimer is lower than that of polylysine.

Zhuo and co-workers[13] synthesized dendritic polymers with 1,4,7,10-tetraazacyclododecane as core. Dendrimer-5FU conjugates were then prepared and the *in vitro* release of 5-Fluorouracil (5FU) was then studied. 5-Fluorouracil is important because of its antitumor activity, but it is very toxic. Therefore, Zhuo and co-workers[13] attempted the preparation of conjugates that will allow the slow release of 5-Fluorouracil which will therefore decrease its toxicity. Figure 1-4 shows a G1 dendrimer prepared by this group. G1 up to G5.5 dendrimers were prepared by subsequent Michael additions. All of the dendrimers were characterized by FT-IR, ^{1}H NMR and elemental analysis.

$$R = NHCH_2CH_2NH_2$$
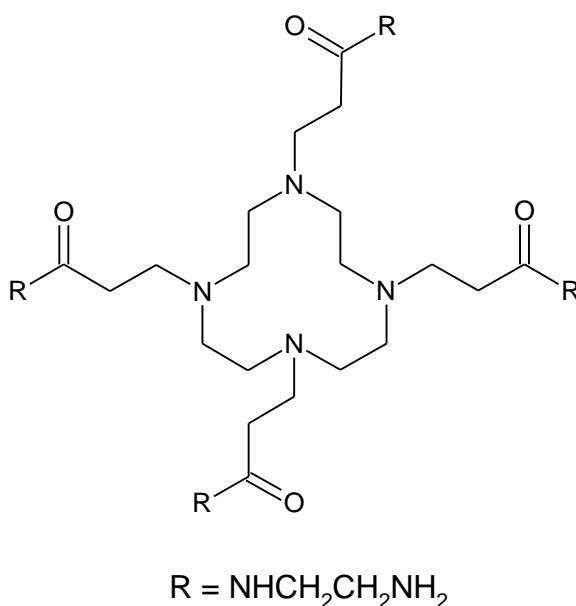
Figure 1-4: Generation 1 dendrimer prepared by Zhuo and co-workers[13]

In order for utilization in *in vitro* studies or *in vivo* studies, the authors enhanced the water solubility of some of these dendrimers by reacting it with acetic anhydride (G4 and G5). The *in vitro* release of 5-Fluorouracil by hydrolysis in a 0.1 M phosphate buffer solution (37 °C, pH = 7.4) was then studied. HPLC was used to study the release of 5-Fluorouracil. Results of

Chapter 1: Literature Review of Dendrimers and Their Applications

this study showed that more 5-Fluorouracil is released over time and that the higher generation dendrimer released more 5-Fluorouracil since it contains more 5-Fluorouracil.

Liu and co-workers[14] reported the preparation of dendritic micelles and applying these as drug delivery agents. For something to be a successful drug delivery agent, it must be water-soluble. To accomplish this objective, 4,4-bis(4'-hydroxyphenyl) pentanol was selected as the dendrimer core surrounded by a hydrophilic shell consisting of poly(ethylene glycol)

$R = O(CH_2CH_2O)_{16}CH_3$
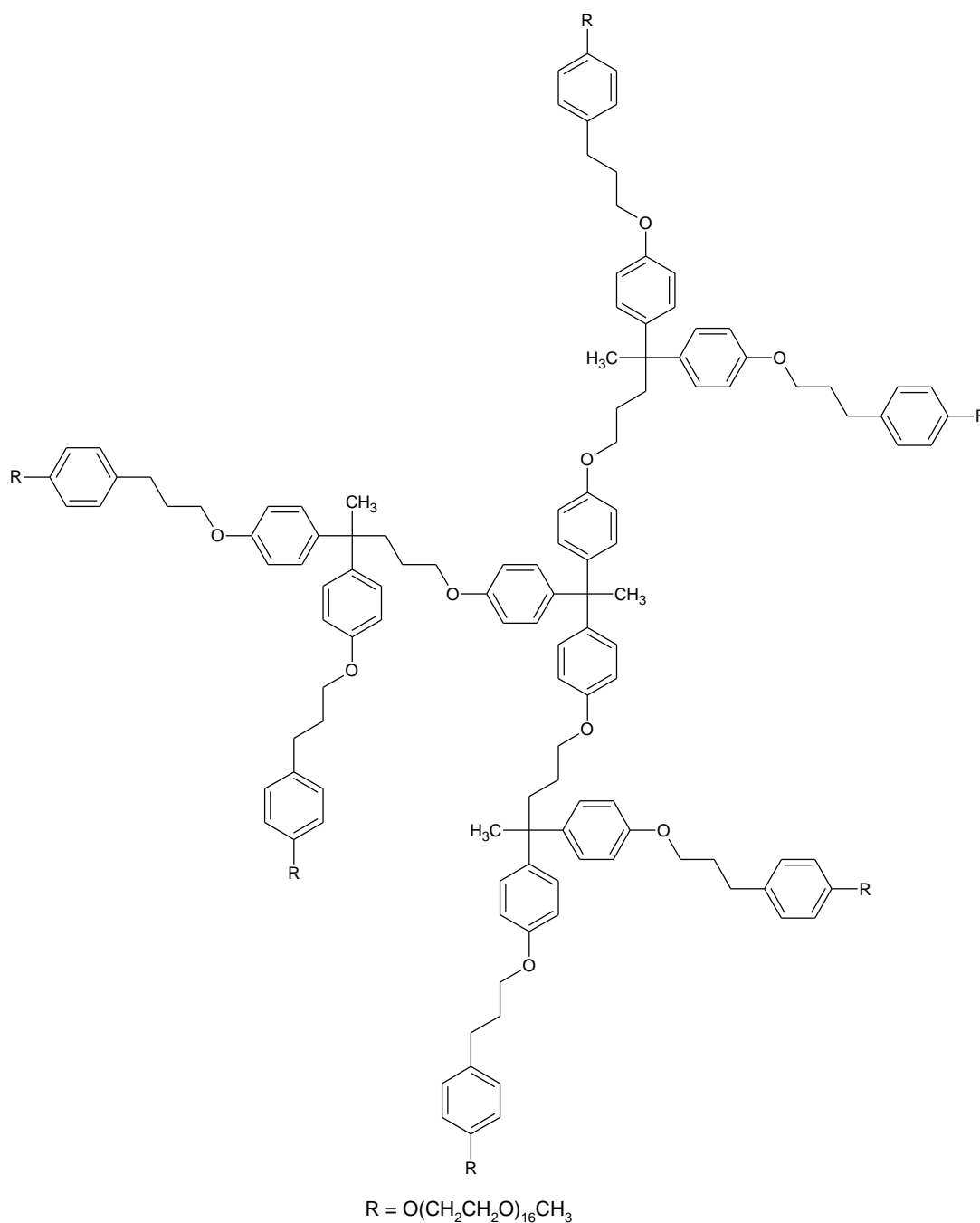
Figure 1-5: G1 Dendrimer prepared by Liu and co-workers[14]

Chapter 1: Literature Review of Dendrimers and Their Applications

mesylate. The interior of the dendrimer was hydrophobic and able to encapsulate small hydrophobic compounds while the surrounding hydrophilic shell renders the material water soluble. The interior of the micelle protects the drug from being deactivated. The synthesized dendrimers were then tested for the solubilisation of pyrene. Pyrene on its own is not highly soluble in water (8×10^{-7} M), but the solubility is increased drastically (2.85×10^{-4} M) in an aqueous solution of the G3 dendrimer. What can be observed from the results is that as the generation of the dendrimer increases, so does the concentration of the pyrene because the bigger dendrimer is able to solubilize more pyrene molecules. Furthermore, encapsulation studies were performed on the model drug indomethacin. After less than 5 h, 100 % of the non-encapsulated drug was released but when the drug is encapsulated in the G-3 micelle, it takes much longer before 100 % of the drug is released. Therefore, it shows that by encapsulating drugs into dendrimers, the release of the drug can be slowed down. If the drug is toxic at high concentrations, slow release will hopefully decrease its toxicity.

Neerman and co-workers[15] reported the synthesis of a melamine cored dendrimer as a drug delivery vehicle. Melamine on its own is a known toxin, and here it is tested for its ability to induce acute and subchronic liver and renal damage. The interior of this dendrimer is hydrophobic which makes it capable of encapsulating small hydrophobic molecules. The exterior is hydrophilic and therefore water soluble which makes it a prime candidate as a drug delivery agent. The studies revealed that this dendrimer performs just as well as the PAMAM dendrimers that were utilized for this purpose. Firstly, the dendrimer were tested for its toxicity towards mice Clone 9 cells. Results showed that the cell viability decreases considerably at a concentration of 0.1 mg/ml while it stays approximately constant for dextran at different concentrations. When the mice were administered with a dosage of 160 mg/kg of the dendrimer, it was found to be lethal. Furthermore, the melamine dendrimer was tested for its ability to induce kidney and liver damage. Changes in blood urea nitrogen (BUN) levels were used as a measure of renal damage while the activity of alanine transaminase (ALT) was used to measure liver damage. An increase in the activity of this enzyme is an indication of damage to the liver. BUN levels were the highest at a dose of 2.5 mg/kg and decreased slowly with increased dosage. This value doesn't differ much from the control. Therefore, the dendrimer does not induce any acute nor subchronic renal damage. Studies with regards to liver damage gave completely different results. The activity of the ALT enzyme increases as the dose of the dendrimer is increased.

Chapter 1: Literature Review of Dendrimers and Their Applications

Goonewardena and co-workers[16] reported the use of a fluorogenic PAMAM dendrimer in which the dendrimer is conjugated to 3-azido-7-hydroxy coumarin as reporter to profile the proliferation of cells. This water-soluble dendrimer conjugate was tested by monitoring the incorporation of 5-ethynyl-2'-deoxyuridine (EdU) into newly synthesized DNA. EdU was not only ligated to the dendrimer conjugate, but also to 3-azido-7-hydroxy coumarin in order to study whether the dendrimer conjugate really shows some promise for this application. KB, a cancer cell line, was incubated with EdU to allow incorporation into DNA. The AF-647 reporter, a standard click-fluorescent reporter, were also tested and compared to the dendrimer conjugate. From the results they observed that the dendrimer conjugate is just as efficient as AF-647 to profile cell proliferation.
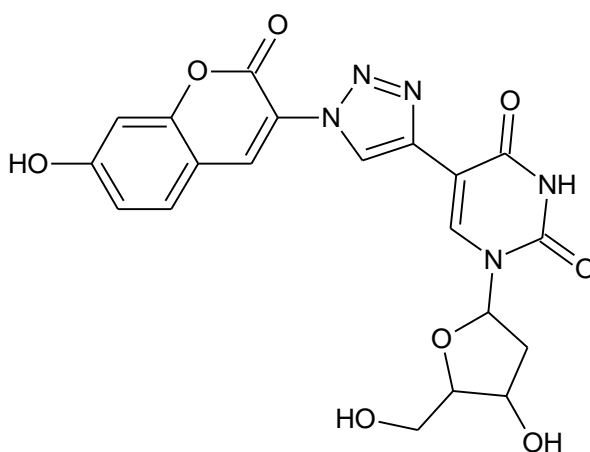
Figure 1-6: EdU ligated to 3-azido-7-hydroxy coumarin[16]

1.2.4.2 Application of Dendrimers in Catalysis

The use of dendrimers in catalysis holds many advantages. As the generation of the dendrimer increases, so the number of metal ions that can be coordinated, increases. This may lead to an enhanced catalytic reaction. Also, due to the large size of metallodendrimers, there is the potential to recover the catalyst using ultrafiltration.

Dendrimers can encapsulate various species within their internal cavities. The type of species present inside these cavities is dependent on the nature of the interior. Usually, the interior is typically hydrophobic and tends to encapsulate small hydrophobic species. Dendrimers, however, can also encapsulate metal ions which can subsequently be reduced to metal nanoparticles stabilized by the dendrimer. Chung and Rhee[17] reported the preparation of a Pd-Rh bimetallic nanoparticle for the partial hydrogenation of 1,3-cyclooctadiene. The dendrimer employed in this case was a fourth generation PAMAM dendrimer with hydroxyl groups on the surface. They also prepared nanoparticles containing Rh and Pd only in order

to study whether the bimetallic nanoparticles holds any advantage over the monometallic nanoparticles. The bimetallic species performed much better than a mixture of Pd and Rh nanoparticles together. Similar observations were previously made by Toshima and Yonezawa[18] who explained this phenomenon in terms of the uneven electron density distribution between the two metals, leading to the more facile coordination of the substrate to the more electron deficient metal. The results show that optimum activity was achieved with a 2:1 Rh:Pd ratio.

Kumar and Gopidas[19] reported the preparation of a palladium nanoparticle-cored Fréchet type dendrimer for the chemoselective hydrogenation of C-C multiple bonds. The catalyst was able to chemoselectively hydrogenate these C-C multiple bonds even in the presence of other reducible groups such as CHO and NO_2. In order to prove the chemoselectivity of their metallodendrimers, they also performed a few reactions using 10 % Pd/C. This latter catalyst is not selective and hydrogenated all groups that are capable of being reduced. Both the C=C double bond and the nitro group were hydrogenated. The palladium nanoparticle-cored dendrimer was able to chemoselectively only hydrogenate the aliphatic C-C multiple bonds while compounds containing aromatic multiple bonds were unaffected. The yields in the majority of the reactions performed were in excess of 75 %.

Smith and co-workers[20] utilized a G1 poly(propylene imine) pyridylimine palladium metallodendrimer in the polymerization of ethylene. They hypothesized that dendrimers affords high local concentrations of active sites as a result of multiple metal ions complexed
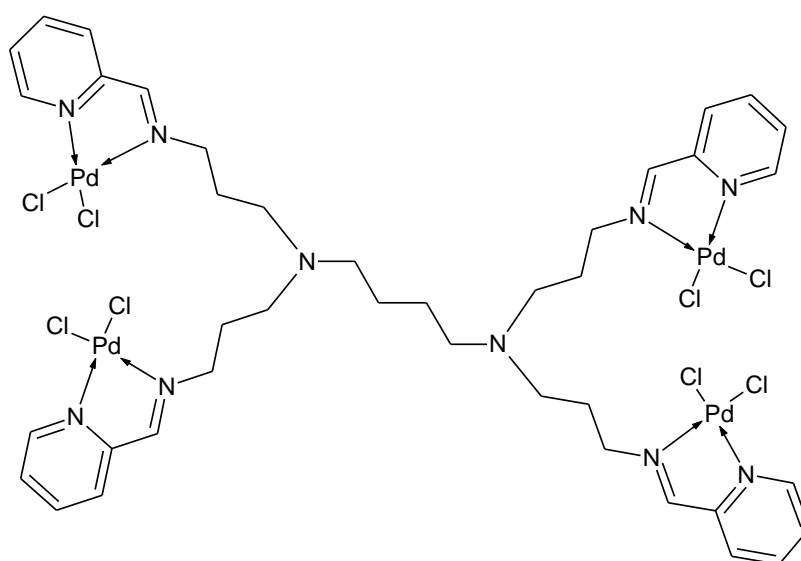
Figure 1-7: DAB G1 metallodendrimer prepared by Smith and co-workers[20]

to the dendrimer, and that this leads to enhanced catalytic activity. Under optimized catalysis conditions, they achieved the highest yield and activity when using a Pd:Al ratio of 1:1000 in the presence of MAO (methylaluminoxane) as activator.

Martínez-Olid and co-workers[21] prepared a monometallic Ni(II) *N,N'*-iminopyridine complex. The ligand was prepared by reacting 2,5-dimethyl-4-{[pyridine-2-ylmethylidene]amino}phenol with the appropriate benzyl bromide to form G0, G1, G2 and G3 dendrimer ligands. These ligands were then complexed to Ni(II) to form four different catalysts which were tested in the oligomerization/polymerization of ethylene. The G3 metallodendrimer is shown in Figure 1-8. The aim here was to study the influence of dendrimer generation on catalyst activity. The G0 metallodendrimer showed the highest activity, while it was the lowest for G1 when tested in ethylene oligomerization reactions. In the case of ethylene polymerization, the G3 dendrimer registered the highest activity. The results also show that for ethylene oligomerization, the generation of the dendrimer has no effect on the activity since there is no clear trend which means that the performance of all the
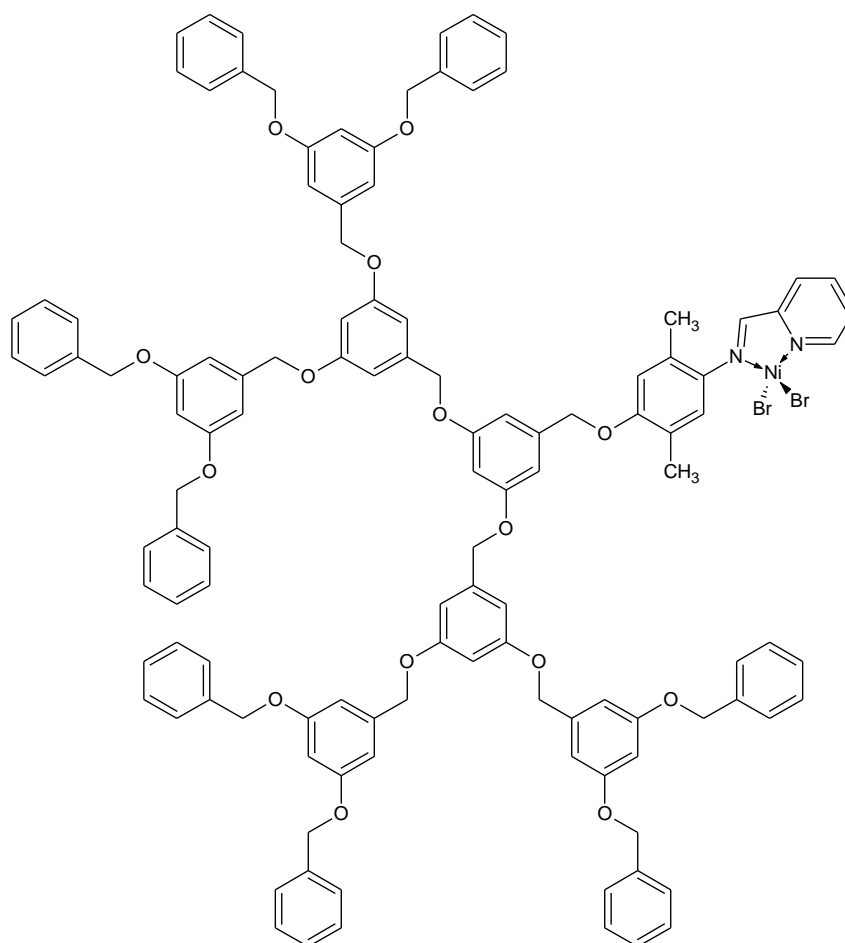
Figure 1-8: G3 metallodendrimer prepared by Martinez-Olid and co-workers[21]

metallodendrimers is roughly similar. However, in the case of ethylene polymerization, the activity increases as the dendrimer generation increases.

Panicker and Krishnapillai[22] synthesized an on resin poly(propylene imine) dendrimer and used it in Knoevenagel condensation reactions. The conditions for the catalysis were optimized and a model reaction was performed by using benzaldehyde and malononitrile. The best performance was achieved by utilizing a 0.5 mol% catalyst loading, ethanol as solvent and doing the reaction for 5 minutes. The catalyst could be recovered after the catalysis by filtration, and reused multiple times. It was also shown that the reaction could be carried out solvent-less, in water and in ethanol making this a green process. After the successful optimization of catalytic conditions, the reaction was performed on other substrates and it was found that all of the reactions proceeded with ease in not more than 10 minutes with close to 100 % yield.

1.3   Hydroformylation

Hydroformylation is the addition of a formyl group and a hydrogen atom over a C-C double bond. It leads to the production of aldehydes which is an important precursor for other more complex compounds. These aldehydes can be hydrogenated to alcohols which can in turn be utilized for the production of plasticizers, fragrances, detergents and other natural products. It was first discovered by Otto Roelen in 1938 during Fischer-Tropsch reactions catalysed by a cobalt catalyst. As such, the early hydroformylation catalysts were mostly based on cobalt and only later did rhodium catalysts become more prominent.[23]

Industrial hydroformylation processes includes the UCC process, Ruhrchemie/Rhône-Poulenc process, BASF process and the Exxon process. The UCC and BASF processes make use of a rhodium phosphine catalyst (TPP), while the Ruhrchemie/Rhône-Poulenc process utilized a water-soluble rhodium complex which enables them to perform aqueous bi-phasic hydroformylation. The Exxon process makes use of a cobalt catalyst.[23]

Since this study is focussing on the development of rhodium and ruthenium catalysts, only the use of these two metals in hydroformylation will be reviewed here.

Chapter 1: Literature Review of Dendrimers and Their Applications

1.3.1 Hydroformylation using Rhodium

1.3.1.1 Rhodium catalyst systems

Rhodium is the most active metal commonly employed in hydroformylation, compared to the other metals (Co, Ir, Ru). This allows for the catalysis to be performed under mild reaction conditions. The early rhodium hydroformylation catalysts were based mostly on phosphine and phosphite ligands. These ligands can have an influence on the activity and selectivity of the catalyst system. In a paper published by Van Rooy and co-workers[24], in which they reported the use of complexes with bisphosphine ligands, they found that the catalyst system can be tailored to favour the formation of linear aldehydes by using a rigid and sterically demanding bridge between the two phosphorous atoms.

Khan and Bhanage[25] synthesized two diphosphinite ligands and the influence of these ligands were compared to phosphite $(P(OR)_3)$ and phosphine (PR_3) ligands, respectively. Excellent regioselectivities were observed for the diphosphinite ligands and it also enabled the catalysis to proceed under very mild conditions (25 bar and 60 °C) and for a relatively short reaction time (4 h). Reactions in the absence of diphosphinite ligand using only $Rh(acac)(CO)_2$ led to low conversion and poor selectivity, which underlines how important the ligand is.

Rhodium complexes bearing *P,N*-bidentate ligands were prepared by Kostas and Screttas[26] for the hydroformylation of styrene. These complexes demonstrated excellent activity at 60 °C, with 100 % chemoselectivity towards aldehydes while favouring the formation of the branched aldehyde.

Furthermore, Duanmu and co-workers[27] synthesized a triphenyl phosphine ligand supported on magnetic nanoparticles for hydroformylation catalysed by rhodium. The complex which is responsible for the catalysis is formed *in situ*. For optimum catalytic activity, the conditions for catalysis were optimized. Initially, the authors wanted to use $RhCl_3$ as the rhodium precursor, however after recycling it and using it in a second round; the reaction did not take place. They lowered the temperature of the reaction because they thought that the high temperature was too harsh for the catalysis, but unfortunately lower yields were registered. They rationalized that this is due to the lower solubility of $RhCl_3$ in THF at lower temperatures. Therefore, $Rh(OAc)_2$ was chosen as the catalyst precursor which yielded encouraging results. The nano-PPh_3Rh complex could be used up to 20 times with the addition of fresh $Rh(OAc)_2$ after every 5 rounds. The PPh_3 contents didn't change much over

Chapter 1: Literature Review of Dendrimers and Their Applications

the 20 cycles, while some Rh(OAc)$_2$ leached out after every round as indicated by ICP-OES analysis. In the 20th cycle, the yield of the reaction was still 40.1 %.

This short overview of rhodium phosphine and phosphite complexes demonstrates how phosphorous ligands allows for the catalysis to be performed under mild reaction conditions. It also demonstrates how the ligand backbone can be tailored in such a way as to influence the regioselectivity of the reaction.

Chiral phosphines, on the other hand, have found application in enantioselective catalysis. Enantioselective catalysis is specifically important in the pharmaceutical industry. Considerable strides have been made with the development of enantioselective hydroformylation catalysts.

Clark and co-workers[28] prepared various bis-3,4-diazaphospholanes ligands with one of them shown in Figure 1-9.

R = C(O)NHCH(CH$_3$)CO$_2$CH$_3$
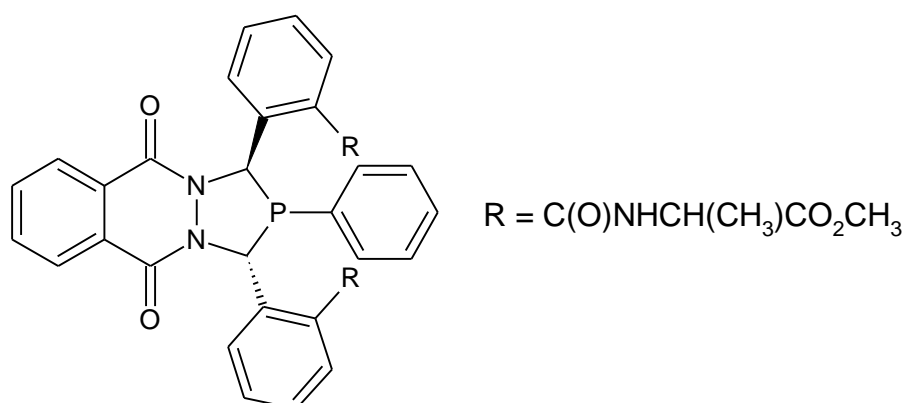
Figure 1-9: Bis-3,4-diazaphospholane ligand used by Clark and co-workers[28]

These ligands were combined with Rh to form catalysts for the enantioselective hydroformylation of styrene, allyl cyanide and vinyl acetate. In order to effectively monitor the performance of the above mentioned ligands, they were compared to other well-established ligands which are known for their success in enantioselective hydroformylation. (S, S)-ESPHOS, one of the ligands used, is shown in Figure 1-10.

R = Ph
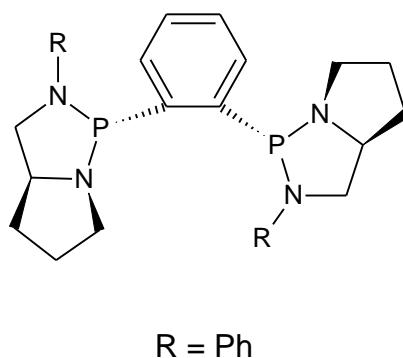
Figure 1-10: (*S, S*)-ESPHOS[28]

The bis-3,4-diazaphospholanes ligands performed quite well in enantioselective hydroformylation and in the majority of the reactions they out-performed other well-established ligands. Furthermore, the influence of reaction conditions on the catalytic reaction was studied using the ligand shown in Figure 1-11. Pressure only had an influence on the enantiomeric excess in the enantioselective hydroformylation of styrene while it stays approximately constant for allyl cyanide and vinyl acetate between 20-500 psig. For styrene hydroformylation, the % ee increases sharply up to ~100 psig and from there onwards it stays constant. The temperature has almost no effect on the % ee achieved for vinyl acetate hydroformylation, but for the styrene and allyl cyanide reaction the temperature does have an effect. High % ee was achieved at lower temperatures for styrene while for allyl cyanide the % ee increases until it reaches a maximum and then decreases again. In terms of the influence of pressure on the branched:linear (b:l) ratio, it was found that in the case of vinyl acetate and allyl cyanide reactions, it stayed approximately the same while for styrene this ratio increases steadily. The temperature has almost no effect on the regioselectivity of the allyl cyanide reaction. For styrene, the b:l ratio decreases as the temperature increases while for vinyl acetate it decreases until it reaches a minimum and then increase again. They concluded that the best regioselectivity and enantioselectivity is achieved by using a temperature of 60 °C and 500 psig syngas pressure.

Thomas and co-workers[29] utilized one of the ligands reported by Clark and co-workers[28] for the asymmetric hydroformylation of vinyl acetate. The specific ligand used is shown in Figure 1-11.

14

Chapter 1: Literature Review of Dendrimers and Their Applications

R = C(O)NHC(CH₃)Ph
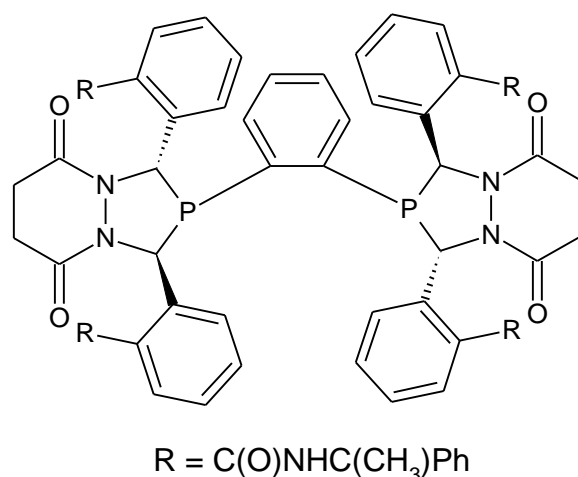
Figure 1-11: (S, S)-Diazaphospholane[29]

The aim was to synthesize branched aldehydes regioselectivity because they were interested in using it for the synthesis of isoxazolines and imidazoles. They found that as the pressure was increased, the % conversion increases up to a maximum (~97 %). Further increases in pressure did not have any effect on the conversion.

1.3.1.2 Rh Metallodendrimers

Triphenylphosphine-functionalized dendrimers were prepared by Huang and co-workers[30] for the hydroformylation of styrene and 1-octene. G1, G2 and G3 dendrimers were synthesized in order to study the effect of dendrimer generation on the catalysis. The catalyst responsible for the catalysis was formed *in situ*.

Chapter 1: Literature Review of Dendrimers and Their Applications
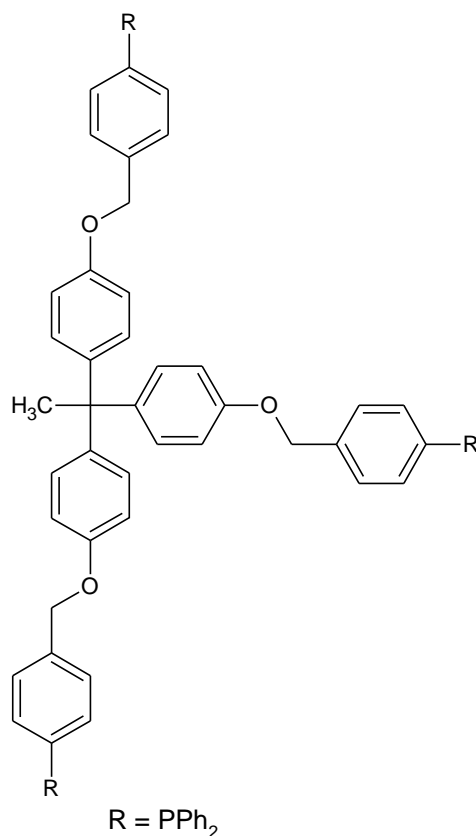
Figure 1-12: G1 dendrimer prepared by Huang and co-workers[30]

After the successful preparation of these dendritic ligands, they were tested in the hydroformylation reaction. Initially, the solvent chosen for the hydroformylation reaction was toluene, but only the $Rh(CO)_2(PPh_3)_2$ and the G1 dendrimer registered good enough conversions (83 % and 76 % respectively) in this solvent with acceptable regioselectivity in which the branched aldehydes are favoured. This was explained by the poor solubility of the G2 and G3 dendrimers in toluene, which lead to a decrease in the conversion and regioselectivity. Therefore, the solvent was changed to dichloromethane and styrene as substrate. In this system, $Rh(CO)_2(PPh_3)_2$ outperformed the dendritic catalysts in terms of conversion but the regioselectivity of the dendritic catalysts was better. For 1-octene, all the catalysts used registered a conversion of 100 % and the preferred products formed are linear aldehydes.

Iminopyridyl and iminophosphine dendritic catalysts were prepared by Smith and co-workers[31] and applied in the hydroformylation of 1-octene. Two different generation catalysts were synthesized (G1 and G2), as well as their mononuclear analogues. The mononuclear analogues were synthesized to act as model complexes for the dendritic catalysts.

Chapter 1: Literature Review of Dendrimers and Their Applications
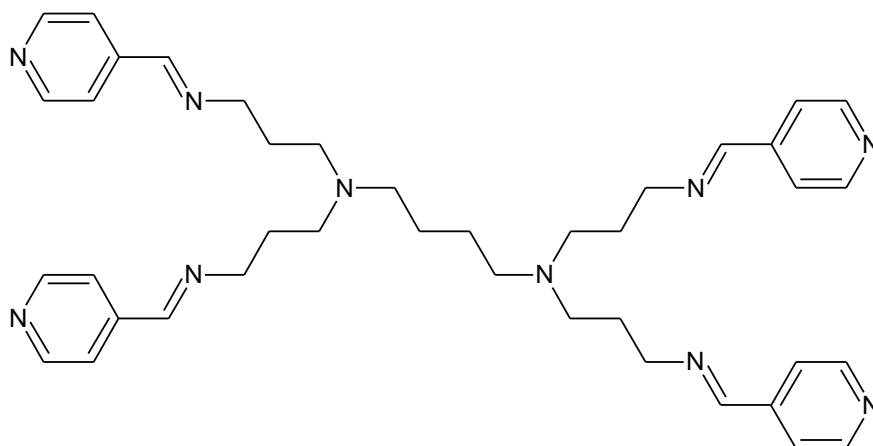
Figure 1-13: G1 Iminopyridyl ligand prepared by Antonels and co-workers[31]

Quite encouraging results were obtained for the different catalyst systems. The conversions for all the Rh(I) complexes were very close to 100 %. For the iminopyridyl complexes, the mononuclear complex yielded 70 % aldehyde which is more than what was recorded for the dendritic catalysts (G1 and G2). Isomerisation was slightly lower and the activity was better (higher TOF) for the mononuclear complex. The regioselectivity of all three iminopyridyl complexes were quite similar. For the iminophosphine complexes, the mononuclear complex outperforms the dendritic catalysts in terms of percentage of aldehydes formed, lower level of isomerisation recorded, better regioselectivity (not much different from G1 metallodendrimer) and much faster catalysis. However, the G2 dendrimer complex led to a higher percentage aldehydes formed, the extent of isomerisation was lower and the reaction rates were faster compared to the G1 dendrimer complex. RhCl(PPh$_3$)$_3$ and Rh(CO)$_2$(acac) were also tested and the results obtained were compared to those of the iminopyridyl and iminophosphine dendrimer complexes. Furthermore, the authors carried out additional studies in order to determine the effect of pressure and temperature on the reaction. One of the major observations was that if the catalysis is performed at low pressures, isomerisation of the alkene occurs and the percentage of aldehyde formed is very low. Consequently, performing the catalysis at higher pressures decreases isomerisation of the alkene leading to the formation of predominantly aldehydes. Regioselectivity determined for the six complexes showed that they are selective for the formation of linear aldehydes compared to branched aldehydes. The complexes were much more selective than Rh(CO)$_2$(acac). Lastly, the authors concluded that the dendrimers have no effect on the regioselectivity since the selectivity observed for the model complexes and dendrimer complexes were quite comparable.

Chapter 1: Literature Review of Dendrimers and Their Applications

Smith and co-workers[32] synthesized hydrophilic sulfonate salicylaldimine dendrimers for the aqueous bi-phasic hydroformylation of 1-octene. Four different types of ligands were tested, of which two complexes were not isolated but formed *in situ* (tris-2-(5-sulfonato salicylaldimine ethyl) amine and DAB-(5-sulfonato salicylaldimine)). Two mononuclear complexes were also prepared, one of which had a hydrogen atom ortho to the hydroxy group (unsubstituted) and the other one a tertiary butyl group (substituted).
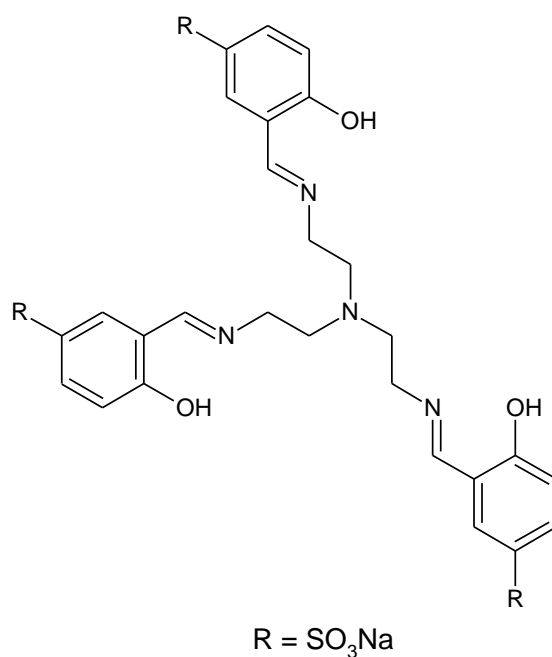
Figure 1-14: Tris-2-(5-sulfonato salicylaldimine ethyl) amine ligand prepared by Smith and co-workers[32]

All the ligands and complexes synthesized were readily soluble in polar solvents (water and alcohols). Biphasic hydroformylation was performed with the complex residing in the water phase and the substrate in the organic phase. These phases came into contact upon heating. After the catalysis, the organic phase containing the product was decanted and the aqueous phase can be re-used in the next catalytic reaction. Thus, biphasic hydroformylation made it possible to recycle the catalyst and the authors could recycle the catalyst up to 5 times without a major loss in activity. In terms of conversion, the DAB-(5-sulfonato salicylaldimine) complex formed *in situ* achieved the highest conversion of 99 %, but gave a product mix of 37 % aldehydes and 63 % iso-octenes thus indicating a large degree of isomerisation. The mononuclear complex containing a hydrogen atom ortho to the hydroxy group is the best performing catalyst since its chemoselectivity is the highest (85 % aldehyde) and registered the highest TOF. When the temperature was increased to 95 °C, the conversions obtained with all of the catalysts increased. In addition, the percentage aldehydes

formed as well as the TOF increased, however, the selectivity of all the catalyst systems seems to favour the formation of branched aldehydes. Furthermore, the influence of pressure on the catalysis was evaluated. Performing the catalysis at 40 bar, compared to the 30 bar, led to higher conversions for all the catalyst systems, the percentage of aldehydes formed increased while the n:iso ratio stayed approximately the same. Also, higher TOF values could be achieved. Increasing the pressure further led to a decrease in the conversion, as well as in the percentage aldehydes formed and also to a lower TOF. Generally, the mononuclear complexes performed better at hydroformylating 1-octene than the dendrimeric catalyst systems.

1.3.2 Hydroformylation using Ruthenium

Hydroformylation is commonly performed using rhodium catalyst systems. This is due to the high activity of rhodium making it possible to use mild reaction conditions. However, rhodium is one of the most expensive metals. Therefore, other metals have been explored to decrease the cost of the catalyst systems. Furthermore, no examples of ruthenium metallodendrimers for hydroformylation were found in literature.

Baricelli and co-workers[33] synthesized and characterized $Ru(H)_2(CO)(TPPMS)_3$ as a catalyst for the hydroformylation of 1-hexene, cyclohexene and 2,3-dimethyl-1-butene. The catalyst was most active for 1-hexene and the least active for 2,3-dimethyl-1-butene. The ruthenium complex was water-soluble which allowed for aqueous biphasic hydroformylation to be performed. The catalyst was also very chemoselective towards aldehydes (90 %). Furthermore, the influence of catalytic conditions was also studied and results showed that the conversion is high when the catalysis is performed at or above temperatures of 90 °C. It was also found that the amount of aldehyde increases over time while the highest conversion is achieved employing a pressure of 1000 psi. Hydroformylation was also performed using a mixture of the three olefins. In this situation, 1-hexene showed the highest conversion (80 %) followed by cyclohexene (14 %) and 2,3-dimethyl-1-butene (6 %).

CO can be replaced with CO_2 when carrying out the hydroformylation reaction, as reported by Tominaga.[34] In this case, a ruthenium catalyst was utilized in the hydroformylation of 1-hexene. The solvent employed was an ionic liquid making this process very environmentally friendly since no organic solvent of any sort is used. During the reaction, the olefin undergoes hydroformylation to form the aldehyde. The aldehyde is then hydrogenated to the alcohol, and this is the product that is isolated at the end of the catalytic run. According to the author,

a halide salt must be present to activate CO_2. From the results it is evident that by using a 1:1 ratio of $Cl:NTf_2$ (bis(trifluoromethylsulfonyl)amide), gave the best results since the yield of the alcohol was the highest in this case. Next, the influence of temperature on catalysis was studied. The conversion of 1-hexene increases as the temperature increases up to a maximum of 160 °C after which it starts to decrease. Initially, heptanal is produced but the amount of aldehyde decreases rapidly since it is completely converted to heptanol. In terms of the recycling of the catalyst, the conversion stayed roughly constant over 5 runs while the yield of heptanol decreased slightly from 82 % in the first run to 75 % in the second run. After the second run the heptanol yield remained roughly unchanged.

Melean and co-workers[35] studied the hydroformylation of substituted allylbenzenes using water-soluble rhodium and ruthenium complexes. Since the complexes were water-soluble, aqueous biphasic hydroformylation was performed. The substrates studied were eugenol, estragole, safrole and trans-anethole. Generally, highest conversions were achieved for eugenol. For the ruthenium catalyst with the TPPMS ligand, the highest conversion was achieved for eugenol compared to the other substrates. The major products formed for eugenol were aldehydes. Although the conversions for the other substrates are low, the catalyst showed greater chemoselectivity towards the formation of aldehydes over unwanted isomerised alkenes. Upon replacing the TPPMS phosphine ligand with TPPTS, the conversions for safrole and estragole increased, but the chemoselectivity were much lower. The authors rationalized that the increase conversions was due to the superior ability of the TPPMS to dissolve in water, making more of the active species available thus increasing the turnover.

Smith and co-workers[36] reported the synthesis of Ru(II) arene complexes of monodendate P-donor ligands [1,3,5-triaza-7-phosphaadamantane (PTA) and $P(OMe)_3$] and a complex containing bidentate salicylaldimine ligands. These complexes were tested in the aqueous biphasic hydroformylation of 1-octene. They rationalized that the basicity of the ligands determines the regioselectivity of the reaction. Higher concentration of aldehydes are formed in the presence of less basic ligands. The complex containing the more basic $P(OMe)_3$ group yielded the highest conversion of 1-octene while the PTA complex yielded the lowest. The $P(OMe)_3$ containing complex were also more chemoselective towards the formation of aldehydes (moderately). The major products obtained using the PTA complex are isomerised alkenes (83.74 %). These products are undesired, meaning that this complex is unable to effectively hydroformylate 1-octene under these conditions. The salicylaldimine complex

performed slightly better than the PTA complex, but isomerised alkenes were still the major products obtained. The authors initially hypothesized that the less basic ligand would favour the formation of aldehydes. The experimental results confirm this proposal. Furthermore, recyclability tests were done and all of the complexes could be recycled and reused without the conversions decreasing significantly.

1.4   Conclusion and Aims

In conclusion, this short review of dendrimers shows how their properties can be exploited in various applications. Its application in catalysis is specifically important since it allows for enhanced catalytic reactions and also the possibility of recovering the catalyst. Although a number of metallodendrimers have been reported in recent years, there is still a need to develop more active and selective dendritic catalysts. Thus, the objectives of this current study were:

1) The synthesis and characterization of novel iminopyridyl ligands. This includes mono-functional, di-functional, tri-functional and tetra-functional ligands.
2) The synthesis and characterization of novel mononuclear and multinuclear complexes. This entails the complexation of the above mentioned ligands to Rh(I) and Ru(II) metal ions.
3) Catalytic testing of the prepared complexes in the hydroformylation of 1-octene. Determining the chemoselectivity and regioselectivity of the catalysts. Investigating the influence of reaction conditions on the activity and selectivity of the catalysts.

1.5   Overview of Thesis

Chapter 2: This chapter contains the synthesis and characterization of new multi-functional iminopyridyl ligands.

Chapter 3: Synthesis and characterization of the various mononuclear and multinuclear complexes is discussed in this chapter.

Chapter 4: Evaluation of the different complexes in the hydroformylation of 1-octene.

Chapter 5: This chapter summarizes the main conclusions that was drawn from the research. It also contains information about future prospects.

Chapter 1: Literature Review of Dendrimers and Their Applications

1.6   References

1. P. Arya, G. Panda, N. V. Rao, H. Alper, S. C. Bourque and L.E. Manzer, *J. Am. Chem. Soc.*, 2001, **123**, 2889-2890.

2. S. C. Bourque and H. Alper, *J. Am. Chem. Soc.*, 2000, **122**, 956-957.

3. E. A. Karakhanov, A. L. Maximov, B. N. Tarasevich and V. A. Skorkin, *J. Mol. Catal. A: Chem.*, 2009, **297**, 73-79.

4. L. H. Bryant, M. W. Brechbiel, C. Wu, J. W. M. Bulte, V. Herynek and J. A. Frank, *J. Magn. Reson. Imaging*, 1999, **9**, 348-352.

5. L. J. Twyman, A. E. Beezer, R. Esfand, M. J. Hardy and J. C. Mitchell, *Tetrahedron Lett.*, 1999, **40**, 1743-1746.

6. J. F. Kukowska-Latallo, E. Raczka, A. Quintana, C. L. Chen, M. Rymaszewski and J. R. Baker, *Hum. Gene Ther.*, 2000, **11**, 1385-1395.

7. J. W. J. Knapen, A. W. van der Made, J. C. de Wilde, P. W. N. M. van Leeuwen, P. Wijkens, D. M. Grove and G. van Koten, *Nature*, 1994, **372**, 659-663.

8. D. A. Tomalia, H. Baker, J. Dewald, M. Hall, G. Kallos, S. Martin, J. Roeck, J. Ryder and J. Smith, *Polym J.*, 1985, **17**, 117-132.

9. G. R. Newkome, Z. Yao, G. R. Baker and V. K. Gupta, *J. Org. Chem.*, 1985, **50**, 2004-2006.

10. C. J. Hawker and J. M. J. Fréchet, *J. Am. Chem. Soc.*, 1990, **112**, 7638-7647.

11. B. Klajnert and M. Bryszewska, *Acta Biochim. Pol.*, 2001, **48**, 199-208.

12. J. Haensler and F. C. Szoka, *Bioconjugate Chem.*, 1993, **4**, 372-379.

13. R. X. Zhuo, B. Du, and Z. R. Lu, *J. Controlled Release.*, 1999, **57**, 249-257.

14. M. Liu, K. Kono and J. M. J. Fréchet, *J. Controlled Release.*, 2000, **65**, 121-131.

15. M. F. Neerman, W. Zhang, A. R. Parrish and E. E. Simanek, *Int. J. Pharm.*, 2004, **281**, 129-132.

16. S. N. Goonewardena, P. R. Leroueil, C. Gemborys, P. Tahiliani, S. Emery, J. R. Baker and H. Zong, *Bioorg. Med. Chem. Lett.*, 2013, **23**, 2230-2233.

17. Y. Chung and H. Rhee, *J. Mol. Catal. A: Chem.*, 2003, **206**, 291-298.

18. N. Toshima and T. Yonezawa, *N. J. Chem.*, 1998, 1179.

19. V. K. R. Kumar and K. R. Gopidas, *Tetrahedron Lett.*, 2011, **52**, 3102-3105.

20. G. Smith, R. Chen and S. F. Mapolie, *J. Organomet. Chem.*, 2003, **673**, 111-115.

21. F. Martínez-Olid, E. de Jesús and J. C. Flores, *Inorg. Chim. Acta*, 2014, **409**, 156-162.

22. R. K. G. Panicker and S. Krishnapillai, *Tetrahedron Lett.*, 2014, **55**, 2352-2354.

23. M. Beller, B. Cornils, C. D. Frohning and C. W. Kohlpaintner, *J. Mol. Catal. A: Chem.*, 1995, **104**, 17-85.

24. A. Van Rooy, P. C. J. Kamer, P. W. N. M. van Leeuwen, K. Goubitz, J. Fraanje, N. Veldman and A. L. Spek, *Organometallics*, 1996, **15**, 835-847.

25. S. R. Khan and B. M. Bhanage, *Appl. Organometal. Chem.*, 2013, **27**, 313-317.

26. I. D. Kostas and C. G. Screttas, *J. Organomet. Chem.*, 1999, **585**, 1-6.

27. C. Duanmu, L. Wu, J. Gu, X. Xu, L. Feng and X. Gu, *Catal. Commun.*, 2014, **48**, 45-49.

28. T. P. Clark, C. R. Landis, S. L. Freed, J. Klosin and K. A. Abboud, *J. Am. Chem. Soc.*, 2005, **127**, 5040-5042.

29. P. J. Thomas, A. T. Axtell, J. Klosin, W. Peng, C. L. Rand, T. P. Clark, C. R. Landis and K. A. Abboud, *Org Letters*, 2007, **9**, 2665-2668.

30. Y. Huang, H. Zhang, G. Deng, W. Tang, X. Wang, Y. He and Q. Fan, *J. Mol. Catal. A: Chem.*, 2005, **227**, 91-96.

31. N. C. Antonels, J. R. Moss and G. S. Smith, *J. Organomet. Chem.*, 2011, **696**, 2003-2007.

32. E. B. Hager, B. C. E. Makhubela and G. S. Smith, *Dalton Trans.*, 2012, **41**, 13927-13935.

33. P. J. Baricelli, E. Lujano, M. Rodríguez, A. Fuentes and R. A. Sánchez-Delgado, *Appl. Catal. A: General*, 2004, **263**, 187-191.

34. K. Tominaga, *Catal. Today*, 2006, **115**, 70-72.

35. L. G. Melean, M. Rodriguez, M. Romero, M. L. Alvarado, M. Rosales and P. J. Baricelli, *Appl. Catal. A: General*, 2011, **394**, 117-123.

36. L. C. Matsinha, P. Malatji, A. T. Hutton, G. A. Venter, S. F. Mapolie and G. S. Smith, *Eur. J. Inorg. Chem.*, 2013, 4318-4328.

Chapter 2 : Synthesis and Characterization of Iminopyridyl Dendrimeric Ligands

2.1   Introduction

This chapter outlines the synthesis and characterization of four novel iminopyridyl ligands. As described in the previous chapter, dendrimers consist of a core, branches and peripheral endgroups. We chose to explore the synthesis of dendrimers containing benzene as a core. This core is rigid which could possibly prevent free rotation and thus yield a more rigid dendrimeric structure. Compounds containing benzene as core have previously been shown to be stable and could be isolated in high yields. Such an example was reported by Ashton and co-workers[1] who synthesized a polycationic dendrimer. There are other examples of such dendrimers in the literature.[2-6] Furthermore, Fréchet and Hawker[7] synthesized dendritic polyether macromolecules using 3,5-diethoxybenzyl bromide with 1,1,1-tris(4'-hydroxyphenyl)ethane as the core of the dendrimer. With the afore-mentioned in mind, benzene-cored dendrimers were synthesized based on some of the approaches outlined above.
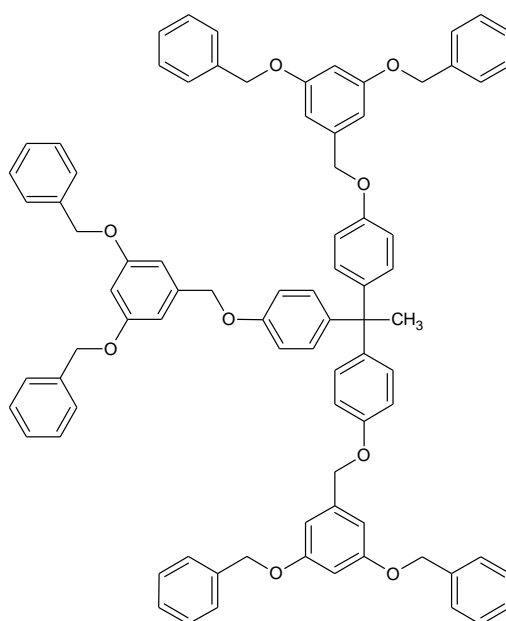
Figure 2-1: A G1 Dendrimer prepared by Fréchet and Hawker[7]

The dendrimers prepared by Fréchet and Hawker[7] were the first examples which were synthesized through a convergent synthetic approach. In this way, they prepared dendrimers up to generation 5 with phenyl rings on the periphery of the dendrimer. The synthesis of these dendrimers entailed the reaction of two equivalents of benzyl bromide with 3,5-

Chapter 2: Synthesis and Characterization of Iminopyridyl Dendrimeric Ligands

dihydroxybenzyl alcohol. The benzyl alcohol functionality is then converted to the corresponding benzyl bromide. This product, which was labelled [G-1]-Br, was then reacted with the core (1,1,1-tris(4'-hydroxyphenyl)ethane) yielding the G1 dendrimer as shown in Figure 2-1. To expand this dendrimer to higher generations, [G-1]-Br was simply reacted with 3,5-dihydroxybenzyl alcohol yielding [G-2]-Br, which could subsequently be reacted with the core to yield the G2 dendrimer. The authors used this approach to construct dendrimers up to the fifth generation.

Similarly to Fréchet and Hawker[7], the aim in this project was to prepare polyether dendritic compounds. Ether bonds are relatively stable and inert, and this property, together with the added stability of the benzene ring, was our motivation to prepare these compounds. Ultimately, the aim was to synthesize *N, N* iminopyridyl chelating ligands. This was achieved by firstly preparing a Schiff base ligand by reacting 2-pyridinecarboxaldehyde with p-aminophenol. This compound was then reacted with the appropriate core to yield different multifunctional ligands. The precursors to the cores utilized in this study were benzyl bromide, 1,4-bis(bromomethyl) benzene, 1,3,5-tris(bromomethyl) benzene and 1,2,4,5-tetrakis(bromomethyl) benzene. All of the ligands were characterized using analytical techniques such as IR spectroscopy, NMR spectroscopy, mass spectrometry, elemental analysis and melting point determinations.

Peacock and co-workers[8] prepared chloro half-sandwich Os(II) complexes containing chelating *N,N*-ligands and studied the influence of these ligands on the hydrolysis, guanine binding and cytotoxicity of these complexes. They found that the presence of these chelating ligands actually improved the stability of these complexes in aqueous solutions. Smith and co-workers[9] prepared chelating *N,O-* and *N,N*-Ru(II) arene complexes and tested the cytotoxicity of these complexes towards A2780 and A2780cisR human ovarian carcinoma cancer cell lines. Both model complexes (mononuclear) and dendrimeric complexes (based on DAB dendrimer) were prepared. Results showed that one of the *N,N*-Ru(II) complexes were the most cytotoxic of all the complexes tested and also more efficient in binding DNA, as determined by gel electrophoresis. Taubmann and Alt[10] prepared Iridium complexes with *N,N*-chelating ligands for the dehydrogenation of cyclooctane to cyclooctene. One of the ligands utilized by these authors is shown in Figure 2-2. Various other ligands were also prepared and most of the complexes exhibited a selectivity of 100 % favouring cyclooctene as product.

Chapter 2: Synthesis and Characterization of Iminopyridyl Dendrimeric Ligands
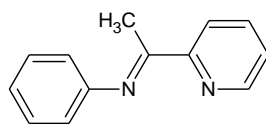
Figure 2-2: Ligand prepared by Taubmann and Alt[10]

Ros and co-workers[11] prepared Ir(III) complexes using hemilabile *N,N*-chelating ligands for the nitrogen-directed borylations of arenes. When the reaction was attempted in the absence of the ligands, no reaction took place underlying the importance of the ligands. Nayab and co-workers[12] prepared *N,N*-bidentate Zn complexes for the ring opening polymerization of *rac*-lactide. All of the complexes tested gave very high conversions between 96-99 %. The conversion were still very close to 100 %, even at reaction temperatures of -25 °C. Furthermore, Tregubov and co-workers[13] anchored *N,N* and *N,P* ligands on glassy carbon electrodes and prepared the Rh(I) complexes thereof. Four different complexes were prepared, three *N,N* complexes and one *N,P* complex. These immobilized complexes were then used as recyclable hydroamination catalysts.
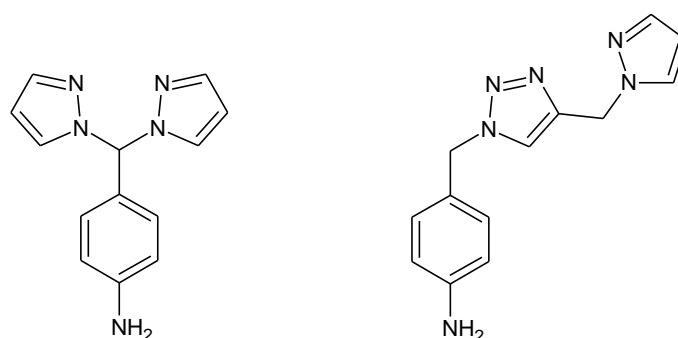
Figure 2-3: Two of the ligands utilized by Tregubov and co-workers[13]

The authors studied the intramolecular hydroamination of 4-pentyn-1-amine to 2-methyl-1-pyrroline. The highest conversion achieved was 50 % for one of the *N,N* donor complexes while the lowest were 15 % for the *N,P* complex.

From the above it is evident how widely the nitrogen donor ligands are being used, including a wide range of applications, from medicinal to catalytic uses.

2.2   Synthesis of dendrimeric ligands and related compounds

2.2.1   Synthesis of 4-{[pyridin-2-ylmethylidene]amino}phenol

Heinze and co-workers[14-16] previously published papers on the utilization of 4-{[pyridin-2-ylmethylidene]amino}phenol in the synthesis of Cr, Mo and W complexes through solid- and solution phase synthesis. These complexes exhibited quite interesting properties. Hydrogen

26

Chapter 2: Synthesis and Characterization of Iminopyridyl Dendrimeric Ligands

bonding is present in the complexes and most interestingly, a hexameric structure was observed for one of the Cr complexes. Furthermore, Chanawanno and co-workers[17] prepared a series of Re(CO)$_3$ pyridine-imine complexes and studied the pH-dependent behaviour of these complexes. In addition to studying the general properties of these compounds, complexes of 4-{[pyridin-2-ylmethylidene]amino}phenol have also been utilized in catalysis.[18-19] Di Serio and co-workers[18] prepared Zn(II) complexes for biodiesel production while Zhang and co-workers[19] synthesized a "click" magnetic nanoparticle-supported Pd catalyst for Suzuki-Miyaura coupling reactions. Due to the success the afore-mentioned groups had utilizing this simple ligand, we decided to utilize this compound to prepare a new range of multifunctional iminopyridyl ligands.
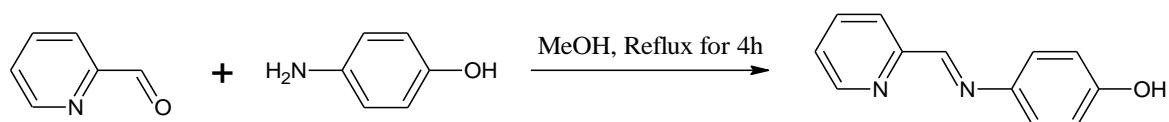
Figure 2-4: Synthesis of 4-{[pyridin-2-ylmethylidene]amino}phenol[19]

We adopted the experimental procedure used by Zhang and co-workers[19] to prepare 4-{[pyridin-2-ylmethylidene]amino}phenol. The synthesis entails a Schiff base condensation reaction between 2-pyridinecarboxaldehyde and p-aminophenol in methanol. The product was isolated as a yellow-orange solid. The carbonyl absorption of the starting material, 2-pyridinecarboxaldehyde, is observed at 1707 cm^{-1} and the amine absorption of p-aminophenol is observed at 3337 cm^{-1} and 3278 cm^{-1}. In the starting material, the υ(C=N) absorption of the pyridyl ring is observed at 1584 cm^{-1} and we expect only a slight, if any at all, shift in this absorption for the product. In the product, the υ(C=N) pyridyl ring absorption shifted slightly to a lower wavenumber (1579 cm^{-1}), while an imine band appeared at 1622 cm^{-1}. The IR spectrum also showed the absence of any carbonyl and amine bands. In the ^{1}H NMR spectrum of 4-{[pyridin-2-ylmethylidene]amino}phenol, the imine proton was observed at 8.60 ppm, while the NMR spectrum, as previously confirmed by IR spectroscopy, did not show the presence of any amine or carbonyl moieties. Ten carbon signals are observed in the ^{13}C NMR spectrum with two signals very close to each other (156.8 and 156.7 ppm), which can be assigned to the pyridyl C=N and free imine carbons. The characterization data for 4-{[pyridin-2-ylmethylidene]amino}phenol compared well to those reported previously in literature.[19]

27

Chapter 2: Synthesis and Characterization of Iminopyridyl Dendrimeric Ligands

2.2.2 Ligand (L1) prepared from benzyl bromide and 4-{[pyridin-2-ylmethylidene]amino}phenol

After the successful preparation and characterization of 4-{[pyridin-2-ylmethylidene]amino}phenol, we proceeded to the synthesis of our multifunctional ligands. Zhang and co-workers[19] performed a nucleophilic substitution reaction where 4-{[pyridin-2-ylmethylidene]amino}phenol was reacted with propargyl bromide in acetone using K_2CO_3 as the base. We employed a similar approach to prepare our ligands as shown in Figure 2-5.

(i) $C_6H_5CH_2Br$, K_2CO_3, Acetone Reflux, 18 h
(ii) $C_6H_4(CH_2Br)_2$, K_2CO_3, Acetone Reflux, 18 h
(iii) $C_6H_3(CH_2Br)_3$, K_2CO_3, Acetone Reflux, 18 h
(iv) $C_6H_2(CH_2Br)_4$, K_2CO_3, Acetone Reflux, 18 h
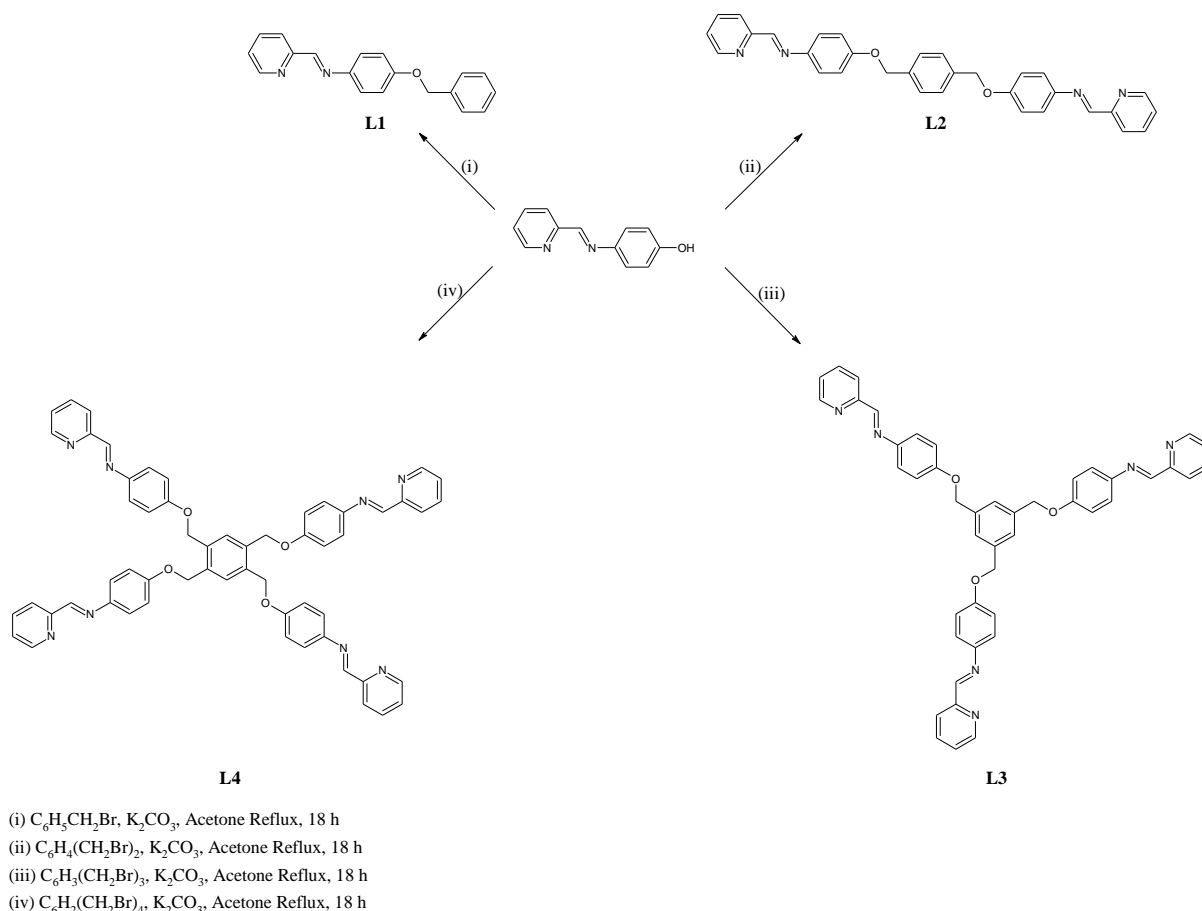
Figure 2-5: Preparation of ligands (L1-L4)

L1, a mono-functional ligand, was prepared by reacting 4-{[pyridin-2-ylmethylidene]amino}phenol with benzyl bromide. It was isolated as a stable light brown solid in 83 % yield. The product melts in the temperature range 109 °C to 111 °C. The IR spectrum revealed the imine and pyridyl absorbances to be at 1621 cm^{-1} and 1574 cm^{-1} respectively. Furthermore, the phenyl and alkyl ether bonds gave two strong bands at 1243 cm^{-1} and 1037 cm^{-1}.

Chapter 2: Synthesis and Characterization of Iminopyridyl Dendrimeric Ligands

In the ^{1}H NMR spectrum (Figure 2-6), the benzylic protons were observed as a singlet at 5.11 ppm. The free imine proton resonates at 8.65 ppm and the imine proton of the pyridyl ring at 8.71 ppm. The rest of the aromatic protons were observed between 7.03 ppm and 8.21 ppm. Further characterization was carried out by ^{13}C NMR spectroscopy. The spectrum showed the presence of the benzylic carbon at 70.6 ppm, while the imine and pyridyl carbon resonances were at 158.4 ppm and 158.6 ppm respectively. The remaining resonances observed between 115.7 ppm and 155.1 ppm are that of the remaining carbon atoms.
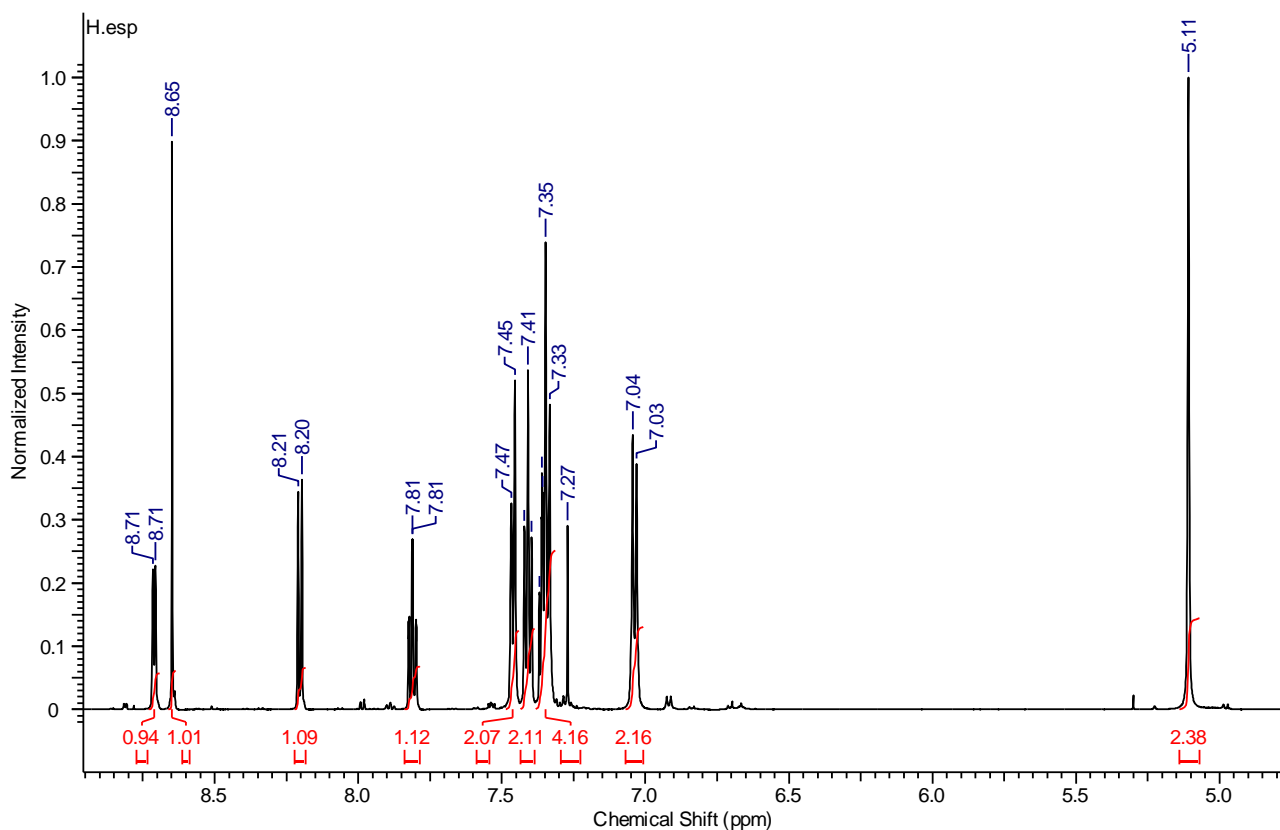
Figure 2-6: ^{1}H NMR Spectrum of L1

Furthermore, in ESI-MS, the molecular ion was absent due to the hydrolysis of the imine bond to an amine under the conditions employed to record the spectrum, resulting in a peak at m/z 200.1. This was the base peak in the spectrum which did not undergo further fragmentation to smaller ions.

Chapter 2: Synthesis and Characterization of Iminopyridyl Dendrimeric Ligands

2.2.3   Ligand (L2) prepared from 1,4-bis(bromomethyl) benzene and 4-{[pyridin-2-ylmethylidene]amino}phenol

L2 was isolated as an off-white solid, unlike **L1** and **L3** which are brown solids. It also differs from the other analogues (**L1** and **L3**) in terms of its solubility properties. It has quite a low solubility in DCM and CHCl$_3$ at room temperature, while it is completely insoluble in DMSO and acetone. It melts in the temperature range of 216 °C – 218 °C. The IR spectra of all the ligands looks similar, and thus the spectrum for **L2** is shown as an example. As for all the other ligands, the imine and pyridyl absorbances are situated at 1622 cm^{-1} and 1576 cm^{-1} respectively. The phenyl and alkyl ether bonds are also observed at 1244 cm^{-1} and 1035 cm^{-1} (Figure 2-7).
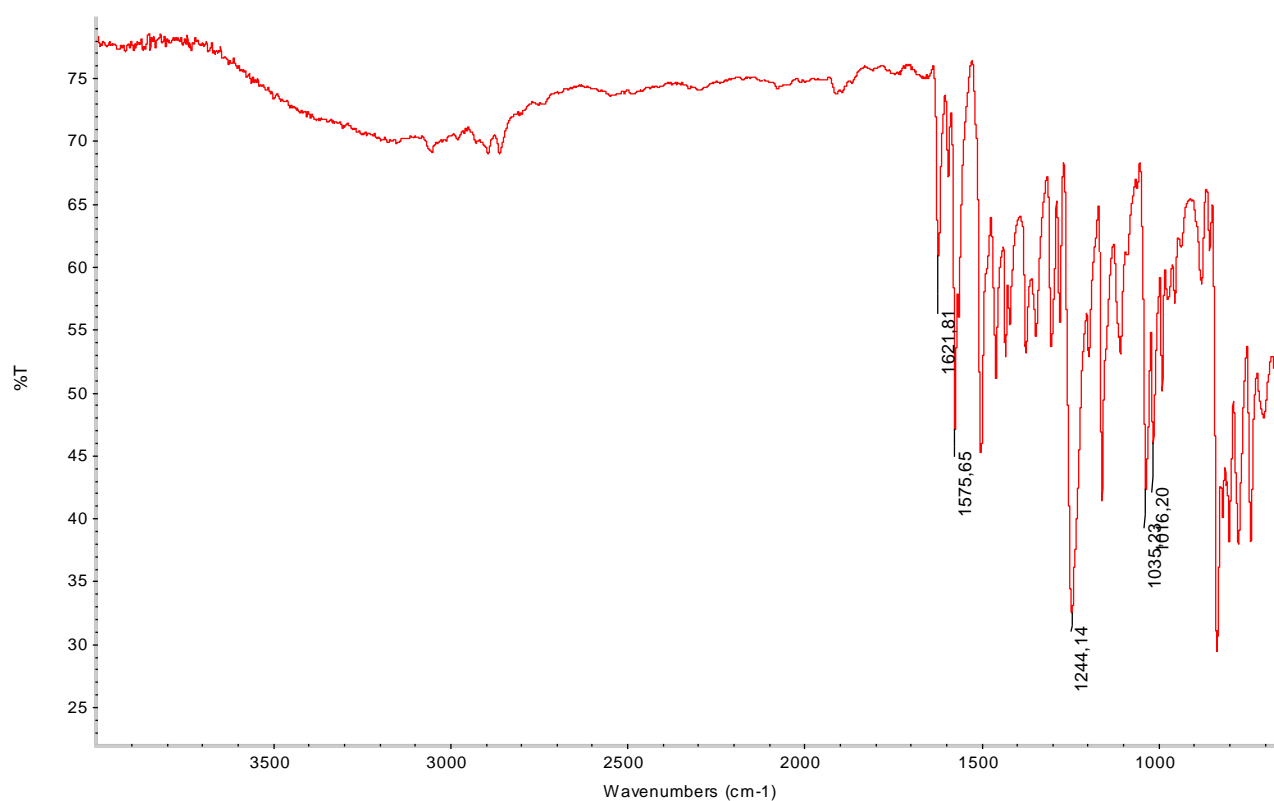
Figure 2-7: IR Spectrum of L2

In the ^{1}H NMR spectrum, the benzylic protons were detected at 5.08 ppm while the signal for the aromatic protons of the core molecule was located at 7.45 ppm in the ^{1}H NMR spectrum. The signals for the other aromatic protons were located between 7.00 ppm and 8.16 ppm. The imine and pyridyl protons were observed at 8.60 ppm and 8.67 ppm respectively. In the ^{13}C NMR spectrum, the benzylic carbon were observed at 69.9 ppm, while the imine and pyridyl carbons were at 158.0 ppm and 158.4 ppm respectively. The other 10 resonances for the other carbons were seen between 115.4 ppm and 154.8 ppm.

30

In the ESI mass spectrum, the protonated molecular ion which coincided with the base peak was observed at m/z 499.2. An additional fragment was observed at m/z 410.2 which is a consequence of the hydrolysis of one of the imine bonds. This was also observed for **L1** above.

2.2.4 Ligand (L3) prepared from 1,3,5-tris(bromomethyl) benzene and 4-{[pyridin-2-ylmethylidene]amino}phenol

A trifunctional ligand, **L3**, was synthesized by the reaction of 4-{[pyridin-2-ylmethylidene]amino}phenol with 1,3,5-Tris(bromomethyl)benzene. **L3** was isolated as a stable brown solid after recrystallization from DCM:Et$_2$O in 90 % yield. It dissolved readily in acetone, dichloromethane and chloroform. The compound was found to melt between 178 °C and 179 °C. In the IR spectrum, two imine bands were observed at 1577 cm^{-1} (pyridyl) and 1623 cm^{-1} (imine). The absorption of the C-O bond of the phenol group of the starting material, 4-{[pyridin-2-ylmethylidene]amino}phenol, was observed at 1237 cm^{-1}. For **L3**, this absorption shifted slightly showing a broad strong peak at 1227 cm^{-1} which can be assigned to the phenyl ether bond. The alkyl ether bond showed a peak at 1030 cm^{-1}.

^{1}H NMR spectroscopy revealed a shift in the benzylic proton signal from 4.47 ppm in 1,3,5-tris(bromomethyl)benzene to 5.15 ppm in **L3**. The protons of the aromatic core were observed at 7.52 ppm, while the other aromatic protons were present at 7.02 – 7.35 ppm. The protons of the pyridyl ring were between 7.32 – 8.71 ppm, with the important proton signal at 8.71 ppm. This signal is due to the pyridyl ring imine proton. The isolated imine proton is present as a singlet at 8.63 ppm. In the ^{13}C NMR spectrum, the benzylic carbon was present at 69.9 ppm. The imine and pyridyl imine carbon gave resonances at 157.9 ppm and 158.4 ppm respectively. Ten other resonances were observed between 115.4 ppm and 154.8 ppm representing the other remaining carbon atoms.

In the ESI mass spectrum, the singly charged molecular ion which coincided with the base peak is observed at m/z 709.3 for **L3** which can be assigned to the [M+H]$^+$ ion. Doubly and triply charged molecular ions are also observed as shown in Figure 2-8.
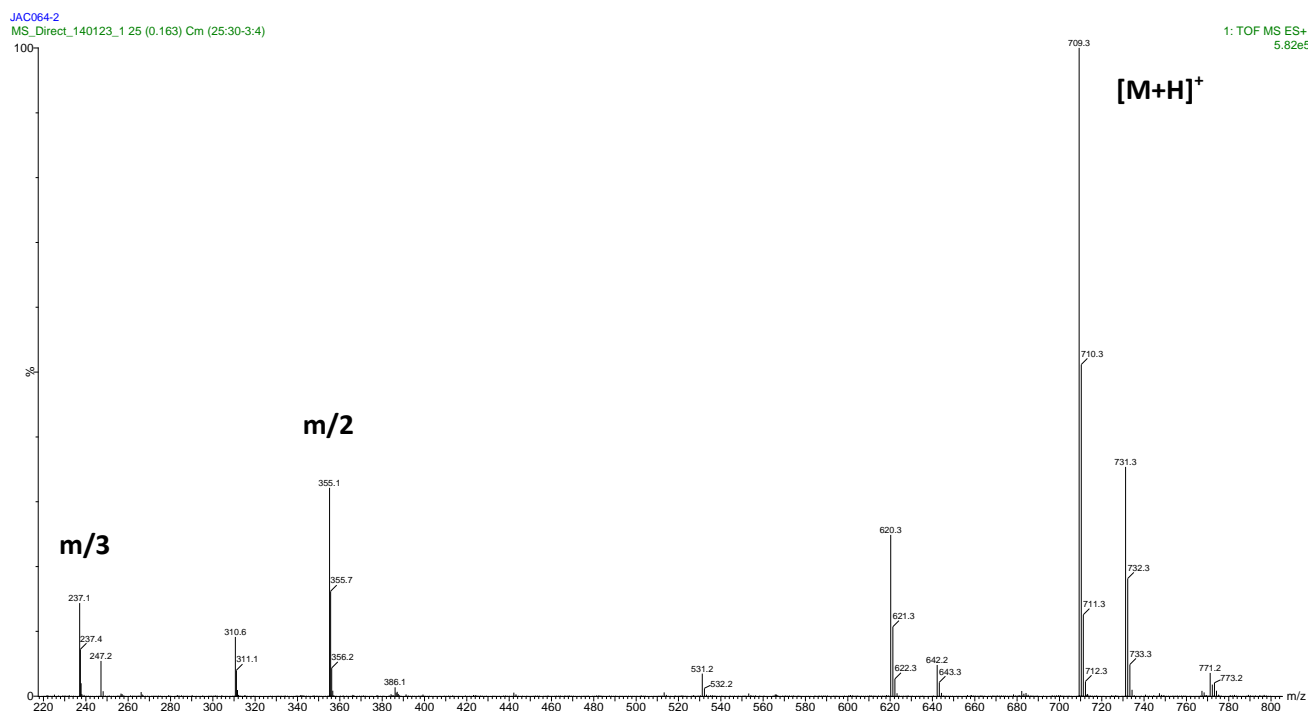
Figure 2-8: ESI-MS Spectrum of L3

2.2.5   Ligand (L4) prepared from 1,2,4,5-tetrakis(bromomethyl) benzene and 4-{[pyridin-2-ylmethylidene]amino}phenol

Another ligand synthesized was a tetra-functionalized compound prepared from 4-{[pyridin-2-ylmethylidene]amino}phenol and 1,2,4,5-tetrakis(bromomethyl)benzene. This ligand was also isolated as an off-white solid in 67 % yield, and the material melts in the temperature range 187 °C to 188 °C. The compound is partially soluble in DCM and CHCl$_3$ at room temperature. The IR spectrum of **L4** appeared fairly similar to those obtained for the other ligands with the imine and pyridyl absorbances observed at 1626 cm^{-1} and 1579 cm^{-1} respectively. The C-O band of the phenyl ether bond is quite strong appearing at 1236 cm^{-1}, while absorption peak of the alkyl ether bond absorption was observed at 1043 cm^{-1}.

The benzylic protons were situated at 5.25 ppm in the ^{1}H NMR spectrum of **L4** while the protons of the central core overlapped with the protons of the pyridyl ring at 7.78 ppm. The imine and pyridyl protons were observed at 8.62 ppm and 8.69 ppm respectively. The other aromatic protons were present between 7.04 ppm and 8.19 ppm. In the ^{13}C NMR spectrum, as shown in Figure 2-9, the benzylic carbon resonated at 67.9 ppm, as expected and as was found for the other ligands, the imine and pyridyl carbons gave peaks at 157.7 and 158.5 ppm. All the other aromatic carbons were observed between 115.4 ppm and 154.8 ppm.

Chapter 2: Synthesis and Characterization of Iminopyridyl Dendrimeric Ligands
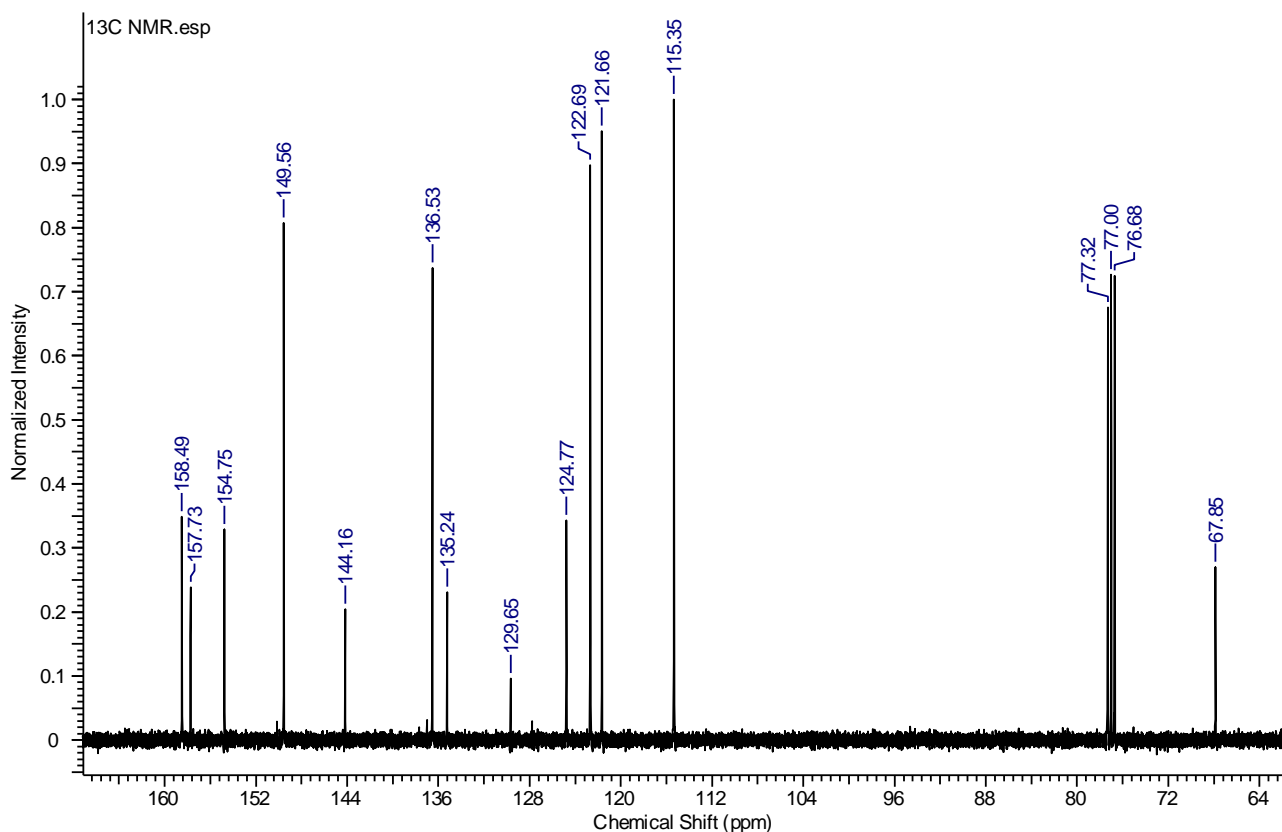
Figure 2-9: ¹³C NMR Spectrum of L4

Further characterization was carried out using high resolution ESI-MS. The molecular ion was observed at m/z 919.3744 which was assigned to the [M+H]$^+$ ion. Additionally, a doubly charged molecular ion was also observed at m/z 460.1895. The base peak was observed at m/z 830.3469. This fragment is due to the hydrolysis of one of the imine bonds with the loss of the pyridyl ring. Moreover, a doubly charged fragment is also present at m/z 415.6759. Lastly, another fragment at m/z 741.3191 is observed due to the cleavage of a second imine bond. Similarly for the others, a doubly charged fragment is observed at m/z 371.1627.

2.3   Conclusion

Four novel ligands (**L1**-**L4**) were prepared by a nucleophilic substitution reaction between 4-{[pyridin-2-ylmethylidene]amino}phenol and the appropriate core. These ligands were prepared in good to high yields and were found to be quite stable. The characterization of **L2** and **L4** was a bit more complicated due to the poor solubility properties of these ligands.

Furthermore, 4-{[pyridin-2-ylmethylidene]amino}phenol can also be utilized as a ligand forming mononuclear complexes.

33

Chapter 2: Synthesis and Characterization of Iminopyridyl Dendrimeric Ligands

2.4   Experimental Section

General Methods and Materials

All of the reagents were purchased from either Merck or Sigma Aldrich and were used without further purification. Solvents were purchased from Merck or Kimix, and were dried by conventional distillation, solvent purifiers or simple storing over molecular sieves.

All reactions were performed in round-bottom flasks under a stream of N_2 gas.

FTIR spectra were recorded on a Thermo Nicolet Avatar 330 FTIR spectrometer equipped with a Smart performer (Zn/Se) ATR attachment. NMR spectra were recorded on a Varian Unity Inova NMR Spectrometer (300, 400 and 600 MHz). ESI mass spectra were obtained using a Waters Synapt G2 spectrometer. Elemental analysis were performed at the University of Cape-Town.

Synthesis of 4-{[pyridin-2-ylmethylidene]amino}phenol

Pyridine-2-carbaldehyde (1.126 g, 10.51 mmol) and p-aminophenol (1.147 g, 10.51 mmol) were added into 20 ml of MeOH forming a dark blackish mixture which turned yellow after about 1 min. The resulting solution was stirred under reflux for 4 h. The mixture was cooled to room temperature and the pure solid product was obtained immediately by filtration (2.02 g, 97 %). IR (ATR) υ (C=N) 1622, 1579 cm^{-1} (pyridyl); ^{1}H NMR (300 MHz, DMSO-d6) δ_H : 6.84 (m, 2 H, Ar-**H**), 7.31 (m, 2 H, Ar-**H**), 7.48 (ddd, J = 7.5, 4.8, 1.2 Hz, 1 H, pyr-**H**), 7.92 (m, 1 H, pyr-**H**), 8.10 (dt, J = 7.9, 1 Hz, 1 H, pyr-**H**), 8.60 (s, 1 H, C**H**=N), 8.68 (m, 1 H, pyr-**H**); ^{13}C NMR (75 MHz, DMSO-d6) δ_C : 115.6, 120.4, 122.7, 124.8, 136.6, 141.2, 149.3, 154.3, 156.7, 156.8 ppm.

Synthesis of L1

A three-neck round-bottom flask was charged with 4-[(pyridine-2-ylmethylene)amino]phenol (108 mg, 0.54 mmol), K_2CO_3 (178 mg, 1.29 mmol), benzyl bromide (65 μl, 93 mg, 0.54 mmol) and acetone (20 ml) forming a yellow suspension which formed a yellow solution upon heating. The resulting mixture was stirred at reflux under a nitrogen atmosphere for 18h, and then allowed to cool to room temperature. After the 18 h period, the solution was brown with an off-white precipitate (salt). It was filtered and the solvent was removed from the filtrate using a rotary evaporator. The product was obtained as a brown solid after recrystallization from DCM:Et$_2$O (0.13 g, 83 %). Mp = 109 – 111 °C; IR (ATR) υ (C=N)

Chapter 2: Synthesis and Characterization of Iminopyridyl Dendrimeric Ligands

1621, 1574 cm^{-1}; ^{1}H NMR (600 MHz, CDCl$_3$) δ_H: 5.11 (s, 2 H, C**H$_2$**-O), 7.04 (d, J = 8.2 Hz, 2 H, Ar-**H**), 7.35 (comp, 4 H, pyr-**H** and *core*), 7.41 (t, J = 7.6 Hz, 2 H, *core*), 7.46 (m, 2 H, Ar-**H**), 7.81 (m, 1 H, pyr-**H**), 8.20 (d, J = 7.6 Hz, 1 H, pyr-**H**), 8.65 (s, 1 H, -C**H**=N-), 8.71 (d, J = 4.7 Hz, 1 H, pyr-**H**)); ^{13}C NMR (101 MHz, CDCl$_3$) δ_C: 70.6, 115.7, 116.5, 122.0, 123.0, 125.1, 127.8, 128.3, 128.9, 137.0, 144.2, 149.9, 155.1, 158.4, 158.6 ppm; ESI-MS: $C_{13}H_{16}N_2O$ (288.34); m/z 200.1 $[C_{13}H_{13}NO]^+$. Elemental analysis $7C_{13}H_{16}N_2O.CH_2Cl_2$: C_{cal} = 76.52 %; C_{exp} = 76.49; H_{cal} = 5.51; H_{exp} = 5.46; N_{cal} = 9.58; N_{exp} = 9.32.

Synthesis of L2

A three-neck round-bottom flask was charged with 4-[(pyridine-2-ylmethylene)amino]phenol (160 mg, 0.81 mmol), K$_2$CO$_3$ (220 mg, 1.6 mmol), 1,4-bis(bromomethyl)benzene (100 mg, 0.38 mmol) and acetone (20 ml) forming a yellow suspension which formed a yellow solution upon heating. The resulting mixture was stirred under reflux under a nitrogen atmosphere for 18h, and then cooled to room temperature. After the 18 h period, the solution was brown with an off-white precipitate (the product). After filtration, the off-white precipitate was washed with water to remove any potassium salt and the crude product recrystallized from hot chloroform (0.134 g, 71 %). Mp = 216 – 218 °C; IR (ATR) v (C=N) 1622, 1576 cm^{-1}; ^{1}H NMR (600 MHz, CDCl$_3$) δ_H: 5.08 (s, 4 H, -C**H$_2$**-O-), 7.00 (d, J = 8.8 Hz, 4 H, Ar-**H**), 7.31 (comp, 5 H, pyr-**H** and Ar-**H**), 7.45 (s, 4 H, *core*), 7.76 (m, 2 H, pyr-**H**), 8.16 (d, J = 7.6 Hz, 2 H, pyr-**H**), 8.60 (s, 2 H, -C**H**=N-), 8.67 (d, J = 4.7 Hz, 2 H, pyr-**H**)); ^{13}C NMR (151 MHz, CDCl$_3$) δ_C: 69.9, 115.4, 121.6, 122.7, 124.8, 127.7, 136.6, 136.7, 143.9, 149.6, 154.8, 158.0, 158.4 ppm; ESI-MS: $C_{32}H_{26}N_4O_2$ (498.57); m/z 499.2 $[M+H]^+$; m/z 410.2 $[C_{26}H_{24}N_3O_2]^+$. Elemental analysis $4C_{32}H_{26}N_4O_2.C_3H_6O$: C_{cal} = 76.66; C_{exp} = 76.21; H_{cal} = 5.40; H_{exp} = 5.17; N_{cal} = 10.92; N_{exp} = 11.30.

Synthesis of L3

A three-neck round-bottom flask was charged with 4-[(pyridine-2-ylmethylene)amino]phenol (300 mg, 1.52 mmol), K$_2$CO$_3$ (404 mg, 2.92mmol), 1,3,5-Tris(bromomethyl)benzene (167 mg, 0.47 mmol) and acetone (20 ml) forming a yellow suspension which formed a clear solution upon heating. The resulting mixture was stirred under reflux under a nitrogen atmosphere for 18h, and then cooled to room temperature. After the 18 h period, the solution was brown with an off-white precipitate (salt). It was filtered and the solvent was removed using a rotary evaporator. The product was obtained as a brown solid which was recrystallized from DCM:Et$_2$O (0.299 g, 90 %). Mp = 178 – 179 °C; IR (ATR) v (C=N) 1623

Chapter 2: Synthesis and Characterization of Iminopyridyl Dendrimeric Ligands

(C=N), 1577 cm^{-1}; ^{1}H NMR (300 MHz, CDCl$_3$) δ_H : 5.15 (s, 6 H, -C**H$_2$**-O-), 7.05 (m, 6 H, Ar-**H**), 7.35 (comp, 9 H, pyr-**H** and Ar-**H**), 7.52 (s, 3 H, *core*), 7.80 (m, 3 H, pyr-**H**), 8.20 (dt, J = 7.9, 1.1 Hz, 3 H, pyr-**H**), 8.63 (s, 3 H, -C**H**=N-), 8.70 (m, 3 H, pyr-**H**); ^{13}C NMR (75 MHz, CDCl$_3$) δ_C : 69.9, 115.4, 121.7, 122.7, 124.8, 126.0, 136.6, 137.8, 144.0, 149.6, 154.8, 157.9, 158.4 ppm; ESI-MS: C$_{45}$H$_{36}$N$_6$O$_3$ (708.82); m/z 709.3 [M+H]$^+$; m/z 620.3 [C$_{39}$H$_{34}$H$_6$O$_3$]$^+$; m/z 531.2 [C$_{33}$H$_{31}$N$_4$O$_3$]$^+$; m/z 355.1 [M+2H]$^{2+}$; m/z 237.1 [M+3H]$^{3+}$. Elemental analysis 4C$_{45}$H$_{36}$N$_6$O$_3$.CH$_2$Cl$_2$: C$_{cal}$ = 74.45; C$_{exp}$ = 74.38; H$_{cal}$ = 5.04; H$_{exp}$ = 4.91; N$_{cal}$ = 11.51; N$_{exp}$ = 11.90.

Synthesis of L4

A three-neck round-bottom flask was charged with 4-[(pyridine-2-ylmethylene)amino]phenol (184 mg, 1.27 mmol), K$_2$CO$_3$ (246 mg, 2.66 mmol), 1,2,4,5-tetrakis(bromomethyl) benzene (100 mg, 0.32 mmol) and acetone (20 ml). The resulting yellow suspension was stirred under reflux under a nitrogen atmosphere for 18 h, and then cooled to room temperature and filtered. After the 18 h period, the solution was brown with an off-white precipitate (the product). After filtration, the off-white precipitate was suspended in water to remove any potassium salt and the product recrystallized from hot chloroform (0.137 g, 67 %). Mp = 187 – 188.0 °C; IR (ATR) υ (C=N) 1626, 1579 cm^{-1}; ^{1}H NMR (300 MHz, CDCl$_3$) δ_H : 5.25 (s, 8 H, -C**H$_2$**-O-), 7.02 (m, 8 H, Ar-**H**), 7.33 (comp, 12 H, pyr-**H** and Ar-**H**), 7.77 (comp, 6 H, pyr-**H** and *core*), 8.17 (d, *J* = 7.9 Hz, 4 H, pyr-**H**), 8.63 (s, 4 H, -C**H**=N-), 8.69 (m, 4 H, pyr-**H**); ^{13}C NMR (101 MHz, CDCl$_3$) δ_C : 67.9, 115.4, 121.7, 122.7, 124.8, 129.7, 135.2, 136.5, 144.2, 149.6, 154.8, 157.7, 158.5 ppm; ESI-MS: C$_{58}$H$_{46}$N$_8$O$_4$ (919.04); m/z 919.3744 [M+H]$^+$; m/z 830.3469 [C$_{52}$H$_{44}$N$_7$O$_4$]$^+$; m/z 741.3191 [C$_{46}$H$_{41}$N$_6$O$_4$]$^+$; m/z 460.1895 [M+2H]$^{2+}$. Elemental analysis C$_{58}$H$_{46}$N$_8$O$_4$.2H$_2$O: C$_{cal}$ = 72.94; C$_{exp}$ = 72.73; H$_{cal}$ = 5.28; H$_{exp}$ = 4.77; N$_{cal}$ = 11.73; N$_{exp}$ = 11.51.

2.5   References

1. P. R. Ashton, K. Shibata, A. N. Shipway and J. F. Stoddart, *Angew. Chem. Int. Ed. Engl*., 1997, **36**, 2781-2783.

2. B. C. Roy, A. Fazal, S. Sun and S. Mallik, *Chem. Commun*., 2000, 547-548.

3. G. L. Balaji, K. Rajesh, M. Venkatesh, S. Sarveswari and V. Vijayakumar, *RSC Adv*., 2014, **4**, 39-46.

4. M. Lee, H. Zali-Boeini, F. Li, L. F. Lindoy, and K. A. Jolliffe, *Tetrahedron*, 2013, **69**, 38-42.

5. D. Soto-Castro, N. E. Magaña-Vergara, N. Farfán and R. Santillan, *Tetrahedron Lett.*, 2014, **55**, 1014-1019.

6. M. Maheshwari, S. Khan and J. D. Singh, *Tetrahedron Lett.*, 2007, **48**, 4737-4741.

7. C. J. Hawker and J. M. J. Fréchet, *J. Am. Chem. Soc.*, 1990, **112**, 7638-7647.

8. A. F. A. Peacock, A. Habtemariam, S. A. Moggach, A. Prescimone, S. Parsons and P. J. Sadler, *Inorg. Chem.*, 2007, **46**, 4049-4059.

9. P. Govender, A. K. Renfrew, C. M. Clavel, P. J. Dyson, B. Therrien and G. S. Smith, *Dalton Trans.*, 2011, **40**, 1158-1167.

10. S. Taubmann and H. G. Alt, *J. Mol. Catal. A: Chem.*, 2008, **284**, 134-140.

11. A. Ros, B. Estepa, R. López-Rodríguez, E. Álvarez, R. Fernández and J. M. Lassaletta, *Angew. Chem. Int. Ed.*, 2011, **50**, 11724-11728.

12. S. Nayab, H. Lee and J. H. Jeong, *Polyhedron*, 2012, **43**, 55-62.

13. A. A. Tregubov, K. Q. Vuong, E. Luais, J. J. Gooding and B. A. Messerle, *J. Am. Chem. Soc.*, 2013, **135**, 16429-16437.

14. K. Heinze and V. Jacob, *J. Chem. Soc., Dalton Trans.*, 2002, 2379-2385.

15. K. Heinze and J. D. Bueno Toro, *Eur. J. Inorg. Chem.*, 2004, 3498-3507.

16. K. Heinze, *Chem. Eur. J.* 2001, **7**, 2922-2932.

17. K. Chanawanno, J. T. Engle, K. X. Le, R. S. Herrick and C. J. Ziegler, *Dalton Trans.*, 2013, **42**, 13679-13684.

18. M. Di Serio, G. Carotenuto, M. E. Cucciolito, M. Lega, F. Ruffo, R. Tesser and M. Trifuoggi, *J. Mol. Catal. A: Chem.*, 2012, **353**-**354**, 106-110.

19. Q. Zhang, H. Su, J. Luo and Y. Wei, *Catal. Sci. Technol.*, 2013, **3**, 235-243.

Chapter 3 : Synthesis and Characterization of Ru(II) and Rh(I) Mononuclear and Multi-nuclear Complexes

3.1 Introduction

Since the first synthesis of dendrimers in 1985 by the group of Tomalia[1], quite a considerable number of reports has been published on the subject.[2-6] Dendrimers possesses distinct properties and therefore find wide application in various fields. They find specific application in medicine[7-9] and catalysis[10-12]. The application in catalysis is due to the fact that they are capable of coordinating multiple metal ions. This, in turn, can enhance catalytic activity compared to analogous mononuclear complexes.[13-16] In addition, dendrimers can also create the possibility of separating the catalyst from the reaction mixture at the completion of the reaction.[17-18]

3.2 Ruthenium Metallodendrimers

In chapter 2, the synthesis and characterization of various iminopyridyl ligands, ranging from mono- to tetra-functional, were discussed. In this chapter, we will describe the complexation of these ligands to both ruthenium and rhodium metals. The complexation was performed in dichloromethane, forming complexes bearing chloride as counter-ion. Subsequent salt metathesis reactions using $NaBPh_4$ in methanol, resulted in the chloride being substituted by $[BPh_4]^-$. These complexes were then characterized using IR and NMR spectroscopy, mass spectrometry, elemental analysis and melting point determinations.

Ruthenium metallodendrimer complexes find wide application in catalysis and medicine. In a paper published by Paira and co-workers[19] on the development of ruthenium quinolinol based complexes, for evaluation of their antibacterial activity, they discussed a few factors which contributes to the usefulness of ruthenium in medicinal applications. The most important factors are the ability of ruthenium to access a wide range of oxidation states. Also, the solubility of the complexes can be determined by the nature of the counter ion present. This also has an effect on the stability of the complex in a biological environment. Furthermore, ruthenium has the ability to mimic iron in its coordination to certain biological molecules.

The anticancer activity of multinuclear ruthenium arene complexes, based on dendritic polypyridyl scaffolds, have been investigated by Smith and co-workers.[20] Two types of

Chapter 3: Synthesis and Characterization of Ru(II) and Rh(I) Mononuclear and Multi-nuclear Complexes

arenes were investigated (p-cymene and hexamethylbenzene) and both generation 1 (G1) and 2 (G2) were prepared. The 'enhanced permeability and retention' (EPR) effect was exploited which allows large molecules to enter and accumulate in cancerous cells. Related mononuclear complexes were also prepared in order to model the dendritic complexes. After successful preparation and characterization of all complexes, the anticancer activity against A2780 ovarian cancer cell line was evaluated. All the complexes displayed only moderate anti-proliferative activity against A2780 ovarian cancer. Furthermore, the G2 ruthenium metallodendrimers were more active than the G1 metallodendrimers, owing to the larger size. The analogous mononuclear complexes were the least active.
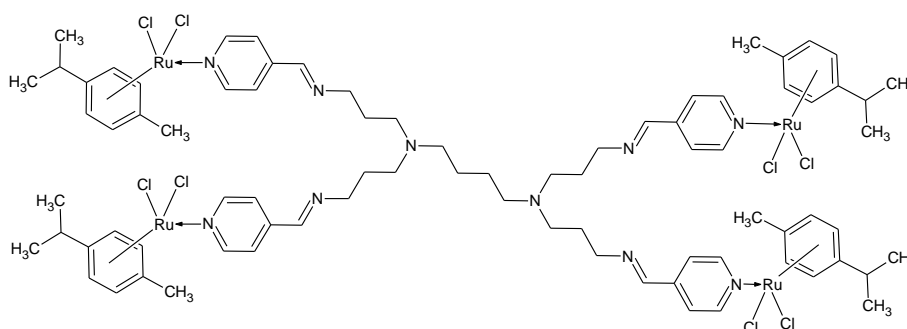
Figure 3-1: G1 Ru Metallodendrimer prepared by Smith and co-workers[20]

Therrien and co-workers[21] also investigated the anticancer activity of ruthenium complexes against A2780 (cisplatin sensitive) ovarian cancer cell line and A2780cisR (acquired resistance to cisplatin). They investigated three generations of pyrenyl bis-MPA (poly(2,2-bis(hydroxymethyl)-propionic acids) dendrimers with either acetonide or alcohols as end-groups. The hydrophobic pyrenyl groups of the dendrimers are encapsulated into the hydrophobic cavity of the arene ruthenium metallacages thereby forming host-guest systems. The dendrimers bearing the alcohol terminal groups were more cytotoxic than the acetonide derivatives due to increased solubility in the culture medium. Furthermore, it was also found that the host-guest systems were more cytotoxic than the individual host and guest system alone.

N-Heterocyclic carbene ligands bearing G0 – G2 dendritic moieties were prepared with a Ru(II) metal centre at the core.[22] The metallodendrimers were utilized in the ring closing metathesis of 4,4-diethoxycarbonyl-1,7-octadiene, with the activity compared to the Grubbs-Hoveyda catalyst. At room temperature, the activity of all the catalysts were above 90 %, irrespective of the generation of the dendrimer. When the reaction was performed at -30 °C,

Chapter 3: Synthesis and Characterization of Ru(II) and Rh(I) Mononuclear and Multi-nuclear Complexes

the activity of the catalysts decreased with increasing generation. However, the activities were higher than the Grubbs-Hoveyda catalyst.

Li and co-workers[23] investigated the role of three generations of fluorinated dendrimers in the asymmetric transfer hydrogenation of acetophenone. Figure 3-2 shows a G2 dendrimer prepared by this group, with a Ru(II) coordinated to the diamine moieties at the core of the dendrimer. All these dendrimers thus contained one metal centre at the core. All three generations of catalysts displayed high catalytic activity, however, activity decreased with increasing generation, which was ascribed to steric hindrance. All the catalysts could be recycled, with the Ru-G-2-F metallodendrimer recycled and re-used 26 times, with no significant drop in activity or enantioselectivity.
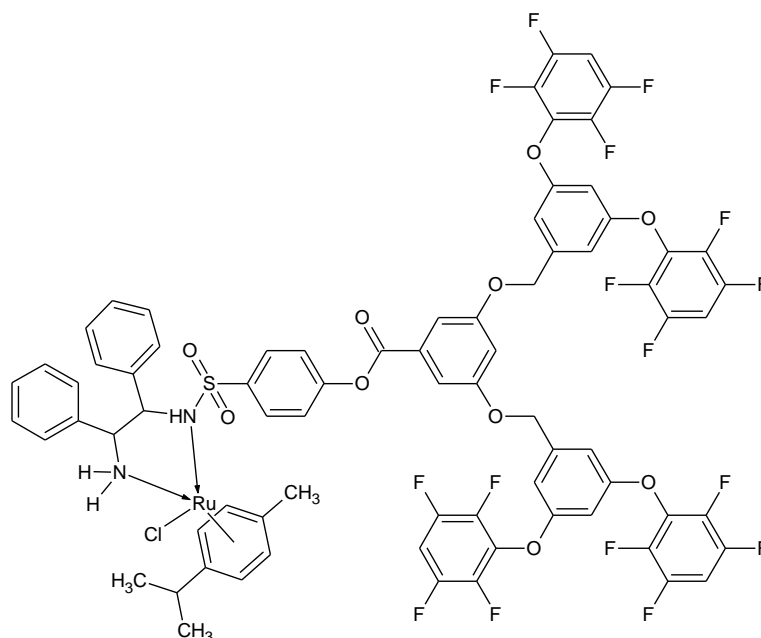
Figure 3-2: A G2 Fluorinated Ru Metallodendrimer[23]

3.2.1 Synthesis and characterization of Ru(II) arene complexes

Ruthenium arene complexes are widespread in literature and it is specifically common when ruthenium is in the +2 oxidation state. This stems from the fact that the arene ring is able to stabilize the ruthenium centre in its +2 oxidation state.[24] These ruthenium complexes also exhibit cytotoxicity and as a result is commonly utilized in ruthenium based drugs as shown in the examples above. We made use of the $[RuCl_2(p\text{-cymene})]_2$ precursor in order to prepare our complexes. This precursor was prepared according to a literature procedure[25] which entails the reaction between $RuCl_3 \cdot xH_2O$ and α-phellandrene in ethanol.

Chapter 3: Synthesis and Characterization of Ru(II) and Rh(I) Mononuclear and Multi-nuclear Complexes

Five novel Ru(II) complexes, ranging from mono- to tetra-nuclear, were synthesized and characterized. The complexation of the ligands to the ruthenium precursor were performed in DCM, while the salt metathesis was carried out in MeOH. All these complexes precipitated out of the MeOH as stable orange-yellow solids, in moderate to high yields (67 – 90 %).
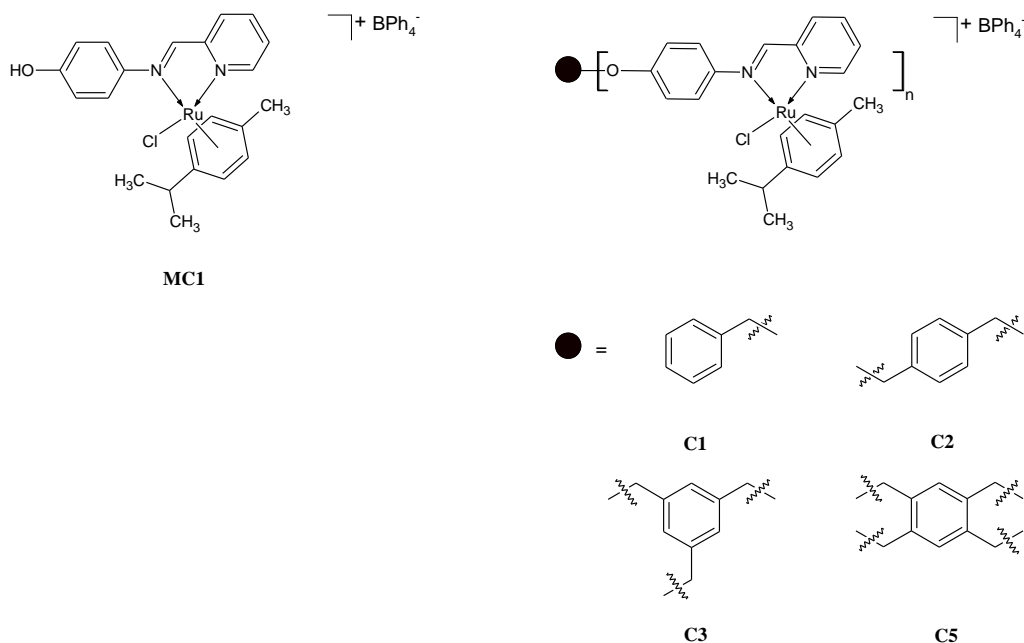
Figure 3-3: Novel Ru(II) arene complexes

The FTIR, ^{1}H NMR and ^{13}C NMR spectra of all complexes are fairly similar and as such the discussion will be limited to the tri-nuclear metallodendrimer, **C3**.

3.2.1.1 Tri-nuclear Iminopyridyl Ru(II) arene complex (C3)

The tri-nuclear Ru(II) arene complex (**C3**) was prepared using **L3** as ligand and the [RuCl$_2$(p-cymene)]$_2$ dimer. **C3** was isolated as a stable yellow-orange solid in 67 % yield. This complex is soluble in dimethyl sulfoxide, while it is partly soluble in acetonitrile and acetone. It decomposes in the temperature range 152 °C – 153 °C.

41

Chapter 3: Synthesis and Characterization of Ru(II) and Rh(I) Mononuclear and Multi-nuclear Complexes
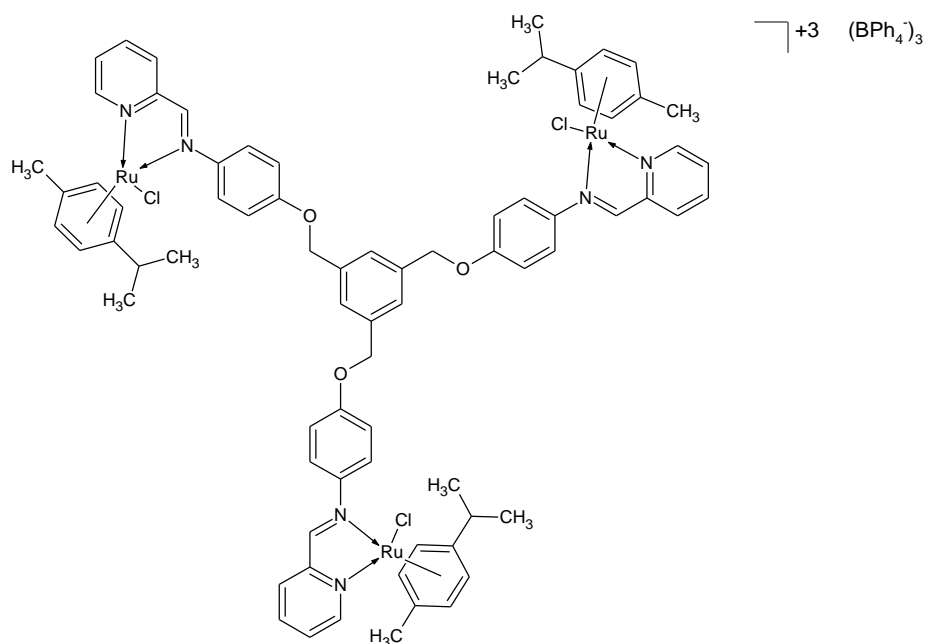
Figure 3-4: Tri-nuclear Ru(II) arene complex

Full characterization of **C3** was then carried using a range of analytical techniques. The free imine and pyridyl imine moieties were complexed to the ruthenium metal, therefore changes in the IR absorbances of these moieties were monitored.
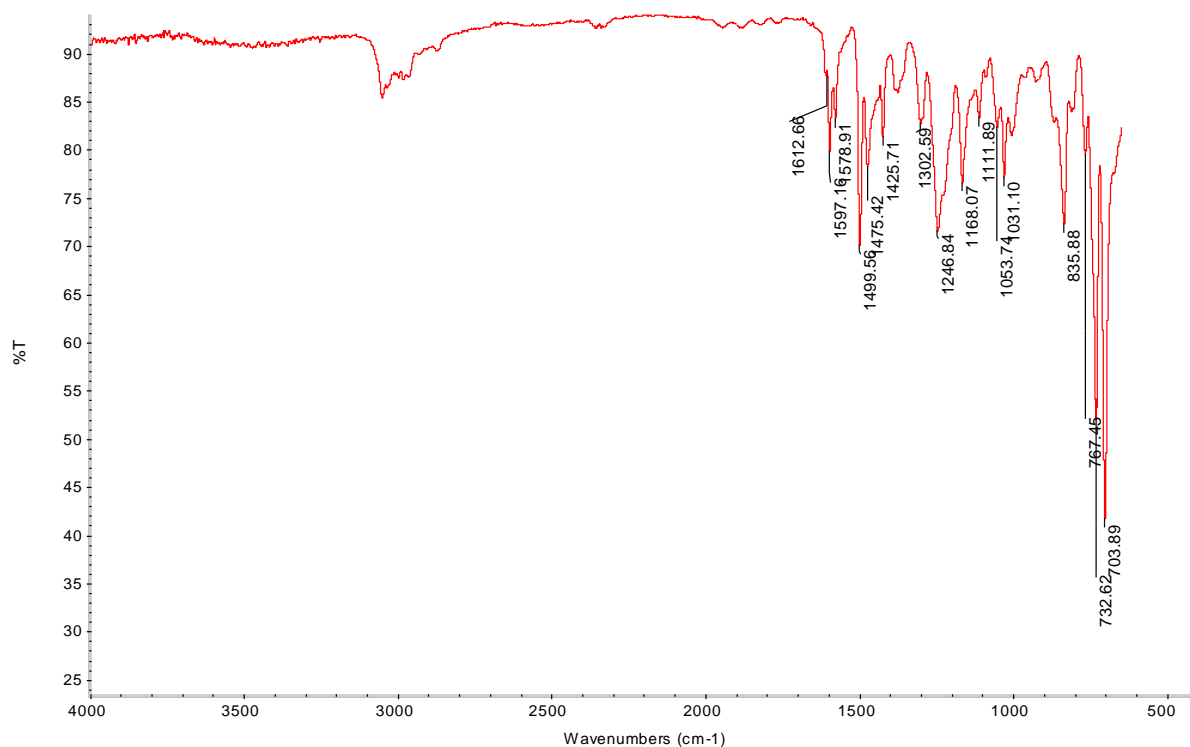
Figure 3-5: IR spectrum of C3

Chapter 3: Synthesis and Characterization of Ru(II) and Rh(I) Mononuclear and Multi-nuclear Complexes

In the IR spectrum of the ligand, **L3**, the imine and pyridyl imine absorbances were observed at 1624 cm^{-1} and 1576 cm^{-1} respectively. In the complex, **C3**, the imine shifted to a lower wavenumber (1613 cm^{-1}) while the pyridyl imine shifted to a higher wavenumber (1597 cm^{-1}). This indicated successful complex formation. The strong absorbances for the [BPh$_4$]$^-$ were also observed at 703 cm^{-1} and 733 cm^{-1}.

Further characterization was carried out using ^{1}H NMR spectroscopy. Similarly, changes in the chemical shifts of the imine and pyridyl imine moieties were monitored.
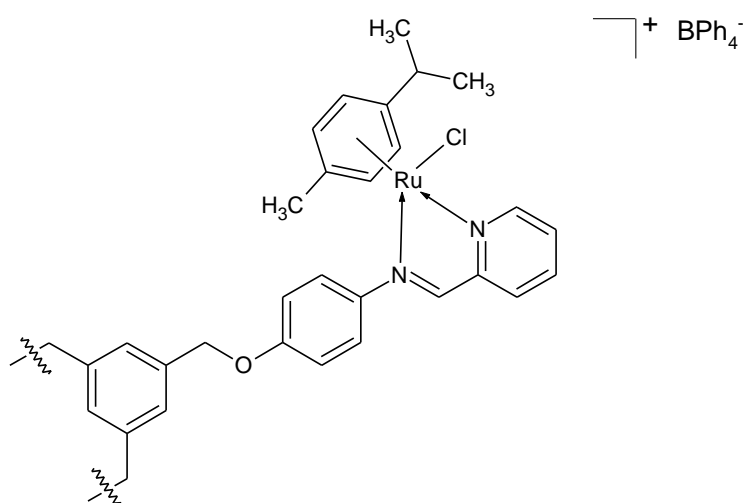
Figure 3-6: C3 wedge

For the ligand, the imine and pyridyl imine shifts occurred at 8.63 and 8.70 ppm respectively. In the complex, the imine proton shifted slightly downfield to 8.81 ppm, while a more significant downfield shift was observed for the pyridyl imine proton to 9.53 ppm. These shifts confirmed successful coordination of the imine moieties to the ruthenium centre. No uncoordinated imine (free or pyridyl) moieties were observed, which confirmed that the metal coordinated at all three *N, N* sites. The protons of the aromatic core was situated at 7.64 ppm, integrating for the expected three protons. The rest of the aromatic protons can be observed between 7.27 – 8.23 ppm, which also includes the remaining protons of the pyridyl ring. Furthermore, the protons of the [BPh$_4$]$^-$ counter-ion resulted in three peaks situated at 6.76, 6.90 and 7.16 ppm. The aromatic protons of the p-cymene ring can be seen as four peaks at 5.57, 5.76, 5.79 and 6.06 ppm. The methyl group was observed as a singlet at 2.14 ppm, while the two methyl groups of the isopropyl group is seen as a doublet at 0.96 ppm. The methine group of the isopropyl group was situated below the solvent peak. Moreover, the benzylic protons were situated at 5.28 ppm.

Chapter 3: Synthesis and Characterization of Ru(II) and Rh(I) Mononuclear and Multi-nuclear Complexes

Characterization of **C3** was also carried out using ^{13}C NMR spectroscopy. The imine shifted from 157.9 ppm in the ligand to 160.0 ppm in **C3**, while the pyridyl imine shifted to 166.8 ppm (158.4 ppm in **L3**). This is complimentary to the ^{1}H NMR spectrum, confirming successful coordination and complex formation. The other aromatic resonances, including those of the pyridyl ring, were observed between 116.0 – 156.6 ppm (10 resonances). Furthermore, the resonances of the [BPh$_4$]$^-$ counter-ion were present at 122.2, 124.9, 136.2 ppm, while there is coupling between the B-C bonds, resulting in a quartet between 163.3 – 164.8 ppm. Six resonances were observed for the aromatic carbons of the p-cymene ring, two peaks at 104.3 and 105.6 ppm, and the other four peaks between 85.4 – 87.2 ppm. The signal of the methyl group of the p-cymene ring resonated at 31.2 ppm, while the signal for methine group of the isopropyl group was seen at 19.0 ppm. The signal for the two methyl groups of the isopropyl group was seen as two peaks at 22.3 and 22.4 ppm. Lastly, the ether carbon was situated at 70.3 ppm.

Furthermore, in ESI-MS (positive mode), the triply charged molecular ion [M – 3BPh$_4$]$^{3+}$ was observed at m/z 507.1 (M_w = 1521.03 g/mol). The theoretical isotopic pattern and the experimental isotopic pattern corresponded to each other. In ESI-MS negative mode, an ion was observed at m/z 319.2, which is as a result of the [BPh$_4$]$^-$ counter-ion.
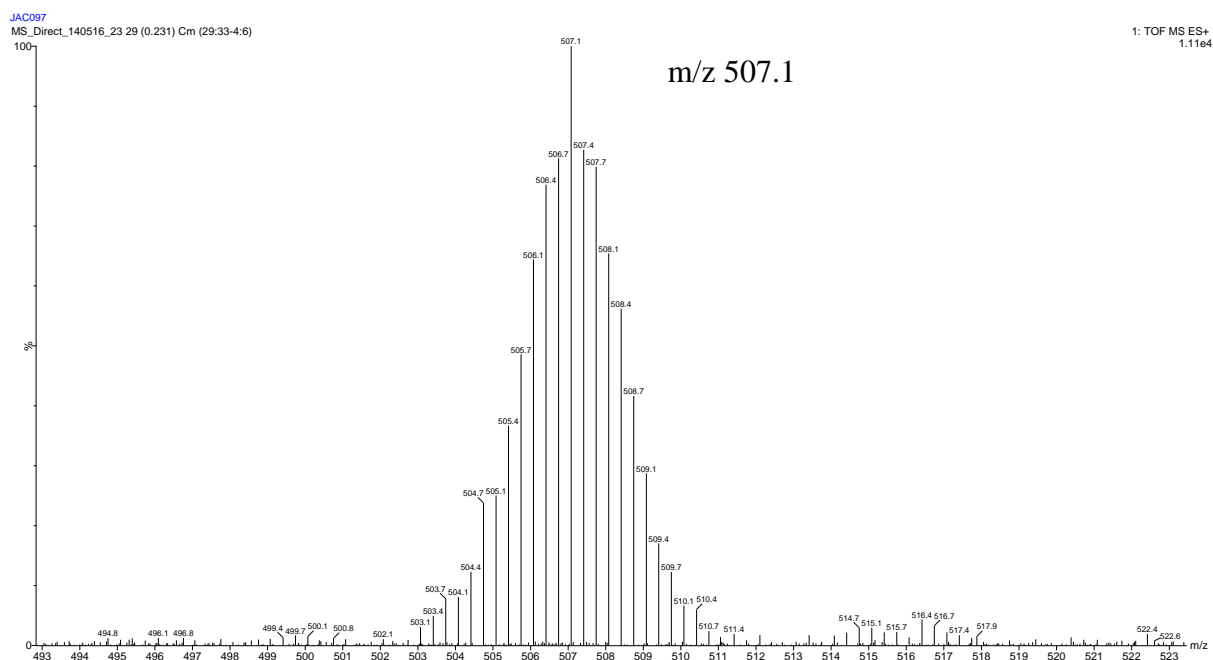
Figure 3-7: MS spectrum of C3

All these characterization data thus confirms the successful synthesis and characterization of **C3**.

Chapter 3: Synthesis and Characterization of Ru(II) and Rh(I) Mononuclear and Multi-nuclear Complexes

3.2.1.2 Characterization data of other Ru(II) complexes

Table 3-1 displays the decomposition temperatures of all the complexes. Furthermore, the molecular ions observed in ESI-MS (positive mode) for all the complexes is also given, confirming the successful preparation and characterization of the five novel Ru(II) complexes.

Table 3-1: Ru(II) arene complexes characterization data

Complex	Melting Points	ESI-MS
MC1	Decomposes T = 158 – 159 °C	m/z 469.1 Singly charged
C1	Decomposes T = 178 – 180 °C	m/z 559.1 Singly charged
C2	Decomposes T = 156 – 159 °C	m/z 520.1 Doubly charged
C3	Decomposes T = 152 – 153 °C	m/z 507.1 Triply charged
C5	Decomposes T = 164 – 166 °C	m/z 500.6 Quadruply charged

3.3   Rhodium Metallodendrimers

Rhodium metallodendrimers are also very common in literature, especially in catalysis. Caminade and co-workers[26] demonstrated the synthesis and characterization of dendrimers modified with PTA ligands on the periphery, in order to improve its solubility in water. Three different dendritic ligands were prepared, a G1 (denoted **1-G$_1$**) dendrimer and two G2 (denoted **1-G$_2$** and **6-G$_2$**) dendrimers, and complexed to rhodium and ruthenium. The rhodium metallodendrimers were utilized in the isomerization of allylic alcohols, however, none of the three metallodendrimers displayed significant activity. A highest conversion of 11 % was achieved with **1-G$_1$** as the ligand. This was subsequently attributed to the poor solubility of the complexes in water, with the solubility decreasing with increasing size. The hydration of alkynes (phenyl acetylene to acetophenone) were then investigated using the ruthenium metallodendrimers. The authors came to the conclusion that the density of the terminal groups determine the efficiency of the catalysts.

Rhodium metallodendrimers have also been used in the asymmetric hydrogenation of methyl 2-acetamidocinnamate.[27] The dendrimer ligand was based on the chiral BICOL backbone which was functionalized with two G3 carbosilane dendrimer wedges at the two carbazole nitrogens. Furthermore, the hydroxyl groups were converted to a phosphoramidite, creating coordinating sites for the rhodium metal.

45

Chapter 3: Synthesis and Characterization of Ru(II) and Rh(I) Mononuclear and Multi-nuclear Complexes
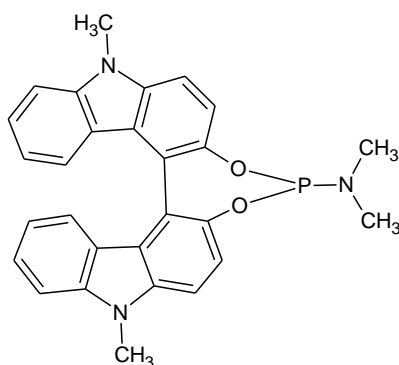
Figure 3-8: BICOL functionalized with phosphoramidite[27]

All the catalysts registered enantioselectivities above 90 % at full conversion.

Natarajan and Jayaraman[28] investigated the hydrogenation of styrene using a range of rhodium metallodendrimers, ranging from G0 – G3.
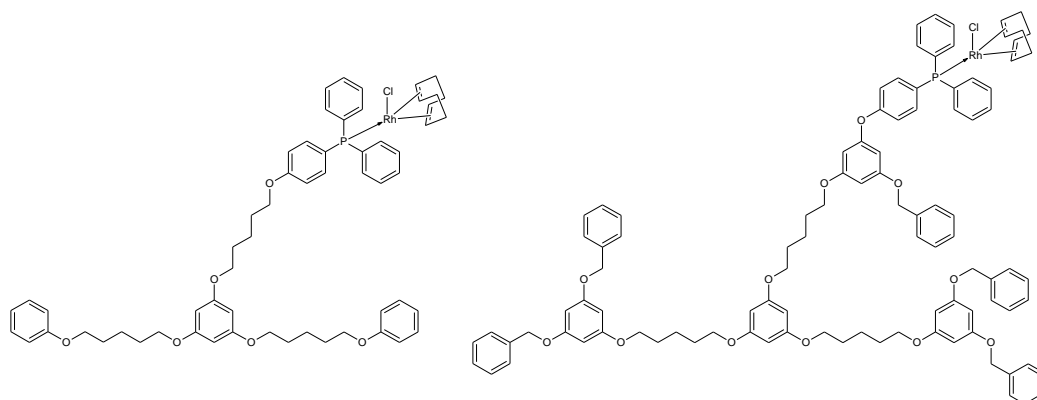
Figure 3-9: G0 (left) and G1 (right) mononuclear metallodendrimers[28]

Figure 3-9 shows a mononuclear G0 (**left**) and a mononuclear G1 (**right**) metallodendrimer. The authors also prepared mononuclear G2 and G3 metallodendrimers in order to investigate the influence of the dendrimer on the catalytic activity. What they observed was that the catalytic efficiency of the mononuclear complexes increases with generation, which they attributed to the growing dendrimer backbone. Furthermore, when analogous multi-nuclear complexes were prepared, these were more active than their mononuclear counterparts, possibly due to the increase in the local concentration of catalytic active sites.

3.3.1   Synthesis and characterization of Rh(I) complexes

Similar as the ruthenium metallodendrimers discussed above, the rhodium metallodendrimers were also prepared in dichloromethane. The [Rh(COD)Cl]$_2$ dimer, prepared according to a literature procedure[29], was dissolve in dichloromethane, forming a bright yellow solution.

46

Chapter 3: Synthesis and Characterization of Ru(II) and Rh(I) Mononuclear and Multi-nuclear Complexes

The ligands were then added as solids, and this resulted in an immediate colour change to a very dark green-brown solution. This solution was stirred for an hour at room temperature. After an hour, the solvent was removed and the resulting residue was dissolved in methanol forming a dark green-brown solution. NaBPh$_4$ was then added as a solid leading to the precipitation of a dark green-brown solid. This was allowed to stir for three hours at 0 °C.
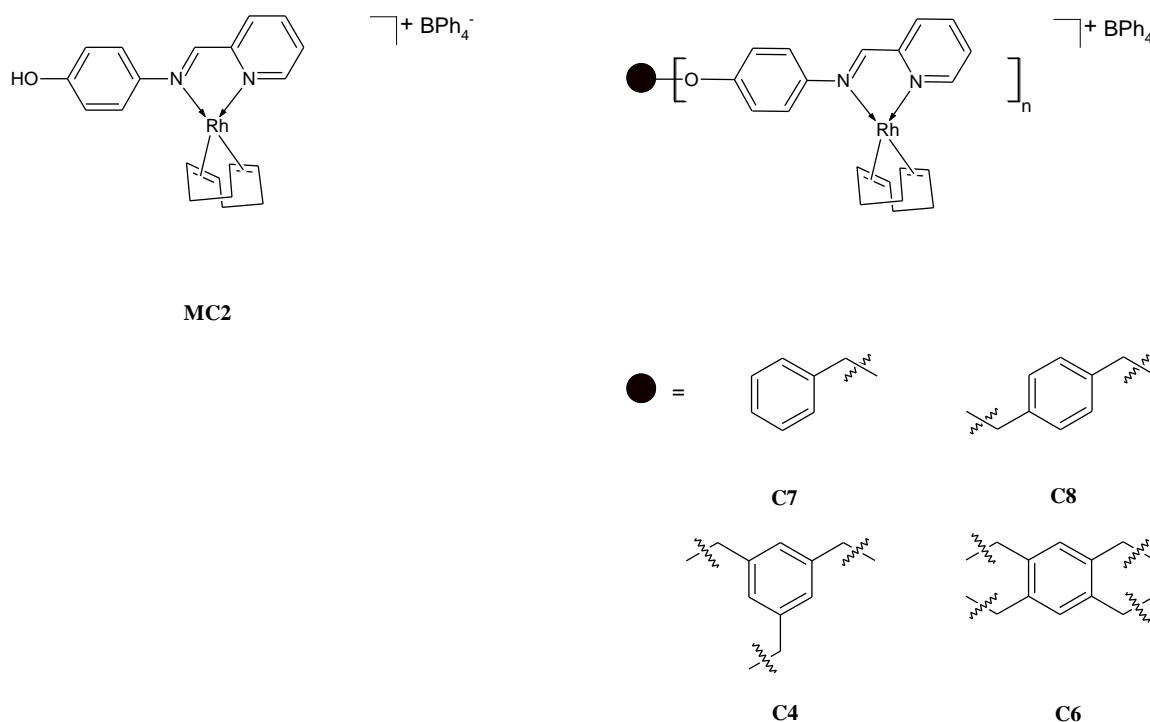
Figure 3-10: Novel Rh(I) complexes

The discussion will be limited to the binuclear complex, **C8**, since the IR, ^{1}H and ^{13}C NMR spectra of all the complexes looks fairly similar.

3.3.1.1 Bi-nuclear Iminopyridyl Rh(I) complex (C8)

The bi-nuclear complex, **C8**, was isolated as a green solid in 88 % yield. It decomposes between the temperature range 158 °C – 159 °C. It dissolves in dimethyl sulfoxide and partially in acetone and tetrahydrofuran.

Chapter 3: Synthesis and Characterization of Ru(II) and Rh(I) Mononuclear and Multi-nuclear Complexes
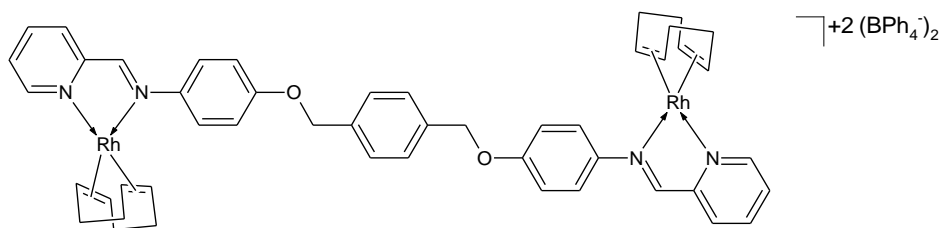
Figure 3-11: Bi-nuclear Rh(I) complex C8

Changes in the imine and pyridyl imine stretches were monitored using IR spectroscopy, in order to confirm successful complexation. The imine occurred at 1613 cm^{-1} (1623 cm^{-1} in **L2**) while the pyridyl imine occurred at 1597 cm^{-1} (1575 cm^{-1} in **L2**). These shifts indicates successful complex formation.

In ^{1}H NMR spectroscopy, a downfield shift was observed for the imine proton from 8.60 ppm in **L2**, to 8.66 ppm in **C8**. A significant upfield shift was observed for the pyridyl imine proton from 8.67 ppm in **L2**, to 8.12 ppm in **C8**. The aromatic protons of the benzene core was observed as a singlet at 7.52 ppm, while the remaining aromatic protons, including those of the pyridyl ring, was observed between 7.11 – 8.28 ppm. Furthermore, the [BPh$_4$]$^-$ counter-ion showed three peaks at 6.78, 6.93 and 7.19 ppm. The CH$_2$-O protons resulted in a peak at 5.14 ppm. Lastly, the protons of the cyclooctadiene (COD) ring gave three peaks at 1.93, 2.41 and 4.25 ppm. This data, together with the integration of all peaks, confirmed the identity of the complex.

Further confirmation of the identity of the complex was carried out using ^{13}C NMR spectroscopy. The imine carbon shifted slightly to 158.0 ppm (158.0 ppm in **L2**), while a more significant shift was observed for the pyridyl imine carbon to 172.0 ppm (158.4 in **L2**). The other aromatic carbons resonated between 115.2 – 154.7 ppm (10 resonances). The resonances of the [BPh$_4$]$^-$ counter-ion is visible at 121.5, 125.3, 135.6 and the four inequivalent B-C resonances between 162.4 – 164.4 ppm. The peaks for the carbon atoms of the COD ligand were observed at 29.9, 84.5 and 84.7 ppm. Lastly, the ether carbon was seen at 69.4 ppm.

Furthermore, the complex was also analysed using ESI-MS in the positive mode. The doubly charged molecular ion, [M – 2BPh$_4$]$^{2+}$, was observed at m/z 460.1. However, the abundance of the molecular ion was quite low, owing to the fact that the base peak occurred at m/z 252.02. This ion at m/z 252.02 corresponds to [Rh(COD)(MeCN)] (acetonitrile was used during the analysis). The [RhCOD] ion can also be seen at m/z 211, while the

48

Chapter 3: Synthesis and Characterization of Ru(II) and Rh(I) Mononuclear and Multi-nuclear Complexes

[Rh(COD)(MeCN)$_2$] ion is present at m/z 293.05. Thus, under ESI-MS conditions, the ligand dissociates from the metal, leading to the coordination of acetonitrile to the rhodium metal centre, and these species dominates the MS spectrum.
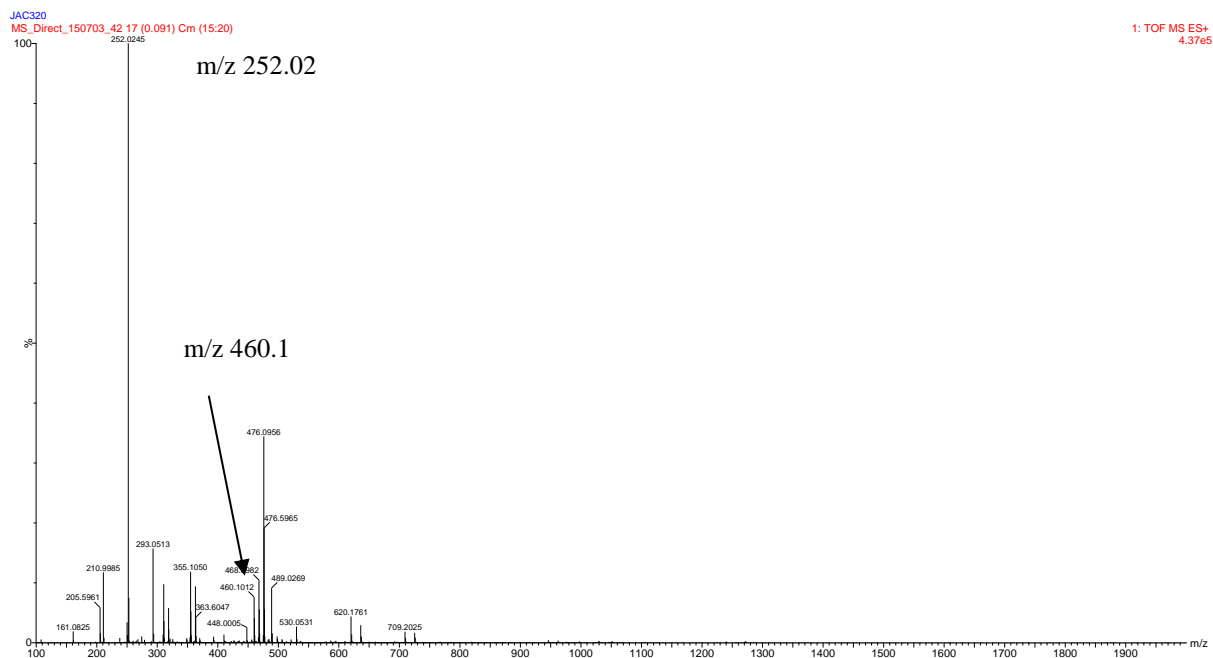
Figure 3-12: MS spectrum of C8

This data thus confirms the successful synthesis and characterization of **C8**.

3.3.1.2 Characterization data of other Rh(I) complexes

The melting points and decomposition temperatures of the other complexes are shown in Table 3-2. The table also shows the ions in the ESI-MS spectra of these complexes. For **C4** and **C6**, the molecular ions were not observed. The base peak in the mass spectra of these complexes were situated at m/z 252. This ion was identified as [Rh(COD)(MeCN)], as was also observed for **C8** above.

Table 3-2: Rh(I) complexes characterization data

Complex	Melting Point	ESI-MS
MC2	Melts T = 146 – 148 °C	m/z 409.1 Singly charged
C7	Melts T = 172 – 174 °C	m/z 499.1 Singly charged
C8	Decomposes T = 158 – 159.0 °C	m/z 460.1 Doubly charged
C4	Decomposes T = 156 – 157 °C	Not observed
C6	Decomposes T = 163 – 164 °C	Not observed

3.4   Conclusion

Ten novel Rh(I) and Ru(II) iminopyridyl complexes, ranging from mono- to tetra-nuclear, were successfully synthesized and characterized using a range of analytical techniques. The Rh(I) complexes were isolated as dark green-brown solids. The NMR characterization of the tri-nuclear (**C4**) and tetra-nuclear complexes (**C5**) proved more difficult. This was due to the presence of the counter-ions, resulting in very small resonances for the other protons and carbons. The Ru(II) complexes were isolated as orange-yellow solids. All these complexes have been isolated in moderate to high yields.

3.5   Experimental Section

General Methods and Materials

All of the reagents were purchased from either Merck or Sigma Aldrich and were used without further purification. Solvents were purchased from Merck or Kimix, and were dried by distillation, solvent purifiers or over molecular sieves (acetone, dichloromethane, diethylether, chloroform and methanol).

All reactions were performed using standard Schlenk techniques under a stream of N_2 gas.

FTIR spectra were recorded on a Thermo Nicolet Avatar 330 FTIR Spectrometer equipped with a Smart performer (Zn/Se) ATR attachment. NMR spectra were recorded on a Varian Unity Inova NMR Spectrometer (300, 400 and 600 MHz). Mass Spectra were obtained by analysis on a Waters Synapt G2 Spectrometer. Elemental analysis was performed at the University of Cape Town. A Stuart Scientific melting point apparatus SMP3 was used for determination of melting points.

Chapter 3: Synthesis and Characterization of Ru(II) and Rh(I) Mononuclear and Multi-nuclear Complexes

Synthesis of MC1

The [RuCl$_2$(p-cymene)]$_2$ dimer (60 mg, 0.098 mmol) was dissolved in DCM (5 ml) forming a dark red solution. 4-{[pyridin-2-ylmethylidene]amino}phenol (39 mg, 0.197 mmol) was added as a solid to the stirring solution of the dimer. After a few minutes, the dark red solution turned orange-yellow. This solution was stirred at room temperature for 1 h leading to the precipitation of an orange-yellow solid. The solvent was then removed and the solid was dissolved in MeOH (5 ml) forming an orange-yellow solution. Sodium tetraphenylborate (67 mg, 0.197 mmol) was then added as a solid and this was stirred for 3 h at 0 °C. During this time, an orange-yellow solid precipitated out of the MeOH solution. It was filtered and washed extensively with MeOH followed by a 2:1 MeOH:H$_2$O solution after which the product was isolated as a orange-yellow solid (0.117 g, 76 %). Decomposition Temperature: 158 – 159 °; IR (ATR) υ (C=N) 1613, 1593 cm^{-1}; ^{1}H NMR (300 MHz, DMSO-d$_6$) δ$_H$: 0.98 (comp, 6 H, CH-(C**H$_3$**)$_2$), 2.16 (s, 3 H, Ar-C**H$_3$**), 5.60 (s, 2 H, p-cy), 5.74 (d, J = 6.2 Hz, 1 H, p-cy), 6.07 (d, J = 6.2 Hz, 1 H, p-cy), 6.79 (m, 4 H, BPh$_4$), 6.95 (comp, 10 H, BPh$_4$ and Ar-**H**), 7.19 (m, 8 H, BPh$_4$), 7.66 (d, J = 8.8 Hz, 2 H, Ar-**H**), 7.82 (m, 1 H, pyr-**H**), 8.24 (comp, 2 H, pyr-**H**), 8.80 (s, 1 H, C**H**=N), 9.52 (d, J = 5.3 Hz, 1 H, pyr-**H**, C**H**=N), 10.23 (broad s, 1 H, C-O**H**); ^{13}C NMR (151 MHz, DMSO-d$_6$) δ$_C$: 18.3, 21.6, 21.7, 30.5, 84.6, 85.1, 86.5, 86.6, 103.7, 104.7, 115.7, 121.5, 124.2, 125.3, 128.4, 129.3, 135.5, 139.8, 143.6, 154.8, 155.8, 159.0, 163.8, 164.9 ppm. ESI-MS: C$_{22}$H$_{24}$ClN$_2$ORu (468.96); m/z 469.06 [M – BPh$_4$]$^+$. Elemental analysis C$_{46}$H$_{44}$BClN$_2$ORu.H$_2$O: C$_{cal}$ = 68.53 %; C$_{exp}$ = 68.95; H$_{cal}$ = 5.75; H$_{exp}$ = 5.73; N$_{cal}$ = 3.47; N$_{exp}$ = 3.23. C.

Synthesis of C1

The [RuCl$_2$(p-cymene)]$_2$ dimer (57 mg, 0.093 mmol) was dissolved in DCM (5 ml) forming a dark red solution. **L1** (54 mg, 0.19 mmol) was added as a solid to the stirring solution of the dimer. After a few minutes, the dark red solution turned orange-yellow. This solution was stirred at room temperature for 1 h. After 1h, the solvent was removed and the solid was dissolved in MeOH (5 ml) forming an orange-yellow solution. Sodium tetraphenylborate (64 mg, 0.19 mmol) was then added as a solid and this was stirred for 3 h at 0 °C. During this time, an orange-yellow solid precipitated out of the MeOH solution. It was filtered and washed extensively with MeOH followed by a 2:1 MeOH:H$_2$O solution after which the product was isolated as a yellow-orange solid (0.128 g, 77 %). Decomposition Temperature: 178 – 180 °C; IR (ATR) υ (C=N) 1610, 1595 cm^{-1}; ^{1}H NMR (400 MHz, CHCl$_3$) δ$_H$: 0.97 (d,

Chapter 3: Synthesis and Characterization of Ru(II) and Rh(I) Mononuclear and Multi-nuclear Complexes

J = 6.6 Hz, 6 H, CH-(**CH$_3$**)$_2$), 1.95 (s, 3 H, Ar-**CH$_3$**), 2.36 (m, 1 H, **CH**-(CH$_3$)$_2$), 4.76 (d, J = 6.2 Hz, 1 H, p-cy), 4.86 (d, J = 6.2 Hz, 1 H, p-cy), 4.96 (d, J = 6.2 Hz, 1 H, p-cy), 5.09 (comp, 3 H, p-cy, **CH$_2$**-O), 6.82 (m, 4 H, BPh$_4$), 6.94 (comp, 10 H, BPh$_4$, Ar-**H**), 7.11 (comp, 2 H, *core*), 7.18 (d, J = 9.0 Hz, 2 H, Ar-**H**), 7.38 (comp, 3 H, **CH**=N, pyr-**H**), 7.45 (comp, 11 H, *core*, BPh$_4$), 7.55 (t, J = 7.8 Hz, 1 H, pyr-**H**), 8.52 (d, J = 5.5 Hz, 1 H, pyr-**H**, **CH**=N); ^{13}C NMR (101 MHz, CHCl$_3$) δ$_C$: 18.9, 22.1, 22.6, 31.2, 70.9, 85.1, 86.0, 86.1, 86.5, 103.4, 106.5, 115.8, 122.5, 124.1, 126.2, 128.0, 128.6, 128.7, 129.0, 129.0, 130.2, 136.3, 136.6, 139.9, 145.2, 154.2, 154.9, 160.3, 165.0 ppm. ESI-MS: C$_{29}$H$_{30}$ClN$_2$ORu (559.08); m/z 559.1 [M − BPh$_4$]$^+$. Elemental analysis C$_{53}$H$_{50}$BClN$_2$ORu.H$_2$O: C$_{cal}$ = 71.02 %; C$_{exp}$ = 71.47; H$_{cal}$ = 5.85; H$_{exp}$ = 5.75; N$_{cal}$ = 3.13; N$_{exp}$ = 2.90.

Synthesis of C2

The [RuCl$_2$(p-cymene)]$_2$ dimer (58 mg, 0.095 mmol) was dissolved in DCM (5 ml) forming a dark red solution. **L2** (47 mg, 0.095 mmol) was added as a solid to the stirring solution of the dimer. After a few minutes, the dark red solution turned orange-yellow. This solution was stirred at room temperature for 1 h. After 1h, the solvent was removed and the solid was dissolved in MeOH (5 ml) forming an orange-yellow solution. Sodium tetraphenylborate (65 mg, 0.19 mmol) was then added as a solid and this was stirred for 3 h at 0 °C. During this time, an orange-yellow solid precipitated out of the MeOH solution. It was filtered and washed extensively with MeOH followed by a 2:1 MeOH:H$_2$O solution after which the product was isolated as a yellow-orange solid (0.143 g, 90 %). Decomposition Temperature: 156 – 159 °C; IR (ATR) υ (C=N) 1614, 1597 cm^{-1}; ^{1}H NMR (600 MHz, DMSO-d$_6$) δ$_H$: 0.98 (d, J = 5.9 Hz, 12 H, CH-(**CH$_3$**)$_2$), 2.16 (s, 6 H, Ar-**CH$_3$**), 5.25 (s, 4 H, **CH$_2$**-O) 5.58 (m, 2 H, p-cy), 5.62 (d, J = 5.9 Hz, 2 H, p-cy), 5.75 (d, J = 6.4 Hz, 2 H, p-cy), 6.08 (d, J = 6.4 Hz, 2 H, p-cy), 6.79 (m, 8 H, BPh$_4$), 6.92 (m, 16 H, BPh$_4$), 7.19 (m, 16 H, BPh$_4$), 7.26 (d, J = 8.8 Hz, 4 H, Ar-**H**), 7.57 (s, 4 H, *core*), 7.79 (d, J = 8.8 Hz, 4 H, Ar-**H**), 7.84 (m, 2 H, pyr-**H**), 8.24 (comp, 4 H, pyr-**H**), 8.84 (s, 2 H, **CH**=N), 9.54 (d, J = 5.3 Hz, 2 H, pyr-**H**, **CH**=N); ^{13}C NMR (151 MHz, DMSO-d$_6$) δ$_C$: 18.3, 21.6, 21.7, 30.5, 69.5, 84.7, 85.1, 86.3, 86.5, 103.6, 104.8, 115.3, 121.5, 124.1, 125.3, 128.1, 128.6, 129.6, 135.5, 136.4, 139.9, 145.0, 154.6, 155.9, 159.3, 163.8, 166.0 ppm. ESI-MS: C$_{52}$H$_{54}$Cl$_2$N$_4$O$_2$Ru$_2$ (1040.05); m/z 520.1 [M − 2BPh$_4$]$^{2+}$. Elemental analysis 2C$_{100}$H$_{94}$B$_2$Cl$_2$N$_4$O$_2$Ru$_2$.H$_2$O: C$_{cal}$ = 70.05 %; C$_{exp}$ = 69.57; H$_{cal}$ = 5.76; H$_{exp}$ = 5.59; N$_{cal}$ = 3.27; N$_{exp}$ = 2.99.

Chapter 3: Synthesis and Characterization of Ru(II) and Rh(I) Mononuclear and Multi-nuclear Complexes

Synthesis of C3

The [RuCl$_2$(p-cymene)]$_2$ dimer (65 mg, 0.11 mmol) was dissolved in DCM (5 ml) forming a dark red solution. **L3** (50 mg, 0.071 mmol) was added as a solid to the stirring solution of the dimer. After a few minutes, the dark red solution turned orange-yellow. This solution was stirred at room temperature for 1 h. After 1h, the solvent was removed and the solid was dissolved in MeOH (5 ml) forming an orange-yellow solution. Sodium tetraphenylborate (72 mg, 0.21 mmol) was then added as a solid and this was stirred for 3 h at 0 °C. During this time, an orange-yellow solid precipitated out of the MeOH solution. It was filtered and washed extensively with MeOH followed by a 2:1 MeOH:H$_2$O solution after which the product was isolated as a yellow-orange solid (0.117 g, 67 %). Decomposition Temperature: 152 – 153 °C; IR (ATR) υ (C=N) 1613, 1597 cm^{-1}; ^{1}H NMR (400 MHz, DMSO-d$_6$) δ$_H$: 0.96 (d, J = 7 Hz, 18 H, CH-(C**H$_3$**)$_2$), 2.14 (s, 9 H, Ar-C**H$_3$**), 5.28 (s, 6 H, C**H$_2$**-O) 5.57 (comp, 6 H, p-cy), 5.76 (comp, 4 H, p-cy), 6.06 (d, J = 6.2 Hz, 2 H, p-cy), 6.76 (m, 12 H, BPh$_4$), 6.90 (m, 24 H, BPh$_4$), 7.16 (m, 24 H, BPh$_4$), 7.27 (d, J = 8.6 Hz, 6 H, Ar-**H**), 7.64 (s, 3 H, *core*), 7.82 (comp, 9 H, Ar-**H**, pyr-**H**), 8.23 (comp, 6 H, pyr-**H**), 8.81 (s, 3 H, C**H**=N), 9.53 (d, J = 5.5 Hz, 3 H, pyr-**H**, C**H**=N); ^{13}C NMR (101 MHz, DMSO-d$_6$) δ$_C$: 19.0, 22.3, 22.4, 31.2, 70.3, 85.4, 85.9, 87.0, 87.2, 104.3, 105.6, 116.0, 122.2, 124.9, 126.0, 127.8, 129.3, 130.3, 136.2, 138.0, 140.6, 145.8, 155.3, 156.6, 160.0, 164.8, 166.8 ppm. ESI-MS: C$_{75}$H$_{78}$Cl$_3$N$_6$O$_3$Ru$_3$ (1521.03); m/z 507.1 [M − 3BPh$_4$]$^{3+}$. Elemental analysis C$_{147}$H$_{138}$B$_3$Cl$_3$N$_6$O$_3$Ru$_3$.6H$_2$O: C$_{cal}$ = 68.25 %; C$_{exp}$ = 68.15; H$_{cal}$ = 5.84; H$_{exp}$ = 5.37; N$_{cal}$ = 3.25; N$_{exp}$ = 3.14.

Synthesis of C5

The [RuCl$_2$(p-cymene)]$_2$ dimer (67 mg, 0.11 mmol) was dissolved in DCM (5 ml) forming a dark red solution. **L4** (50 mg, 0.054 mmol) was added as a solid to the stirring solution of the dimer. After a few minutes, the dark red solution turned orange-yellow. This solution was stirred at room temperature for 1 h. After 1h, the solvent was removed and the solid was dissolved in MeOH (5 ml) forming an orange-yellow solution. Sodium tetraphenylborate (74 mg, 0.22 mmol) was then added as a solid and this was stirred for 3 h at 0 °C. During this time, an orange-yellow solid precipitated out of the MeOH solution. It was filtered and washed extensively with MeOH followed by a 2:1 MeOH:H$_2$O solution after which the product was isolated as a yellow-orange solid (0.125 g, 70 %). Decomposition Temperature: 164 – 166 °C; IR (ATR) υ (C=N) 1614, 1597 cm^{-1}; ^{1}H NMR (400 MHz, DMSO-d$_6$) δ$_H$: 0.96

Chapter 3: Synthesis and Characterization of Ru(II) and Rh(I) Mononuclear and Multi-nuclear Complexes

(d, J = 7 Hz, 24 H, CH-(**CH$_3$**)$_2$), 2.13 (s, 12 H, Ar-**CH$_3$**), 5.44 (s, 8 H, **CH$_2$**-O) 5.55 (comp, 6 H, p-cy), 5.77 (comp, 6 H, p-cy), 6.05 (d, J = 6.2 Hz, 4 H, p-cy), 6.78 (m, 16 H, BPh$_4$), 6.92 (m, 32 H, BPh$_4$), 7.18 (m, 32 H, BPh$_4$), 7.29 (m, 8 H, Ar-**H**), 7.82 (comp, 14 H, Ar-**H**, pyr-**H**, *core*), 8.16 (comp, 8 H, pyr-**H**), 8.76 (m, 4 H, **CH**=N), 9.53 (d, J = 5.1 Hz, 4 H, pyr-**H**, **CH**=N); ^{13}C NMR (151 MHz, DMSO-d$_6$) δ_C : 18.3, 21.6, 21.7, 30.4, 67.5, 84.7, 85.2, 86.2, 86.5, 103.5, 104.8, 115.3, 121.5, 124.1, 125.3, 126.1, 126.7, 128.6, 129.5, 135.5, 139.8, 145.1, 154.5, 155.9, 159.2, 163.8, 166.0 ppm. ESI-MS: C$_{98}$H$_{102}$Cl$_4$N$_8$O$_4$Ru$_4$ (2002.00); m/z 500.5 [M – 4BPh$_4$]$^{4+}$. Elemental analysis C$_{194}$H$_{182}$B$_4$Cl$_4$N$_8$O$_4$Ru$_4$.9H$_2$O: C$_{cal}$ = 67.71 %; C$_{exp}$ = 67.46; H$_{cal}$ = 5.86; H$_{exp}$ = 5.10; N$_{cal}$ = 3.26; N$_{exp}$ = 3.06.

Synthesis of MC2

The [RhCODCl]$_2$ dimer (50 mg, 0.10 mmol) was dissolved in DCM (5 ml) forming a bright yellow solution. 4-{[pyridin-2-ylmethylidene]amino}phenol (40 mg, 0.20 mmol) was then added as a solid to the stirring solution of the dimer forming a dark-green solution and this solution was stirred for 1 h at room temperature. This led to the precipitation of a green solid. After 1 h, the solvent was filtered off and the solid was dissolved in MeOH (5 ml) forming a dark-green solution. Sodium tetraphenylborate (70 mg, 0.20 mmol) was then added as a solid and this was stirred for 3 h at 0 °C. During this time, a green solid precipitated out of the MeOH solution. It was filtered and washed extensively with MeOH followed by a 2:1 MeOH:H$_2$O solution after which the product was isolated as a green solid (0.098 g, 67 %). Mp = 146 – 148 °C. IR (ATR) υ (C=N) 1614, 1593 cm^{-1}; ^{1}H NMR (300 MHz, DMSO-d$_6$) δ_H : 1.93 (m, 4 H, COD), 2.42 (m, 4 H, COD), 4.25 (broad s, 4 H, COD), 6.84 (comp, 6 H, Ar-**H**, BPh$_4$), 6.94 (m, 8 H, BPh$_4$), 7.18 (comp, 10 H, Ar-**H**, BPh$_4$), 7.80 (m, 1 H, pyr-**H**), 8.12 (comp, 2 H, pyr, **CH**=N, pyr-**H**), 8.29 (m, 1 H, pyr-**H**), 8.63 (d, J = 1.5 Hz, 1 H, **CH**=N); ^{13}C NMR (151 MHz, DMSO-d$_6$) δ_C : 29.9, 84.5, 84.6, 115.5, 121.5, 122.9, 125.3, 129.1, 129.5, 135.5, 139.3, 141.2, 149.9, 154.7, 157.4, 163.8, 171.4 ppm. ESI-MS: C$_{20}$H$_{22}$N$_2$ORh (409.31); m/z 409.1 [M – BPh$_4$]$^+$. Elemental analysis C$_{44}$H$_{42}$BN$_2$ORh: C$_{cal}$ = 72.54 %; C$_{exp}$ = 72.39; H$_{cal}$ = 5.81; H$_{exp}$ = 4.65; N$_{cal}$ = 3.85; N$_{exp}$ = 3.44.

Synthesis of C7

The [RhCODCl]$_2$ dimer (70 mg, 0.14 mmol) was dissolved in DCM (5 ml) forming a bright yellow solution. **L1** (82 mg, 0.28 mmol) was then added as a solid to the stirring solution of the dimer forming a dark-green solution and this solution was stirred for 1 h at room temperature. After 1 h, the solvent was removed and the solid was dissolved in MeOH (5 ml)

Chapter 3: Synthesis and Characterization of Ru(II) and Rh(I) Mononuclear and Multi-nuclear Complexes

forming a dark-green solution. Sodium tetraphenylborate (97 mg, 0.28 mmol) was then added as a solid and this was stirred for 3 h at 0 °C. During this time, a green solid precipitated out of the MeOH solution. It was filtered and washed extensively with MeOH followed by a 2:1 MeOH:H_2O solution after which the product was isolated as a green solid (0.207 g, 89 %). Mp = 172 – 174 °C. IR (ATR) υ (C=N) 1614, 1589 cm^{-1}; ^{1}H NMR (400 MHz, DMSO-d_6) δ_H : 1.93 (m, 4 H, COD), 2.41 (m, 4 H, COD), 4.25 (broad s, 4 H, COD), 5.14 (s, 2 H, **CH$_2$**-O), 6.79 (m, 4 H, BPh$_4$), 6.92 (m, 8 H, BPh$_4$), 7.15 (comp, 10 H, Ar-**H**, BPh$_4$), 7.28 (m, 2 H, Ar-**H**), 7.40 (comp, 5 H, *core*), 7.82 (m, 1 H, pyr-**H**), 8.13 (comp, 2 H, pyr, C**H**=N, pyr-**H**), 8.30 (m, 1 H, pyr-**H**), 8.67 (s, 1 H, C**H**=N); ^{13}C NMR (101 MHz, DMSO-d_6) δ_C : 30.6, 70.3, 85.2, 85.3, 115.9, 122.2, 123.7, 126.0, 128.5, 128.7, 129.2, 129.9, 130.3, 136.2, 137.3, 141.4, 142.0, 150.7, 155.4, 158.7, 164.8, 172.7 ppm. ESI-MS: $C_{27}H_{28}N_2ORh$ (499.43); m/z 499.1 [M − BPh$_4$]$^+$. Elemental analysis $C_{51}H_{48}BN_2ORh$: C_{cal} = 74.82 %; C_{exp} = 72.39; H_{cal} = 5.91; H_{exp} = 5.97; N_{cal} = 3.42; N_{exp} = 3.07.

Synthesis of C8

The [RhCODCl]$_2$ dimer (70 mg, 0.14 mmol) was dissolved in DCM (5 ml) forming a bright yellow solution. **L2** (71 mg, 0.14 mmol) was then added as a solid to the stirring solution of the dimer forming a dark-green solution and this solution was stirred for 1 h at room temperature. After 1 h, the solvent was removed and the solid was dissolved in MeOH (5 ml) forming a dark-green solution. Sodium tetraphenylborate (97 mg, 0.28 mmol) was then added as a solid and this was stirred for 3 h at 0 °C. During this time, a green solid precipitated out of the MeOH solution. It was filtered and washed extensively with MeOH followed by a 2:1 MeOH:H_2O solution after which the product was isolated as a green solid (0.194 g, 88 %). Decomposition Temperature: 158 – 159 °C. IR (ATR) υ (C=N) 1613, 1597 cm^{-1}; ^{1}H NMR (300 MHz, DMSO-d_6) δ_H : 1.93 (m, 8 H, COD), 2.41 (m, 8 H, COD), 4.25 (broad s, 8 H, COD), 5.14 (s, 4 H, C**H$_2$**-O), 6.78 (m, 8 H, BPh$_4$), 6.93 (m, 16 H, BPh$_4$), 7.11 (m, 4 H, Ar-**H**), 7.19 (m, 16 H, BPh$_4$), 7.28 (m, 4 H, Ar-**H**), 7.52 (s, 4 H, *core*), 7.82 (m, 2 H, pyr-**H**), 8.12 (comp, 4 H, pyr, C**H**=N, pyr-**H**), 8.28 (m, 2 H, pyr-**H**), 8.66 (s, 2 H, C**H**=N); ^{13}C NMR (75 MHz, DMSO-d_6) δ_C : 29.9, 69.4, 84.5, 84.7, 115.2, 121.5, 123.0, 125.3, 128.0, 128.3, 135.6, 136.5, 140.7, 141.3, 150.1, 154.7, 158.0, 164.4, 172.0 ppm. ESI-MS: $C_{48}H_{50}N_4O_2Rh_2$ (920.74); m/z 460.1 [M − 2BPh$_4$]$^{2+}$. Elemental analysis $C_{96}H_{91}B_2N_4O_2Rh_2$: C_{cal} = 73.90 %; C_{exp} = 71.77; H_{cal} = 5.88; H_{exp} = 6.05; N_{cal} = 3.59; N_{exp} = 3.16.

Chapter 3: Synthesis and Characterization of Ru(II) and Rh(I) Mononuclear and Multi-nuclear Complexes

Synthesis of C4

The [RhCODCl]$_2$ dimer (57 mg, 0.12 mmol) was dissolved in DCM (5 ml) forming a bright yellow solution. **L3** (55 mg, 0.078 mmol) was then added as a solid to the stirring solution of the dimer forming a dark-green solution and this solution was stirred for 1 h at room temperature. After 1 h, the solvent was removed and the solid was dissolved in MeOH (5 ml) forming a dark-green solution. Sodium tetraphenylborate (79 mg, 0.23 mmol) was then added as a solid and this was stirred for 3 h at 0 °C. During this time, a green solid precipitated out of the MeOH solution. It was filtered and washed extensively with MeOH followed by a 2:1 MeOH:H$_2$O solution after which the product was isolated as a green solid (0.123 g, 69 %). Decomposition Temperature: 156 – 157 °C. IR (ATR) υ (C=N) 1613, 1597 cm^{-1}; ^{1}H NMR (300 MHz, DMSO-d$_6$) δ$_H$: 1.93 (m, 12 H, COD), 2.41 (m, 12 H, COD), 4.26 (broad s, 12 H, COD), 5.17 (s, 6 H, C**H$_2$**-O), 6.78 (m, 12 H, BPh$_4$), 6.92 (m, 24 H, BPh$_4$), 7.20 (comp, 36 H, Ar-**H**, BPh$_4$), 7.53 (s, 3 H, *core*), 7.81 (m, 3 H, pyr-**H**), 8.14 (comp, 6 H, pyr, C**H**=N, pyr-**H**), 8.28 (m, 3 H, pyr-**H**), 8.66 (s, 3 H, C**H**=N); ESI-MS: C$_{69}$H$_{72}$N$_6$O$_3$Rh$_3$ (1342.06); Molecular ion not observed. Elemental analysis C$_{141}$H$_{132}$B$_3$N$_6$O$_3$Rh$_3$.10H$_2$O: C$_{cal}$ = 68.29 %; C$_{exp}$ = 67.99; H$_{cal}$ = 6.18; H$_{exp}$ = 5.72; N$_{cal}$ = 3.39; N$_{exp}$ = 3.37.

Synthesis of C6

The [RhCODCl]$_2$ dimer (61 mg, 0.12 mmol) was dissolved in DCM (5 ml) forming a bright yellow solution. **L4** (57 mg, 0.06 mmol) was then added as a solid to the stirring solution of the dimer forming a dark-green solution and this solution was stirred for 1 h at room temperature. After 1 h, the solvent was removed and the solid was dissolved in MeOH (5 ml) forming a dark-green solution. Sodium tetraphenylborate (85 mg, 0.25 mmol) was then added as a solid and this was stirred for 3 h at 0 °C. During this time, a green solid precipitated out of the MeOH solution. It was filtered and washed extensively with MeOH followed by a 2:1 MeOH:H$_2$O solution after which the product was isolated as a green solid (0.146 g, 78 %). Decomposition Temperature: 163 – 164 °C. IR (ATR) υ (C=N) 1614, 1597 cm^{-1}; ^{1}H NMR (400 MHz, DMSO-d$_6$) δ$_H$: 1.90 (m, 16 H, COD), 2.40 (m, 16 H, COD), 4.23 (broad s, 16 H, COD), 5.28 (s, 8 H, C**H$_2$**-O), 6.77 (m, 16 H, BPh$_4$), 6.92 (m, 32 H, BPh$_4$), 7.20 (comp, 48 H, Ar-**H**, BPh$_4$), 7.48 (s, 2 H, *core*), 7.82 (m, 4 H, pyr-**H**), 8.13 (comp, 8 H, pyr, C**H**=N, pyr-**H**), 8.30 (m, 4 H, pyr-**H**), 8.62 (s, 4 H, C**H**=N); ESI-MS: C$_{90}$H$_{94}$N$_8$O$_4$Rh$_4$ (1763.38); Molecular ion not observed. Elemental analysis C$_{186}$H$_{174}$B$_4$N$_8$O$_4$Rh$_4$.15H$_2$O: C$_{cal}$ = 67.48 %; C$_{exp}$ = 67.14; H$_{cal}$ = 6.21; H$_{exp}$ = 5.67; N$_{cal}$ = 3.38; N$_{exp}$ = 3.16.

Chapter 3: Synthesis and Characterization of Ru(II) and Rh(I) Mononuclear and Multi-nuclear Complexes

3.6   References

1. D. A. Tomalia, H. Baker, J. Dewald, M. Hall, G. Kallos, S. Martin, J. Roeck, J. Ryder and J. Smith, *Polym J.*, 1985, **17**, 117-132.

2. J. Zhang, J. Aszodi, C. Chartier, N. L'hermite and J. Weston, *Tetrahedron Lett.*, 2001, **42**, 6683-6686.

3. J. G. Weintraub, S. Broxer, N. M. Paul and J. R. Parquette, *Tetrahedron*, 2001, **57**, 9393-9402.

4. B. Pan, F. Gao and H. Gu, *J. Colloid Interface Sci.*, 2005, **284**, 1-6.

5. J. Zhang, Y. Yuan, S. Xie, Y. Chai and R. Yuan, *Biosens. Bioelectron.*, 2014, **60**, 224-230.

6. M. Algarra, M. I. Vázquez, B. Alonso, C. M. Casado, J. Casado and J. Benavente, *Chem. Eng. J.*, 2014, **253**, 472-477.

7. E. Gong, B. Matthews, T. McCarthy, J. Chu, G. Holan, J. Raff and S. Sacks, *Antiviral Res.*, 2005, **68**, 139-146.

8. P. Kesharwani, R. K. Tekade and N. K. Jain, *Biomaterials*, 2014, **35**, 5539-5548.

9. B. Kavosi, R. Hallaj, H. Teymourian and A. Salimi, *Biosens. Bioelectron.*, 2014, **59**, 389-396.

10. R. J. Korkosz, J. D. Gilbertson, K. S. Prasifka and B. D. Chandler, *Catal. Today*, 2007, **122**, 370-377.

11. G. R. Krishnan and K. Sreekumar, *Appl. Catal., A*, 2009, **353**, 80-86.

12. E. Murugan and I. Pakrudheen, *Appl. Catal., A*, 2012, **439**-**440**, 142-148.

13. T. Mizugaki, M. Ooe, K. Ebitani and K. Kaneda, *J. Mol. Catal. A: Chem.*, 1999, **145**, 329-333.

14. G. Smith, R. Chen and S. F. Mapolie, *J. Organomet. Chem.*, 2003, **673**, 111-115.

15. R. Chen, J. Bacsa, and S. F. Mapolie, *Inorg. Chem. Commun.*, 2002, **5**, 724-726.

16. R. Chen and S. F. Mapolie, *J. Mol. Catal. A: Chem.*, 2003, **193**, 33-40.

17. Y. Li, X. Liu and G. Zhao, *Tetrahedron: Asymmetry*, 2006, **17**, 2034-2039.

18. K. Fujita, M. Yamazaki, T. Ainoya, T. Tsuchimoto and H. Yasuda, *Tetrahedron*, 2010, **66**, 8536-8543.

19. M. Malipeddi, C. Lakhani, M. Chhabra, P. Paira and R. Vidya, *Bioorg. Med. Chem. Lett.*, 2015, **25**, 2892-2896.

20. P. Govender, N. C. Antonels, J. Mattsson, A. K. Renfrew, P. J. Dyson, J. R. Moss, B. Therrien and G. S. Smith, *J. Organomet. Chem.*, 2009, **694**, 3470-3476.

21. A. Pitto-Barry, O. Zava, P. J. Dyson, R. Deschenaux and B. Therrien, *Inorg. Chem.*, 2012, **51**, 7119-7124.

22. T. Fujihara, T. Nishida, J. Terao and Y. Tsuji, *Inorg. Chim. Acta*, 2014, **409**, 174-178.

23. W. Wang, Z. Li, L. Su, Q. Wang and Y. Wu, *J. Mol. Catal. A: Chem.*, 2014, **387**, 92-102.

24. J. G. Małecki, *Struct. Chem.*, 2012, **23**, 461–472.

25. M. A. Bennett, T. N. Huang, T. W. Matheson and A. K. Smith, *Inorg. Synth.*, 1982, **21**, 74-78.

26. P. Servin, R. Laurent, H. Dib, L. Gonsalvi, M. Peruzzini, J. Majoral and A. Caminade, *Tetrahedron Lett.*, 2012, **53**, 3876-3879.

27. P. N. M. Botman, A. Amore, R. van Heerbeek, J. W. Back, H. Hiemstra, J. N. H. Reek and J. H. van Maarseveen, *Tetrahedron Lett.*, 2004, **45**, 5999-6002.

28. B. Natarajan and N. Jayaraman, *J. Organomet. Chem.*, 2011, **696**, 722-730.

29. G. Giordano and R. H. Crabtree, *Inorg. Synth.*, 1979, **19**, 218-220.

Chapter 4 : Evaluation of Rh(I) and Ru(II) Catalyst Precursors in the Hydroformylation of 1-Octene

4.1   Introduction

Hydroformylation is one of the largest industrial homogeneously catalyzed reactions.[1] Annually, large quantities of aldehydes are produced via this process and these are used to access other secondary products such as alcohols and amines.[1] Hydroformylation leads to the production of both linear and branched products. The selectivity in this reaction is important and it is usually determined by the reaction conditions. However, the ligands surrounding the metal centre also have an influence. The branched aldehyde has specific applications in the pharmaceutical industry. BASF, for instance, utilize hydroformylation in the production of vitamin A from 1,2-diacetoxy-3-butene.[1] Hydroformylation also finds application in the fragrance industry. Dos Santos and co-workers[2] reported the hydroformylation of sterically crowded monoterpenes under quite mild reaction conditions. These monoterpenes included 2-carene, 3-carene and α-pinene. Furthermore, hydroformylation has successfully been applied in the preparation of 2-aryloxypropanals which are important precursors for 2-aryloxypropanoic acids.[3] These acids are applied as herbicides. Thus, hydroformylation is quite an important industrial process. Most hydroformylation catalysts nowadays are based on rhodium, but the downside about using rhodium is its high cost. Therefore, more active and selective catalysts need to be developed which must also allow the recovery and reusability of these catalytic systems.

4.1.1   Mechanism

In 1961, Heck and Breslow[4] proposed a mechanism for the cobalt catalyzed hydroformylation reaction. Today, this is the mechanism that is widely accepted. They proposed that $HCo(CO)_4$ undergoes CO dissociation, forming a hydridotricarbonyl cobalt species. The following step is the coordination of the olefin to the metal centre, forming a π-complex followed by the subsequent insertion into the Co-H bond forming a cobalt alkyl species which is in equilibrium with an acyl cobalt species. The next step is oxidative addition of H_2 and the subsequent reductive elimination, forming the aldehyde. $HCo(CO)_4$ was the first cobalt complex that was used for hydroformylation and it is therefore referred to as the unmodified cobalt catalyst. This complex has subsequently been modified by introducing various types of ligands in order to influence the selectivity of the reaction.

Chapter 4: Evaluation of Rh(I) and Ru(II) Catalyst Precursors in the Hydroformylation of 1-Octene
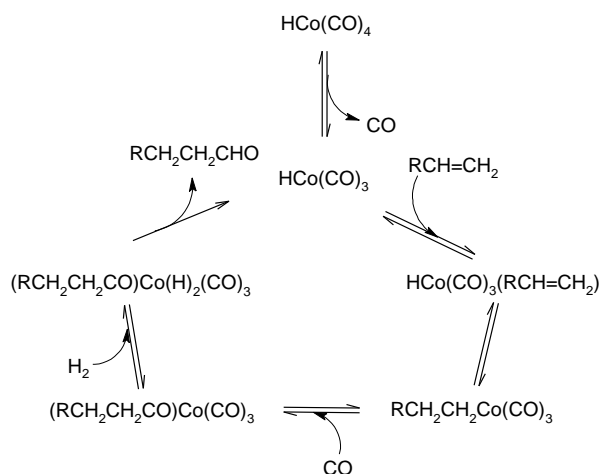
Figure 4-1: HCo(CO)$_4$ hydroformylation mechanism[4]

Therefore, a few variations of this mechanism is prevalent in the literature as researchers are applying it to their systems. One such an example is the work reported by Caporali *et al.*[5] who studied the hydroformylation reaction using high pressure FT-IR spectroscopy. They proposed a mechanism for the reaction using RhH(CO)(PPh$_3$)$_3$ as catalyst, and this is shown in Figure 4-2.

Figure 4-2: HRh(CO)(PPh$_3$)$_3$ hydroformylation mechanism[5]

60

Chapter 4: Evaluation of Rh(I) and Ru(II) Catalyst Precursors in the Hydroformylation of 1-Octene

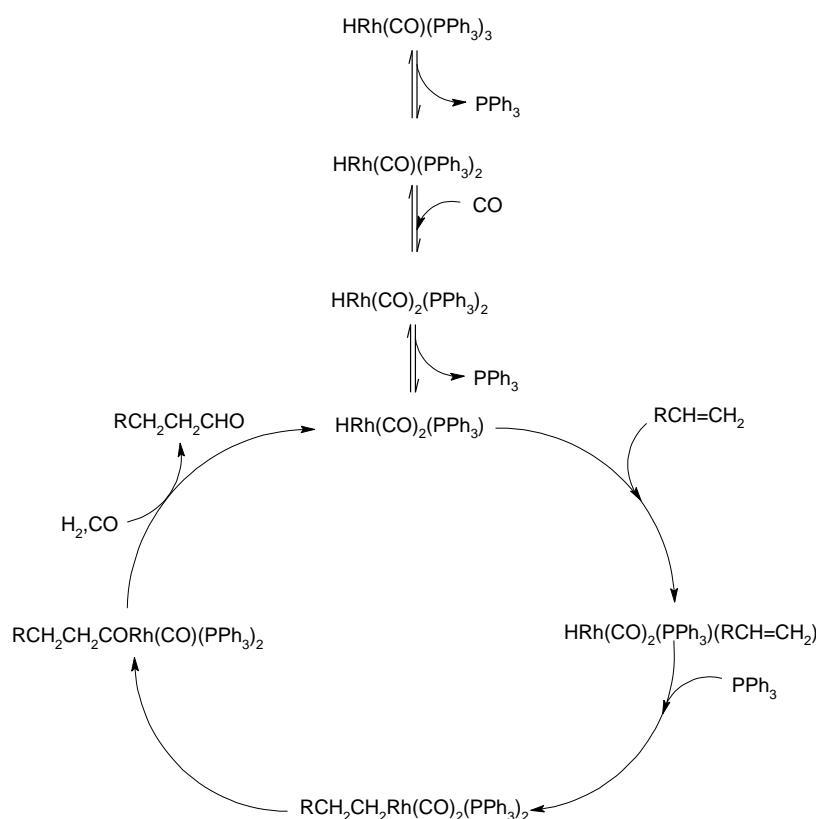### 4.1.2 Factors that influence the activity and selectivity

4.1.2.1 Temperature

Studies have shown that by increasing the temperature of the reaction, the conversion of the substrate increases.[6-8] However, temperature has the most profound effect on the chemo – and regioselectivity of the reaction. Researchers has found that by carefully controlling the temperature of the hydroformylation reaction, one can get a handle on the selectivity of the reaction. As the temperature of the reaction is increased, so does the rate of isomerization.[9] Isomerization is a major side reaction in hydroformylation. As the terminal alkenes are converted to the linear aldehydes, the isomerized (internal) alkenes also undergo hydroformylation to branched aldehydes. It is therefore found that by increasing the temperature of the reaction, you can tune the system to be regioselective towards branched aldehydes.[6, 9-10]

4.1.2.2 Pressure

Increasing the syngas pressure leads to an increase in the conversion of the substrate.[6,8,11] However, once optimum pressure has been reached, further increases will lead to a decrease in the conversion.[6] Moreover, syngas pressure has a significant effect on the rate of isomerization. An increase in pressure led to a decrease in isomerization.[6,9-10,12] Referring back to the mechanism, CO insertion takes place once the cobalt alkyl species is formed. At low CO pressure, this insertion is probably inhibited, leading to the isomerization of the alkene. Optimum pressure of the reaction is thus a prerequisite in order to get acceptable conversions and selectivities.

4.1.2.3 Ligand effects

The ligands can have an influence on both the selectivity and stability of the catalyst. Hanson and Davis[13] showed how the presence of excess PPh_3 suppresses the isomerization of the alkene using $RhH(CO)(PPh_3)_3$ as the catalyst. This can be best understood by referring to the mechanism of the reaction shown in Figure 4-2. After the coordination of the olefin to the metal centre, free phosphine ligand coordinates to the metal at the same time as the insertion of the olefin into the Rh-H bond occurs to form a rhodium-alkyl species. Isomerized olefins are the result of the formation of a branched rhodium-alkyl species and subsequent β-hydrogen transfer to form the internal olefins. The presence of large ligands such as PPh_3 prevents the formation of branched rhodium-alkyl species due to steric interactions and

therefore suppresses isomerization. Furthermore, the presence of a large excess of PPh_3 will prevent phosphine dissociation and therefore retard the formation of branched alkyl species. This will also have an influence on the second step of isomerization, β-hydrogen transfer which requires an open coordination site which is created by the insertion of the olefin into the Rh-H bond. Excess phosphine will occupy this vacant site.

4.1.3   Mechanistic Investigations

NMR and IR spectroscopy have been utilized to study the mechanism of the hydroformylation reaction. These techniques can be used to monitor the presence of M-H and M-CO species. They are normally used in conjunction, since IR spectroscopy is much more sensitive compared to NMR. In monitoring the progression of the hydroformylation reaction, ^{1}H NMR spectroscopy is normally used to detect metal hydride species for which the signals generally occur between 0 and -40 ppm. Furthermore, IR spectroscopy is a useful tool to detect the presence of metal carbonyls. Moreover, the disappearance of the alkene substrate and the appearance of the aldehydic product can be monitored. Caporali *et al.*[5] studied the hydroformylation of 1-hexene and cyclohexene using *in situ* high pressure FT-IR. The catalyst precursors studied were $RhH(CO)(PPh_3)_3$ and $Co_2(CO)_8$. Various experiments were conducted, of which the important experiments were the ones under CO and syngas. These experiments were performed in the presence of the substrate (1-hexene). Under CO only, FT-IR showed the presence of two acyl species around 1676 cm^{-1} which is attributed to the linear and branched acyl complexes. They also observed a high amount of $[Rh(CO)_2(PPh_3)_2]_2$. However, after addition of H_2 gas, a significant decrease in the intensity of these peaks were observed. The same experiment was performed using cyclohexene as the substrate. In the presence of syngas, the FT-IR spectrum only showed the presence of the substrate, aldehydes, $[Rh(CO)_2(PPh_3)_2]_2$ and $RhH(CO)_2(PPh_3)_2$. This led them to believe that $RhH(CO)_2(PPh_3)_2$ is the intermediate before the transition state of the reaction. Therefore, they concluded that the coordination of the alkene to the rhodium hydride is the rate determining step.

In another study carried out by Masdue-Bultó and co-workers[14], they observed the formation of $[RhH(CO)_2(\text{sulfonated diphosphine})]$ species under hydroformylation conditions from $[Rh(\mu\text{-OMe})(cod)]_2$ (cod = 1,5-cyclooctadiene) as catalyst precursor and two different ligands dpppts (tetrasulfonated 1,3-bis(diphenylphosphino)propane) and (*S,S*)-bdppts (2,4-bis(diphenylphosphino)pentane). For the catalyst precursor and dpppts, experiments were performed in the presence of H_2 only, followed by syngas. Both $^{31}P\{^1H\}$ and ^1H NMR

Chapter 4: Evaluation of Rh(I) and Ru(II) Catalyst Precursors in the Hydroformylation of 1-Octene

spectra were recorded. Under H_2 only, the important species observed were [RhH(dpppts)$_2$] and [RhH$_2$(dpppts)$_2$]$^+$. Evidence of this was found in both ^{31}P{^{1}H} and ^{1}H NMR. Under syngas, [RhH(CO)$_2$(dpppts)] was one of the species formed and is thought to probably be the active species. This was confirmed by HP-IR which showed absorbances at 1955, 1990 and 2034 cm^{-1}.

4.2   Application of novel Rh(I) and Ru(II) Metallodendrimers in the Hydroformylation of 1-Octene

A total of ten novel Rh(I) and Ru(II) complexes were evaluated as catalyst precursors in the hydroformylation of 1-octene. The reactions were performed in a 1:1 THF:Toluene mixture. THF was employed since the mononuclear complexes were found to be soluble in this solvent, however, the multi-nuclear complexes are not soluble in THF at room temperature. Toluene is a solvent commonly employed in hydroformylation and allows the reaction to be performed at temperatures above 100 °C.

Table 4-1: Rh(I) and Ru(II) catalyst precursors

Nuclearity of Complexes	Rh(I)	Ru(II)
Mononuclear	MC2	MC1
Mononuclear	C7	C1
Bi-nuclear	C8	C2
Tri-nuclear	C4	C3
Tetra-nuclear	C6	C5

4.2.1   Hydroformylation using Rh(I) catalyst precursors

The conditions for the catalysis were adopted from a paper published by Smith and co-workers[10] on the application of low generation *N,N* Rh(I) metallodendrimers in the hydroformylation of 1-octene: P = 30 bar, T = 75 °C. We performed the reactions for 8 and 21 hours utilizing a Rh:substrate ratio of 1:2000 (0.05 mol%). A 1:2000 ratio was used for all catalyst systems, irrespective of the nuclearity of the catalysts. Thus, the specific amount of moles were varied for each catalyst in order to maintain a constant rhodium concentration. The chemo − and regioselectivity were also determined at these reaction times. The best performing catalyst was then identified and used to investigate the influence of temperature and syngas pressure on the activity and selectivity.

Chapter 4: Evaluation of Rh(I) and Ru(II) Catalyst Precursors in the Hydroformylation of 1-Octene

4.2.1.1 Conversion vs Time
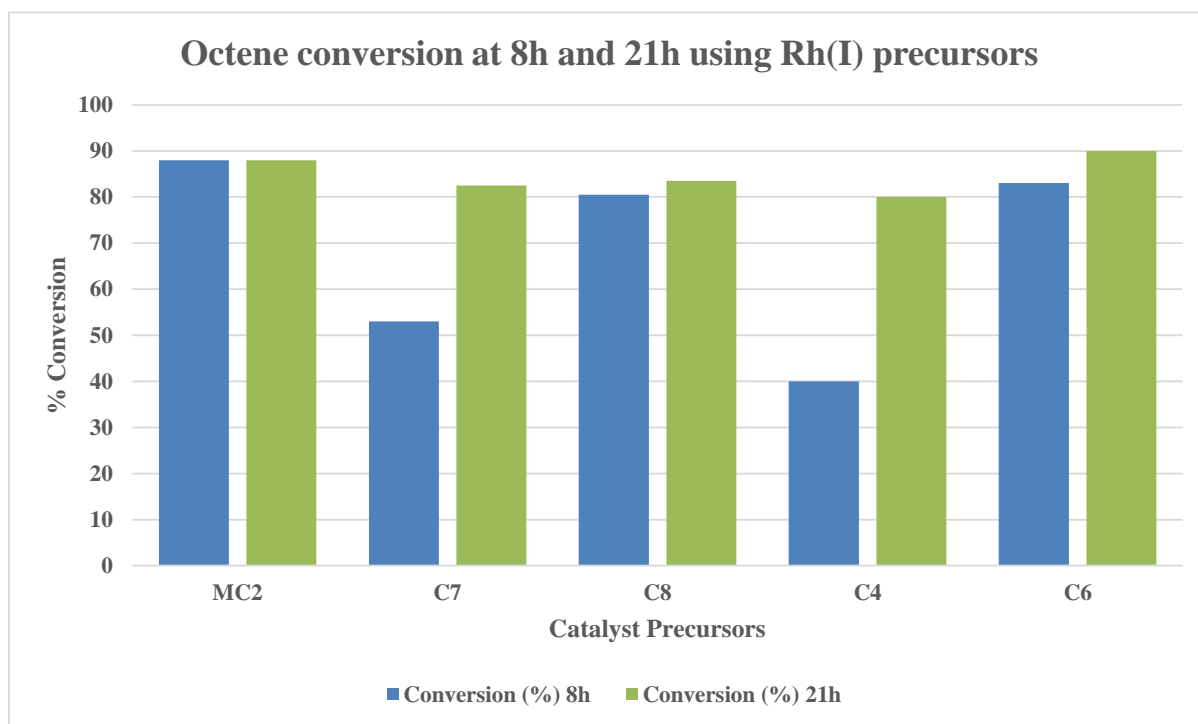
Figure 4-3: Conversion vs Time for Rh(I) catalyst precursors; 1-octene (38 mmol), 30 bar CO:H_2 (1:1), 75 °C, 10 ml THF:Toluene (1:1), 0.05 mol % Rh(I)

The rationale behind the preparation of multinuclear complexes was to investigate whether it will enhance the reaction due to the higher local concentration of metal ions. Once again it must be emphasized that all experiments were conducted at the same rhodium concentration, irrespective of the nuclearity of the complex. For the catalysts investigated in this current study we observed that the model catalyst, **C7**, registered lower conversions than the multi-nuclear catalysts (**C6** and **C8**). There is quite a significant increase in the conversion in going from the mononuclear complex (**C7**) to the bi-nuclear analogue (**C8**) when tested for 8 h. This increase in activity can be ascribed to the higher local concentration of catalytic sites for **C8**, thereby enhancing the rate of the reaction.[15-18] Previously, it has been shown that multi-nuclear complexes can produce catalysts that are more active than their mononuclear counterparts.[15-18] The conversion (83 %) obtained for the tetra-nuclear (**C6**) catalyst at 8 h was only slightly higher than that obtained for the bi-nuclear (**C8**) catalyst (81 %). However, at 21 h, all the catalysts display roughly similar activities (80 – 90 %).

Chapter 4: Evaluation of Rh(I) and Ru(II) Catalyst Precursors in the Hydroformylation of 1-Octene
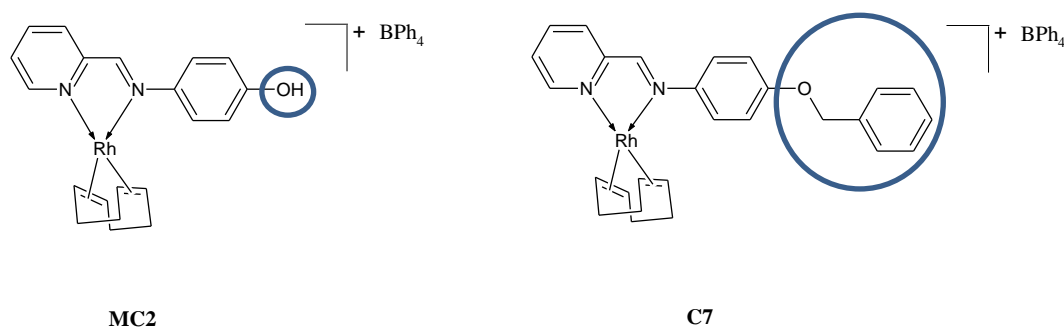
Figure 4-4: Structures of MC2 and C7

The mononuclear complex with the phenolic substituent on the aromatic ring, **MC2**, was found to be more active than **C7**, especially for the 8 h reactions. The structures of **MC2** and **C7** are shown in Figure 4-4, with the difference between them indicated by the blue circles. We rationalized that this is due to the electron donating ability of the phenol versus that of the ether. It is probably more significant in the case of the ether that the phenol. This increases the electron density on the metal and therefore decreases its electrophilicity. This makes the coordination of the substrate slower.[19]

No significant increase in the conversion from 8 to 21 h was observed when using catalysts **MC2**, **C6** and **C8**. However, there was a vast difference in the selectivity obtained at the two different reaction times, which will be discussed under section **4.2.1.2** below.

C4 (tri-nuclear) did not follow the expected trend, and only registered a conversion (40 %) that is lower than what was observed for **C8** (bi-nuclear), when tested over an 8 h period. It is important to note that both **C4** and **C8** are insoluble in the reaction solvents at room temperature. At the conclusion of the 8 h reaction period, **C8** (a) was completely in solution, whereas for **C4** (b), some of the material remained undissolved.
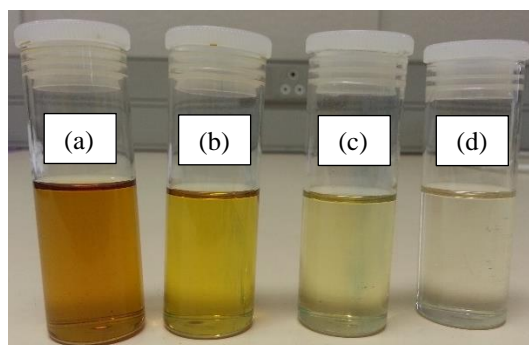
Figure 4-5: Reaction solutions; (a) C8, (b) C4, (c) C4 second cycle, (d) C4 third cycle

Chapter 4: Evaluation of Rh(I) and Ru(II) Catalyst Precursors in the Hydroformylation of 1-Octene

The higher activity of **C8** compared to **C4** is due to its higher solubility at the reaction temperatures, which was also confirmed by the colour of the solutions. Furthermore, the insoluble material that was isolated after the 8 h reaction period for **C4**, could be reused in a second cycle (c). A conversion of 30 % was observed in this second cycle using the recovered catalyst, with the colour of the solution lighter compared to that of the fresh catalyst (b). However, the catalyst could not be reused in a third cycle (d), even though some of the material remained insoluble at the conclusion of the reaction. The hydroformylation reaction is thus essentially homogeneous, and for **C4**, the catalyst is only partially soluble and it's the complex in solution which then catalyses the hydroformylation reaction. **C6**, the tetra-nuclear analogue, was surprisingly much more soluble at the reaction temperatures, explaining the higher conversions observed for this catalyst.

The chemo – and regioselectivity for **C4** were determined in both the first and second cycle. No significant differences were observed.

The IR spectrum of **C4** before catalysis was compared to the IR spectra of **C4** after the first and third cycle.
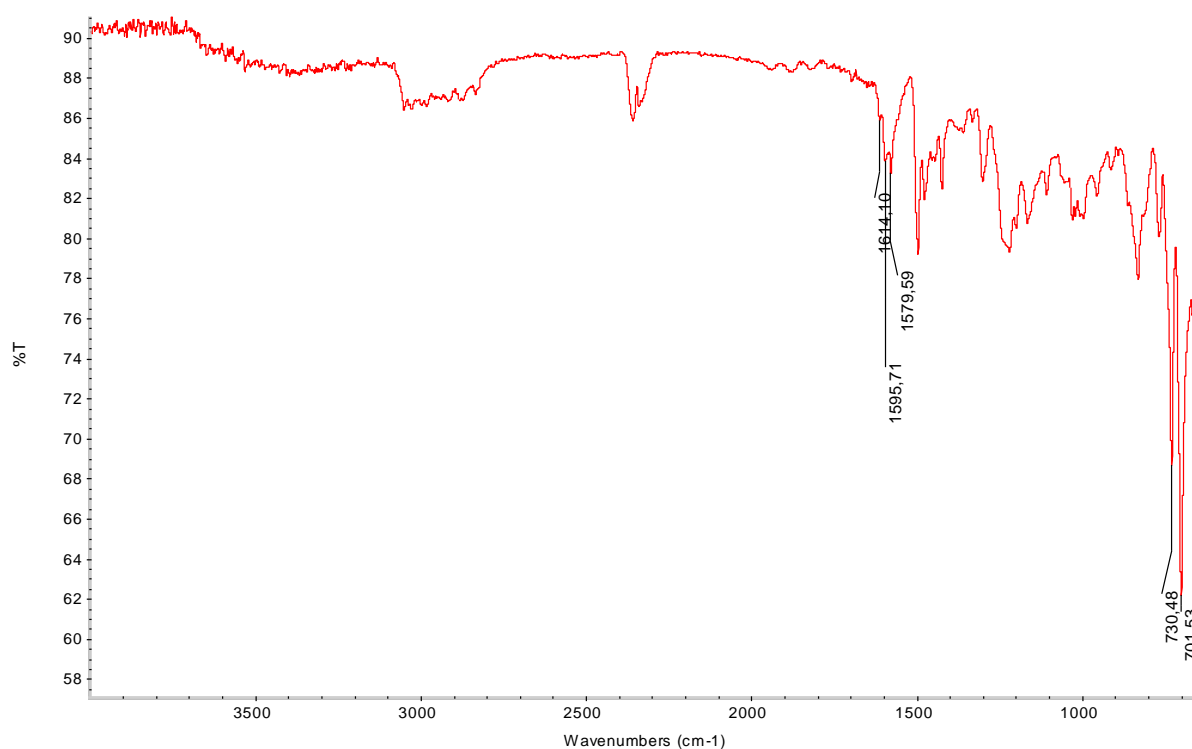
Figure 4-6: C4 IR spectrum before catalysis

Chapter 4: Evaluation of Rh(I) and Ru(II) Catalyst Precursors in the Hydroformylation of 1-Octene

The IR spectrum of **C4** after the first cycle is shown below. The absorbances around 2006 – 2077 cm^{-1} represents the Rh-CO and Rh-H moieties.[5] This indicates how the catalyst precursor is converted to what is thought to be the active species *in situ*.
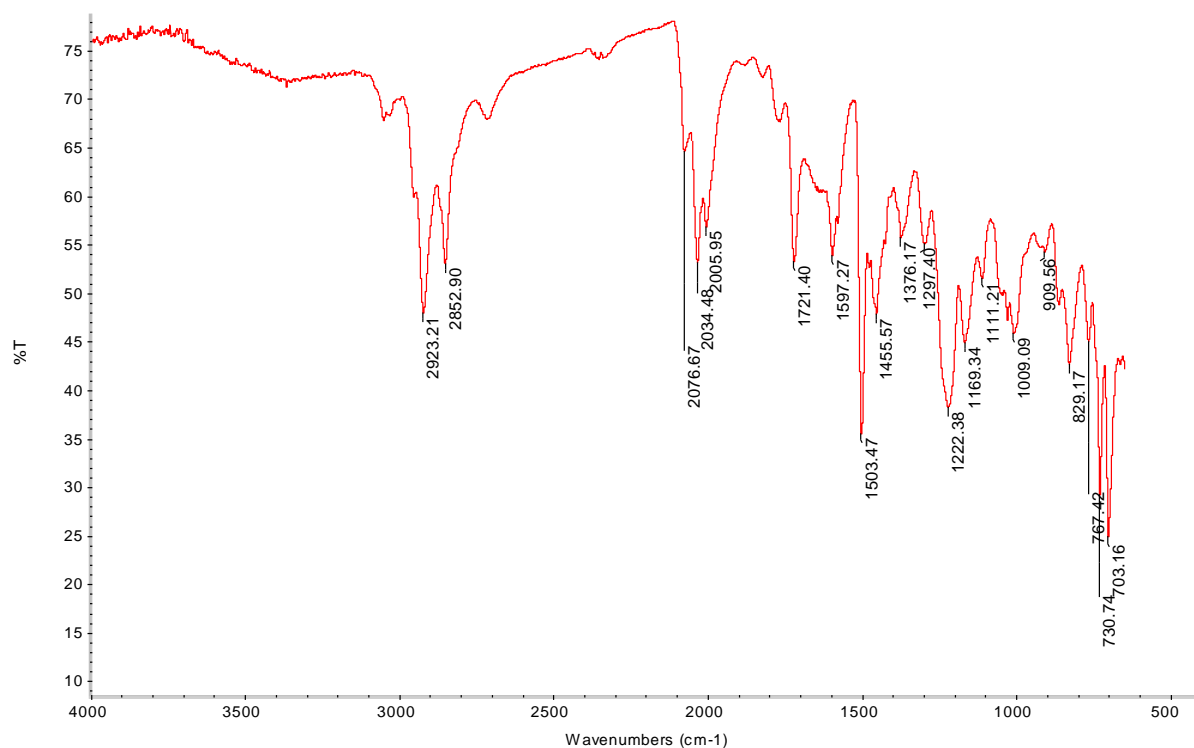
Figure 4-7: IR spectrum of C4 after first cycle

Chapter 4: Evaluation of Rh(I) and Ru(II) Catalyst Precursors in the Hydroformylation of 1-Octene
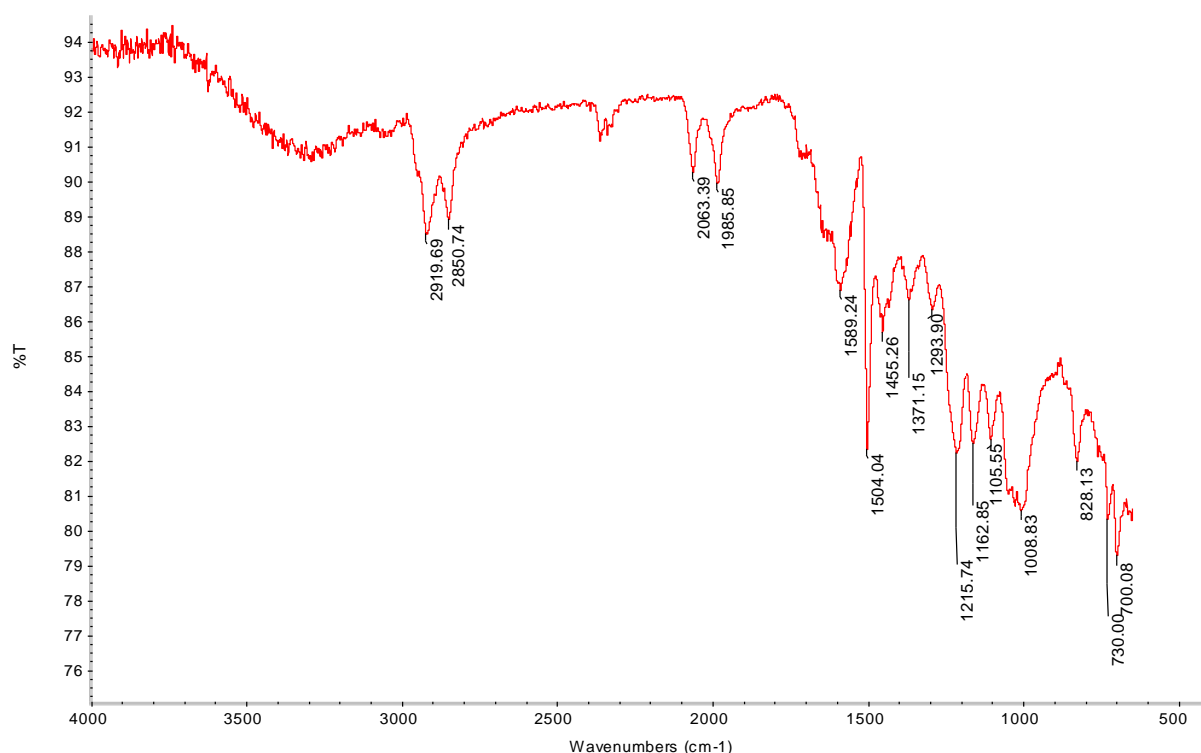
Figure 4-8: IR spectrum of C4 after third cycle

The IR spectrum of the insoluble material isolated at the conclusion of the third cycle is shown in Figure 4-8. The Rh-H and Rh-CO absorbances in this case are very weak compared to those observed in Figure 4-7. This might be an explanation as to why no activity was observed after the third cycle.

The activity of the catalysts were also expressed in terms of Turnover Number (TON).

Table 4-2: TON's at 8h and 21 h

Catalysts	TON[a]	
	8 h	21 h
MC2	1758	1768
C7	1059	1661
C8	1616	1676
C4	802	1597
C6	1667	1803

[a]**TON = (mol product/mol Rh)**

The TON's shown above are based on the total conversion of 1-octene. It thus includes the isomerization of 1-octene to its internal analogues, the hydrogenation of 1-octene to octane, as well as the hydroformylation of 1-octene to the corresponding aldehydes. However, this does not give one a clear indication of the activity of the catalysts in hydroformylation (production of aldehydes). Therefore, the TON's based on aldehyde formation (TON_{ald}) alone

Chapter 4: Evaluation of Rh(I) and Ru(II) Catalyst Precursors in the Hydroformylation of 1-Octene

were determined and compared to those reported in literature using rhodium catalysts and 1-octene as substrate as shown in Table 4-3.

Table 4-3: Rhodium catalyst activity comparison

Catalysts	Conditions				TON_{ald}^a	Ref
	P (bar)	**Temp (°C)**	**t (h)**	**Cat:sub**		
[Rh(acac)(CO)$_2$]dibenzophosphole	30	60	6	1:1000	999	20
Rh Iminophosphine	40	75	4	1:500	500	21
Rh phosphine-imidazolium	40	100	2	1:2000	1920	22
C6	30	75	8	1:2000	1017	This work

^{a}**TON$_{ald}$ = (mol aldehyde/mol Rh)**

The TON$_{ald}$ achieved for **C6** were slightly higher than that achieved by Leroux and co-workers[20], however, they utilized a lower temperature and a shorter reaction time for their catalysis. They used [Rh(acac)(CO)$_2$] with added phosphine ligands (dibenzophospholes) as catalysts. The activity of our catalyst compare quite well to the catalyst system employed by Leroux and co-workers[20] seeing that we obtained roughly the same TON$_{ald}$ while utilizing double the substrate loading. Furthermore, Smith and co-workers[21] developed fluorocarbon-containing Rh(I) complexes, bearing iminophosphine and salicylaldimine ligands, for the biphasic hydroformylation of 1-octene. They achieved a TON$_{ald}$ around 500 for all the iminophosphine complexes. **C6** is thus more efficient than the catalyst systems reported by Smith and co-workers[21], considering we employed a substrate to catalyst ratio four times higher and at a lower syngas pressure, albeit at a longer reaction time of 8 h. Moreover, Liu and co-workers[22] utilized a Rh(III) salt, in the presence of various phosphine-imidazolium ligands, for the hydroformylation of 1-octene in a water suspension. These catalysts performed much better than our catalysts, most likely due to the ion-pair synergistic effect of the ligands.

It would appear that the activity of our rhodium catalysts is quite comparable to a number of other rhodium systems reported.

Chapter 4: Evaluation of Rh(I) and Ru(II) Catalyst Precursors in the Hydroformylation of 1-Octene
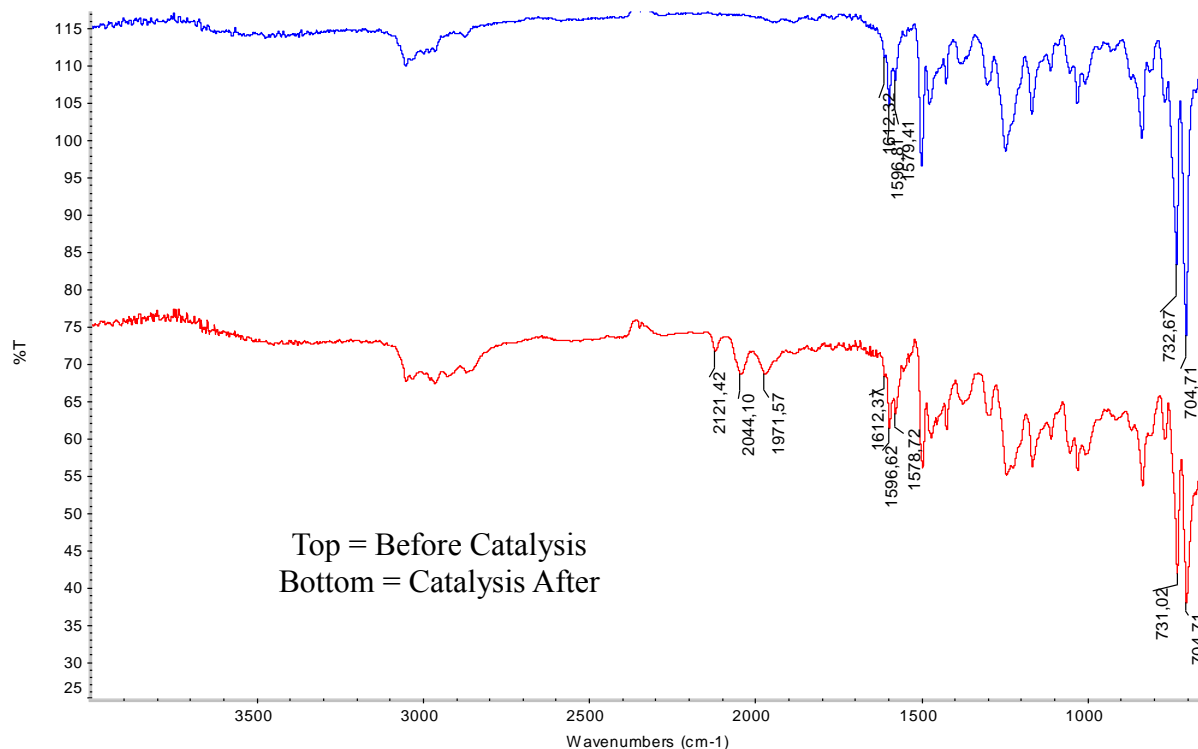
Figure 4-9: C3 before (top) and after (bottom) catalysis

The five Ru(II) catalyst precursors were also tested under the same reaction conditions used for the Rh(I) catalysts. However, they only showed low conversion of 1-octene. Of the low amount of 1-octene converted, none were converted to aldehydes or internal octenes. Only a small amount of octane was obtained as product. The FT-IR spectra of the catalyst were recorded before and after catalysis reactions with **C3**. Before use, the isolated imine and pyridyl imine absorbances were observed at 1612 and 1597 cm^{-1} respectively. The signal for the [BPh$_4$]$^-$ counter ion can also be observed around 700 cm^{-1}. After catalysis, all these bands are still intact and at the same wavenumbers in these regions. In addition to these bands, three new but relatively weak bands appeared around 1971 – 2121 cm^{-1} in the spectrum of the recovered catalyst. This is the region where Ru-CO and Ru-H bands normally occur. Since the bands are relatively weak, this led us to believe that the catalyst precursor is not significantly converted to the active species under these conditions, which could account for the low activity of the Ru(II) catalyst precursors under these conditions. From these results it would appear that harsher reaction conditions are required. The results obtained are in line with what is expected as rhodium is known to give more active hydroformylation catalysts thus requiring milder reaction conditions compared to other metals such as Ru, Co and Ir.[23]

70

4.2.1.2 Selectivity

As mentioned briefly earlier, the first catalyst used for hydroformylation was $HCo(CO)_4$, which was subsequently called unmodified cobalt catalyst. $HCo(CO)_4$ is formed *in situ* from $Co_2(CO)_8$ after cleavage by H_2 under hydroformylation conditions. This catalyst was found to be highly active, however, it required high pressures for stability. Furthermore, when a 1:1 ratio of H_2:CO is employed, the regioselectivity is low forming a 50:50 mixture of normal:branched products.[24] Slaugh and Mullineaux[24] found that by increasing the ratio of H_2:CO, one can effectively increase the regioselectivity towards linear products.

The aldehydes that are produced during the hydroformylation reaction can subsequently be hydrogenated to alcohols. However, it has been shown that alcohols can also form directly from the acyl complex which forms during the catalytic cycle.[25-26] $HCo(CO)_4$ has a very low hydrogenation ability and therefore the yield of alcohols is normally low. Slaugh and Mullineaux[24] investigated possibilities of replacing one of the CO ligands and introducing phosphine ligands, thereby forming so-called modified cobalt catalysts. The result was a more stable catalyst allowing reactions to proceed at lower pressures, however, the activity of these catalysts were lower than the unmodified cobalt catalysts. Moreover, it was found that these modified cobalt catalysts increased the yield of alcohols due to the increase electron density on the cobalt metal. If alcohols are the desired target product, this is actually advantageous.

It is thus clear that the presence of highly donating ligands (especially phosphine containing ligands) can increase the yield of alcohols. This was further illustrated by the group of Cole-Hamilton[25-26] who showed the direct formation of alcohols from 1-hexene using $[RhH(PEt_3)_3]$ as catalyst precursors. Using labelling studies, they showed that alcohols are the primary product in the hydrocarbonylation of 1-hexene and that it did not proceed through the formation of aldehydes. However, for this to occur, they concluded that a tri(primary alkyl)phosphine must be present as well as a proton source (alcohols and H_2O).

Chapter 4: Evaluation of Rh(I) and Ru(II) Catalyst Precursors in the Hydroformylation of 1-Octene

4.2.1.2.1 Chemoselectivity of Rh(I) catalysts in the hydroformylation of 1-octene

Table 4-4: Chemoselectivity for Rh(I) catalyst precursors[a]

Catalysts	Time (h)	% Conversion	% Internal Octenes	% Octane	% Aldehydes
MC2	8	88	38	2	60
MC2	21	88	6	1	93
C7	8	53	26	4	70
C7	21	83	6	2	92
C8	8	81	26	2	71
C8	21	83	8	2	90
C4	8	40	24	5	71
C4	21	80	7	2	92
C6	8	83	36	2	61
C6	21	90	6	2	92

[a] 1-octene (38 mmol), 30 bar $CO:H_2$ (1:1), 75 °C, 10 ml THF:Toluene (1:1), 0.05 mol % Rh(I)

By performing the reaction at 8 and 21 h, valuable information regarding the chemo – and regioselectivity could be obtained. For **MC2**, **C6** and **C8**, even though the conversion of 1-octene at the two reaction times were high, quite a high degree of alkene isomerization took place over the initial 8 h period. This often is a major side reaction in hydroformylation.[27] Isomerization can be influenced by temperature, pressure and the nature of the ligand. Karapinka and Orchin[28] found that 1-pentene isomerizes to 2-pentene at room temperature and that the isomerization is decreased with increasing CO pressure. The effect of temperature on isomerization is best illustrated by the work of Hughes and Kirshenbaum[29] who showed that isomerization increases with temperature and that it is quite rapid at temperatures above 170 °C. They found that at reaction temperatures above 150 °C, both 1-heptene and 2-heptene registered the same product distributions in the hydroformylation reaction. This was subsequently attributed to isomerization of the alkenes.

For **MC2**, **C6** and **C8**, the amounts of internal octenes obtained were between 25 – 40 % after 8 h reaction time. Therefore, at 8 h the catalysts are chemoselective towards the formation of aldehydes. Since a higher percentage of aldehydes compared to internal octenes is observed, it would suggest that the rate of isomerization of 1-octene is slower than the rate of hydroformylation of 1-octene. In agreement with results by Wender and co-workers[27], in their study of the hydroformylation of 1-hexene using $Co_2(CO)_8$ as catalyst. When they treated 1-hexene at 110 °C and 233 bar $CO:H_2$ (1:1), the product stream consisted of 75 % aldehydes whereas the remaining olefin had a composition of 84 % internal hexenes and 16 % 1-hexene. Since the internal octenes can also undergo hydroformylation to form branched aldehydes, it means that by stopping the reaction after 8 h, the hydroformylation reaction is effectively

Chapter 4: Evaluation of Rh(I) and Ru(II) Catalyst Precursors in the Hydroformylation of 1-Octene

interrupted. This is corroborated by the fact that at 21 h, the percentage internal octenes has considerably decreased and all catalysts are highly chemoselective towards the formation of aldehydes. Chemoselectivity towards aldehydes thus increases with time, which is to be expected. Similarly, Leroux and co-workers[20] also found that by increasing the reaction time from 3 h to 6 h, an increase in the % aldehydes were observed.

The hydrogenation ability of our catalysts is very low since the % octane observed was never significantly high. Furthermore, no hydrogenation of aldehydes to alcohols were observed.

4.2.1.2.2   Regioselectivity of Rh(I) catalysts in the hydroformylation of 1-octene
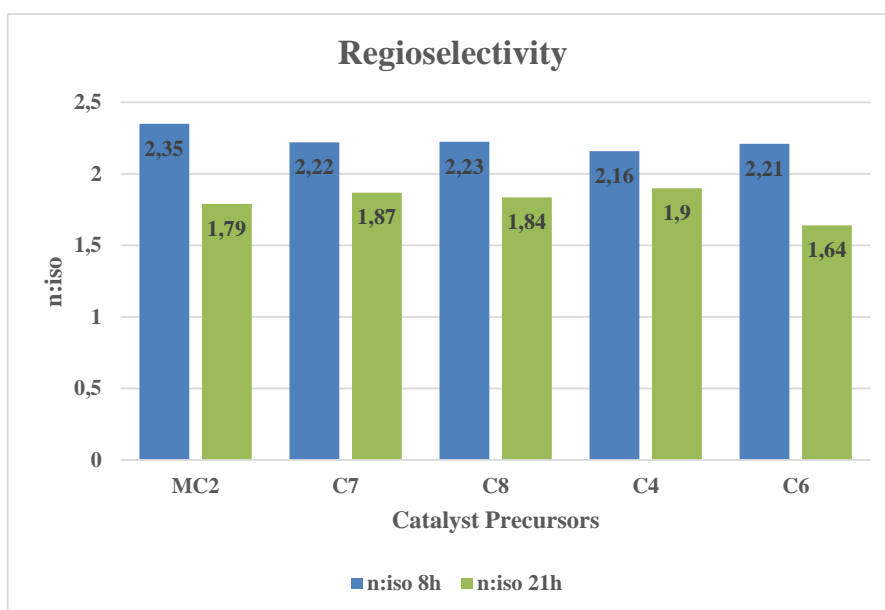
Figure 4-10: Regioselectivity vs time for Rh(I) catalyst precursors; 1-octene (38 mmol), 30 bar CO:H$_2$ (1:1), 75 °C, 10 ml THF:Toluene (1:1), 0.05 mol % Rh(I)

The selectivity between linear and branched aldehydes are very important, since they have such different applications in industry. Linear aldehydes are specifically important for the production of plasticizers and detergents, while branched aldehydes finds application in the pharmaceutical industry. Carpentier and co-workers[30] demonstrated the selective hydroformylation of 10-undecenenitrile to the corresponding linear aldehyde. This linear aldehyde can undergo auto-oxidation when expose to air at room temperature, forming the 10-cyano-2-methyldecanoic acid, which is a precursor for polyamide-12 (nylon-12). The hydroformylation reaction were carried out using [Rh(acac)(CO)$_2$] as catalyst precursor with various phosphine ligands. Of all the phosphine ligands screened, xantphos and biphephos gave the best selectivity towards the linear aldehyde (97 % and 99 % respectively), albeit at

very low conversion of the substrate. When additional experiments were carried out using the [Rh(acac)(CO)$_2$biphephos] catalyst, they found that if the reaction time is significantly extended, the internal olefins can be converted to the linear aldehyde product due to the isomerization of the double bond to the terminal position.

The selective synthesis of the branched aldehyde was demonstrated by Clark and co-workers[31] by the asymmetric hydroformylation of vinyl acetate. Both the *R* and *S* enantiomers were prepared on kilogram scale and used as precursors for the preparation of optically active isoxazolines and imidazoles. The high selectivity towards the branched aldehyde was due to the use of the highly selective (*S*, *S*)-Diazaphospholane ligand.

For our catalyst systems, we observe that they are selective towards the formation of nonanal at short reaction times, however, when the reaction times were extended, this selectivity decreased. The decrease in regioselectivity towards the linear aldehyde is observed due to the hydroformylation of the internal octenes to branched aldehydes. To confirm this, a reaction was performed on 2-octene as substrate using **C6** as catalyst at 30 bar, 75 °C, 8 h and a 1:200 (Rh:substrate) ratio. In terms of the product distribution, 36 % of the 2-octene converted was isomerized products (including 1-octene) and 64 % was aldehydes. The n:iso ratio were 0.19, with 2-methyloctanal the major branched aldehyde formed. The presence of nonanal in the product stream was due to the isomerization of 2-octene to 1-octene.

1-Octene can in theory yield both nonanal and 2-methyloctanal, but it seems that the majority of the 2-methyloctanal formed is due to the hydroformylation of 2-octene (2-octene formed due to the isomerization of 1-octene). It is generally known that terminal olefins are more reactive in hydroformylation compared to their internal counterparts.[27] This was illustrated by Wender and co-workers[27] when they measured the rates of the hydroformylation reaction using various substrates. The rates decreased in the order: straight-chain terminal > straight-chain internal > branched terminal > branched internal > cyclic olefins.
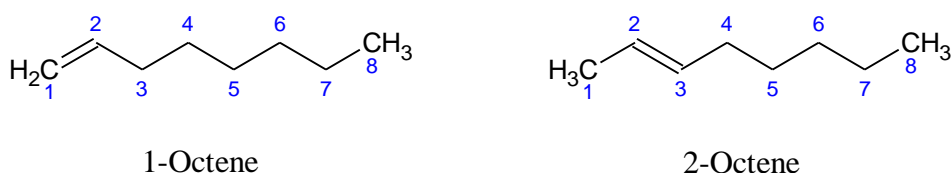

Figure 4-11: Octene substrates

Chapter 4: Evaluation of Rh(I) and Ru(II) Catalyst Precursors in the Hydroformylation of 1-Octene

The major aldehydes formed from the hydroformylation of 1-octene and 2-octene, are nonanal and 2-methyloctanal respectively. For 1-octene, this means that the hydrogen atom from the rhodium hydride species is transferred to C-2, while the formyl group is situated on C-1, forming the linear aldehyde nonanal. In the case of 2-octene, the formyl group is transferred to C-2 with the hydrogen atom on C-3. This is thought to be as a result of steric interactions, since the formation of the least hindered rhodium alkyl species is favoured.

Generally, by extending the reaction time from 8 to 21 h, an increase in the conversion was observed (for **MC2** the conversion remained the same). In addition, a decrease in the % internal octenes and an increase in the % aldehydes is observed which leads to a decrease in the n:iso ratio. This was also previously observed by Leroux and co-workers[20] when they studied the hydroformylation of 1-octene using [Rh(CO)$_2$acac] as catalyst precursor in the presence of dibenzophosphole ligands.

Table 4-5: Hydroformylation using [Rh(CO)$_2$acac][20]

Time (h)	% Conversion	% Internal Octenes	% Aldehydes	n:iso
3	96	6	94	66:34
6	98	1.5	98.5	61:39

When they extended the reaction time from 3 to 6 h, the conversion and the % aldehydes increased slightly while a decrease in the % internal octenes was observed. Similarly to our systems, they observed an increase in the amount of the iso product with increasing time and conversion.

75

4.2.1.3 Influence of pressure and temperature on the activity and selectivity for C6

The influence of pressure and temperature on the activity and selectivity of the reaction was investigated. All reactions were performed at 8 h using **C6** as the catalyst precursor. The first parameter investigated was the pressure at a constant temperature of 75 °C:

Influence of pressure on conversion
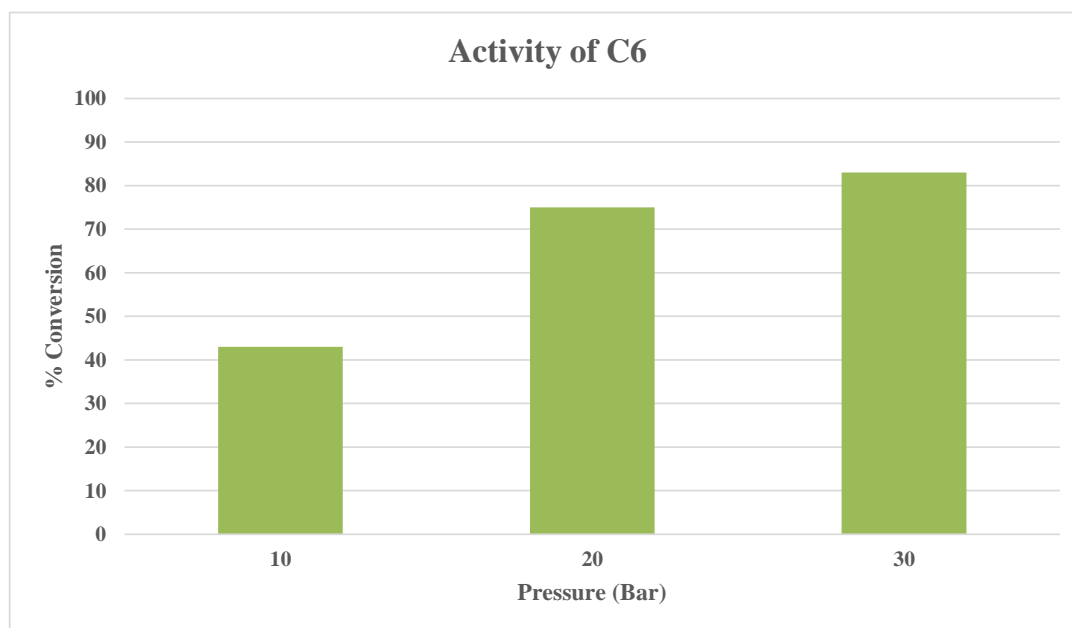
Figure 4-12: Influence of pressure on the conversion of C6; CO:H$_2$ (1:1) 1-octene (38 mmol), 75 °C, t = 8 h, 10 ml THF:Toluene (1:1), 0.05 mol % Rh(I)

Performing the reaction at lower pressures led to a decrease in the conversion of 1-octene. The catalyst precursor, **C6**, needs to be converted to the active species *in situ*. The active species involves the formation of Rh-H and Rh-CO moieties. We rationalize that in the presence of a lower syngas pressure, the formation of the active species is retarded, and thus results in a decrease in the catalytic activity. A significant increase in the conversion was observed when the pressure was increased from 10 bar to 20 bar (increase of 32 % in conversion), while only a small increase is observed when the pressure is raised between 20 bar and 30 bar (increase of 8 %). It is assumed that at higher pressures, the formation of the active species is faster, allowing for an increase in the hydroformylation rate. Similar results were observed by Wang and co-workers[32], when they studied the hydroformylation of 1-octene using poly(ethylene glycol)-stabilized Rh nanoparticles. When they decreased the pressures, they observed a slight decrease in the conversion of 1-octene. A more significant decrease in the conversion at lower pressure was observed by Khan and Bhanage[33], when

they investigated the regioselective hydroformylation of vinyl acetate using $Rh(acac)(CO)_2$ and diphosphinite ligands.

This thus illustrates how the pressure of the reaction can influence the catalytic efficiency of a particular catalyst. It is thus paramount to always work at the optimum pressure for a particular catalyst.

Influence of pressure on selectivity

Table 4-6: Influence of pressure on the selectivity for C6[a]

P (Bar)	% Conversion	% Internal Octenes	% Octane	% Aldehydes	n:iso	TON_{ald}[b]
10	43	54	5	41	2.82	353
20	75	39	3	58	2.54	874
30	83	36	3	61	2.21	1017

[a] $CO:H_2$ (1:1), 1-octene (38 mmol), t = 8 h, 75 °C, 10 ml THF:Toluene (1:1), 0.05 mol % Rh(I)

[b] TON_{ald} = (mol aldehyde/mol Rh)

Pressure did not only have an effect on the catalytic activity of the catalyst, it also had a marked effect on the chemo – and regioselectivity. By decreasing the pressure of the reaction to 10 bar, 54 % of the product stream consisted of internal octenes. This is an indication that as you decrease the pressure, isomerization becomes more prominent, which is in agreement with reports in literature.[34] This observation can be explained by referring to the mechanism of the reaction. After coordination of the substrate to the rhodium centre, a π-complex is formed followed by the insertion of the olefin into the Rh-H moiety resulting in a rhodium alkyl species. This is followed by the insertion of CO. The insertion of CO is normally fast, however, at lower pressure the insertion is slowed down, allowing for isomerization to take place via a series of β-hydride transfers and alkene insertion reactions. At higher pressures, isomerization is suppressed and hydroformylation starts dominating. This can be observed in Table 4-6. The % aldehydes increases as the pressure is increased (41 % at 10 bar and 61 % at 30 bar). The effect of pressure is better illustrated by the TON_{ald} (moles of aldehydes formed divided by the moles of rhodium). The TON almost triples as the pressure is increased from 10 bar to 30 bar.

Table 4-7: Hydroformylation using Rhodium nanoparticles[34]

P (Bar)	% Conversion	% Internal Octenes	% Aldehydes	n:iso
20	100	60	40	0.8
30	100	42	58	0.7
40	100	13	87	0.8
50	100	<1	>99	1.2

Chapter 4: Evaluation of Rh(I) and Ru(II) Catalyst Precursors in the Hydroformylation of 1-Octene

Table 4-7 summarizes work published by Wang and co-workers[34] where they studied the hydroformylation of 1-octene using Rh nanoparticles in a thermoregulated ionic liquid and organic biphasic system. The influence of pressure on the chemoselectivity is quite clear from the table.

The influence of pressure on the regioselectivity of **C6** is demonstrated by the n:iso ratios. We observed that as the pressure decreased, so an increase in the regioselectivity towards the linear aldehyde was observed. This is due to the fact that at lower pressures, the conversion of the internal octenes to the branched aldehydes is much slower due to the higher reactivity of terminal alkenes such as 1-octene, resulting in the linear aldehyde to be the major product.[27] As the pressure increases, internal octenes are hydroformylated to branched aldehydes, which explains the decrease in the n:iso ratio.

Influence of temperature on conversion and selectivity

Table 4-8: Influence of temperature on the conversion and selectivity for C6[a]

Temp (°C)	% Conversion	% Internal Octenes	% Octane	% Aldehydes	n:iso	TON$_{ald}$[b]
50	0	~	~	~	~	~
75	83	36	3	61	2.21	1017
100	89	16	1	83	1.43	1481

[a] **1-octene (38 mmol), 30 bar CO:H$_2$ (1:1), t = 8 h, 10 ml THF:Toluene (1:1), 0.05 mol % Rh(I)**

[b] **TON$_{ald}$ = (mol aldehyde/mol Rh)**

When the temperature was decreased to 50 °C, no conversion of 1-octene was observed. Increasing the temperature to 100 °C leads only to a slight increase in the conversion. Temperature, however, had the greatest influence on the selectivity. From literature[29] we know that isomerization becomes faster with increasing temperature. Comparing the % internal octenes at 75 and 100 °C does not reveal this directly, since the increase in temperature did not only increase the rate of isomerization, but also increased the rate of hydroformylation. This is confirmed by the 22 % increase in the % aldehydes as well as the increase in the TON$_{ald}$ from 1017 at 75 °C to 1481 at 100 °C. Furthermore, the n:iso ratio decrease significantly. There is thus more branched aldehydes at 100 °C compared to 75 °C. As mentioned previously, branched aldehydes are essentially the result of the hydroformylation of the internal octenes. This significant decrease in the n:iso ratio thus confirms that at higher temperatures, isomerization of the olefin is faster, and this increases the yield towards branched aldehydes. However, the n:iso is now closer to unity, making the catalyst system not that selective towards a specific aldehyde product at this temperature.

In conclusion, the aforementioned results underlined how the conditions of the reaction can influence the activity and selectivity of the catalysts. The selectivity towards nonanal is high and it seems to increase with a decrease in pressure. However, at lower pressures, the isomerization also increased. Temperature had a marked effect on the rates of isomerization and hydroformylation.

4.2.2 Catalysis using Ru(II) catalyst precursors

Alternative metals are being investigated for utilization in hydroformylation, due to the high cost of rhodium. In a review published by Beller and co-workers[23], they described the application of Ru, Ir, Pd, Pt and Fe complexes in the hydroformylation process. It was shown that complexes based on these "alternative" metals are far less active compared to Rh catalysts, and that the TOF's need to improve by two orders of magnitude in order for it to become economically viable.

Herein we describe the use of five different Ru(II) complexes (prepared in Chapter 3) as catalyst precursors in the hydroformylation of 1-octene. When these ruthenium catalyst precursors were tested under the same conditions as the Rh(I) catalyst precursors discussed earlier, it was found that the former showed no activity. This is in agreement with previous observations that ruthenium tends to be less active than rhodium in hydroformylation and often requires more stringent reaction conditions. In addition, higher catalyst loadings are usually also required. It has previously been found that ruthenium catalyzed hydroformylation tends to be accompanied with a high level of hydrogenation of both olefins and aldehydes. Huakka and co-workers[35] studied the hydroformylation of 1-hexene using the linear chain polymeric ruthenium carbonyl cluster $[Ru(CO)_4]_n$. The activity of the polymer was higher than the commonly utilized trinuclear ruthenium carbonyl cluster, $Ru_3(CO)_{12}$. However, the former led to the hydrogenation of the aldehydes to alcohols. If alcohols are the target products, then this is not a problem, however, ways to circumvent aldehyde reduction is to perform a so-called tandem reaction. An example of this is a report published by Börner and co-workers[36], where they studied the tandem hydroformylation-acetalization of 1-octene using a ruthenium catalyst. In this case, they trapped the aldehydes as cyclic acetals using ethylene glycol, but various other alcohols could also be employed.

Since the Ru(II) systems were inactive at 30 bar and 75 °C, more harsher conditions were employed. In a paper published by Smith and co-workers[37], various Ru(II) arene complexes were utilized as catalyst precursors in the hydroformylation of 1-octene. They utilized a

Chapter 4: Evaluation of Rh(I) and Ru(II) Catalyst Precursors in the Hydroformylation of 1-Octene

pressure of 50 bar and temperatures between 100 – 125 °C. We decided to employ modified conditions from this paper for our catalyst precursors: 45 bar, 120 °C, t = 8, 21, 24 h and a catalyst loading of 0.5 mol% (1:200). Similarly to the rhodium catalysts discussed earlier, the specific amount of moles for each catalyst were varied in order to work at a constant ruthenium concentration.
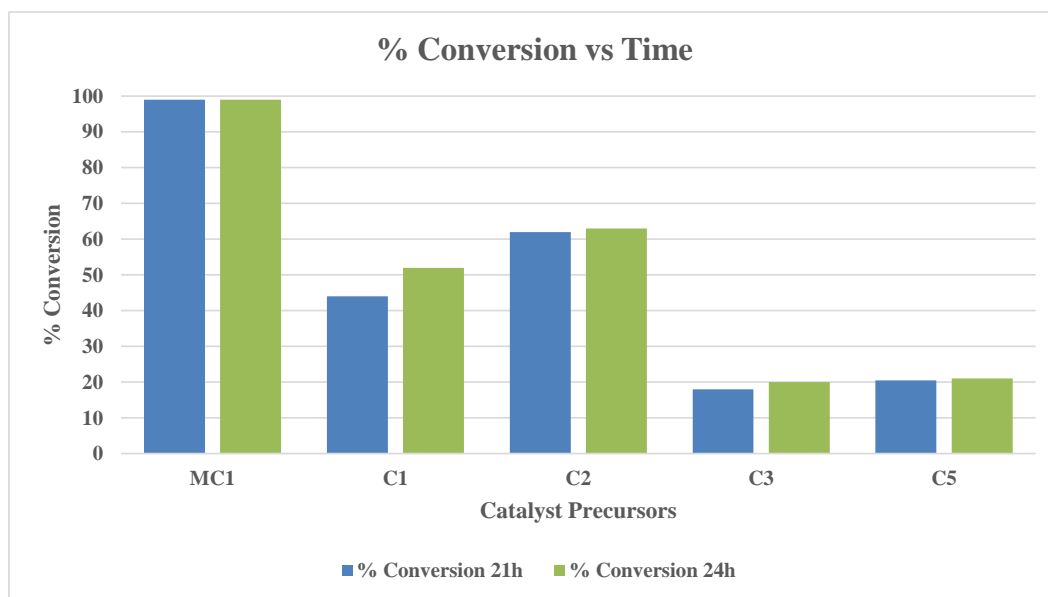
4.2.2.1 Conversion vs Time

Figure 4-13: Conversion vs Time for Ru(II) catalyst precursors; 1-octene (3.8 mmol), 45 bar CO:H$_2$ (1:1), 120 °C, 10 ml THF:Toluene (1:1), 0.5 mol % Ru(II)

The catalyst precursors were tested at three different reaction times as mentioned above. At 8 h, all the catalyst precursors converted only traces of 1-octene, except for **MC1** which converted 11 % of the 1-octene. The Ru(II) catalysts thus seem to have relatively long induction periods, with the result that they require longer reaction times.

As was the case for the Rh(I) systems discussed earlier (**MC2** vs **C7**), **MC1** is more active than **C1**.

Figure 4-14 shows the structures of **MC1** and **C1**. The influence of the phenol group on the metal centre was discussed earlier under section **4.2.1.1**.

80

Chapter 4: Evaluation of Rh(I) and Ru(II) Catalyst Precursors in the Hydroformylation of 1-Octene
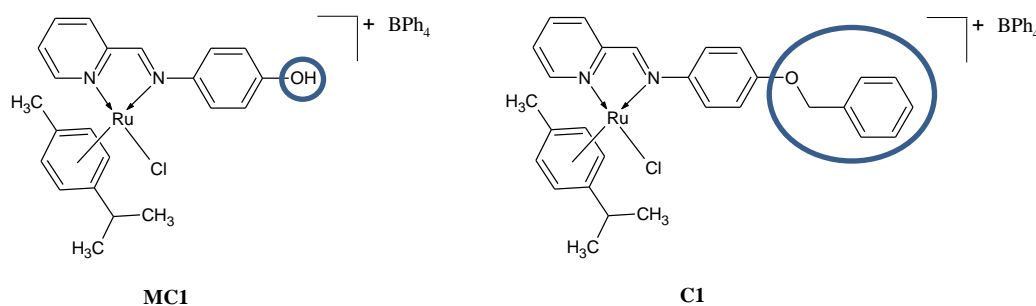

Figure 4-14: MC1 and C1

MC1 converted 99 % of 1-octene over 21 h. The highest conversion achieved with **C1** was 52 % at 24 h. **MC1** is thus twice as active as **C1**. The bi-nuclear catalyst, **C2**, gave a conversion of 63 % after 24 h, which is higher than what was obtained using **C1**. This we attribute to the extra Ru centre, making the catalyst more active. Similarly, Mapolie and co-workers[38] studied the oligomerization of ethylene using G1 (generation 1) and G2 (generation 2) dendritic nickel catalysts. The overall activity of the G2 nickel catalyst (4 Ni(II) centres) was higher than the analogous G1 nickel catalyst (2 Ni(II) centres), albeit at higher Al:Ni ratios (aluminium co-catalyst). However, in the case of the hydroformylation reactions studied here, the tri-nuclear (**C3**) and tetra-nuclear catalyst (**C5**) precursors did not follow the expected trend, and registered very low conversions of around 20 %. **C3** and **C5** were found to be insoluble in the reaction solvents under the reaction conditions tested. It would thus appear as if these catalysts were behaving as heterogeneous catalysts, and this might explain the low activity of these systems. **MC1**, **C1** and **C2**, on the other hand, are soluble and can thus behave as homogeneous catalysts which were more active than the "heterogeneous" catalysts. Having said that, these "heterogeneous" catalysts, **C3** and **C5**, could be recovered from the reaction medium and this will be discussed further on.

The activity of the ruthenium catalysts were also expressed in terms of TON's.

Table 4-9: TON's for Ru catalyzed reactions of 1-octene hydroformylation at 24 h

Catalysts	TON[a]
MC1	198
C1	105
C2	126
C3	41
C5	43

[a]TON = (mol product/mol Ru)

4.2.2.2 Selectivity

4.2.2.2.1   Chemoselectivity

Table 4-10: Chemoselectivity for the Ru(II) catalyst precursors at 24 h[a]

Catalysts	% Conversion	% Internal Octenes	% Octane	% Aldehydes
MC1	99	2	1	97
C1	52	53	5	42
C2	63	48	4	48
C3	20	50	11	39
C5	21	61	11	29

[a]1-octene (3.8 mmol), 45 bar CO:H_2, 120 °C, 10 ml THF:Toluene (1:1), 0.5 mol % Ru(II)

Hydroformylation performed by ruthenium catalysts systems often suffer from high isomerization capacities. It is thus no surprise when our systems showed similar behaviours. For all the catalyst systems, except for **MC1**, the % internal octenes were around 50 % and in some cases even higher levels. In the case of **MC1**, the % internal octenes is low due to the higher hydroformylation activity of this catalyst compared to the other systems (**C1 – C3** and **C5**). Thus, any internal octenes formed using **MC1** is rapidly converted to aldehydes. It is thus found that this catalyst is ultimately chemoselective towards the formation of aldehydes under these reaction conditions (P = 45 bar (1:1 CO:H_2), T = 120 °C, t = 24 h), while the other ruthenium catalysts evaluated display poor chemoselectivity.

The Huakka group[39-41] has published a number of reports on the development of supported Ru catalysts for olefin hydroformylation. They developed a ruthenium 2,2'-bipyridine catalyst, supported on silica, for the hydroformylation of 1-hexene.[39] These types of catalysts showed a high tendency to isomerize the 1-hexene to its internal counterparts. Even when different types of impregnation solvents or silica supports were utilized, the isomerization was still high. They also developed pyrazine based ruthenium catalysts for the same substrate.[40] The activity of the catalysts were relatively low (54 % conversion) with 23 % of the product distribution constituting internal hexenes. In another study, $[Ru(CO)_3Cl_2]_2$ was microencapsulated into poly(4-vinylpyridine) cross-linked with 25 % divinylbenzene, and utilized in the hydroformylation of 1-hexene.[41] This catalyst displayed high conversions of the substrate (93 %) in NMP, however, 19 % of the product stream consisted of internal hexenes. When toluene was used as the solvent, there was a dramatic increase in the isomerization of 1-hexene (75 %). It is thus clear that ruthenium catalysts have quite high isomerization capabilities which is also dependant on the nature of the solvent in which the catalysis is performed.

Chapter 4: Evaluation of Rh(I) and Ru(II) Catalyst Precursors in the Hydroformylation of 1-Octene

In addition to its high isomerization abilities, ruthenium catalysts also have the capability to hydrogenate the aldehydes formed during hydroformylation, to alcohols. In the paper by Huakka and co-workers[39] on the ruthenium 2,2'-bipyridine catalyst, they attributed the hydrogenation ability of the catalyst to the presence of the *N,N* chelating ligand, 2,2'-bipyridine. This ligand increases the electron density on the ruthenium metal centre, thereby increasing its hydrogenation ability. This was also previously found in the case of cobalt hydroformylation, after the introduction of highly electron donating phosphine ligands. However, high hydrogenation of the aldehydes were also observed when the unsupported $[Ru(CO)_3Cl_2]_2$ catalyst were used.[41] This complex does not contain any N or P donating ligands and therefore the hydrogenation must be due to the ruthenium metal centre. For our systems, no hydrogenation of the aldehydes to alcohols was observed, even in the presence of chelating nitrogen ligands. The only hydrogenation that occurred was that of 1-octene to octane, but this was almost never significant. This results are specifically significant for **MC1**, since the yield of aldehydes using this catalyst is quite high. The aldehydes can thus be isolated and utilized as precursors for other more value-added materials.

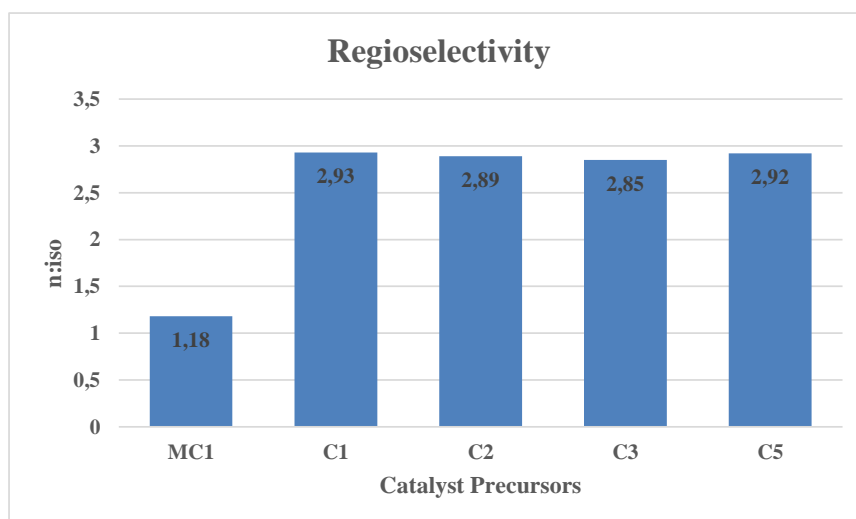### 4.2.2.2.2   Regioselectivity of Ru(II) catalysts

Figure 4-15: Regioselectivity for the Ru(II) catalyst precursors at 24 h; 1-octene (3.8 mmol), 45 bar CO:H$_2$, 120 °C, 10 ml THF:Toluene (1:1), 0.5 mol % Ru(II)

The importance of the regioselectivity between linear and branched aldehydes has been discussed previously. For our ruthenium systems we found that the most active catalyst, **MC1**, registered a n:iso ratio of 1.18 (l:b, 54:46). Under these conditions, very little regio-control is thus observed while the other ruthenium catalyst systems (**C1** – **C3**, **C5**) displays

higher regioselectivity towards the linear aldehyde, nonanal. Under these conditions, these catalysts are more regioselective than **MC1**, however this is accompanied with lower conversions and poor chemoselectivity (extensive isomerization of 1-octene). Since the internal octenes are subsequently converted to branched aldehydes, this will result in an increase in the regioselectivity towards branched aldehydes and therefore a lower n:iso ratio. The low n:iso ratio of **MC1** is thus an indication that quite extensive isomerization must have taken place, with the subsequent hydroformylation of the internal octenes to the branched aldehydes, resulting in the n:iso ratio of 1.18.

It is clear that hydroformylation of 1-octene using **C1**-**C3** and **C5** mostly results in the production of nonanal under these reaction conditions. These ruthenium catalysts, as was the case with the rhodium catalysts discussed earlier, prefer the formation of the least hindered ruthenium alkyl species, owing to steric interactions.
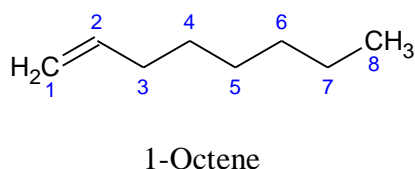

1-Octene

Figure 4-16: 1-Octene substrate

In addition to steric interactions, the electron donation ability of the ligand must also be taken into account. This will increase the electron density on the metal. The more electron rich the metal hydride is, the less likely it is to behave as a proton. This, in turn, will direct the hydride to the carbon containing the least number of hydrogens (C-2), resulting in the normal aldehyde to be the major product (nonanal).

C3 and **C5** could be recovered after catalysis and analysed using FT-IR spectroscopy. Figure 4-17 shows the IR spectrum of **C5** before catalysis, while Figure 4-18 shows the spectrum of the recovered catalyst after catalysis.

Chapter 4: Evaluation of Rh(I) and Ru(II) Catalyst Precursors in the Hydroformylation of 1-Octene
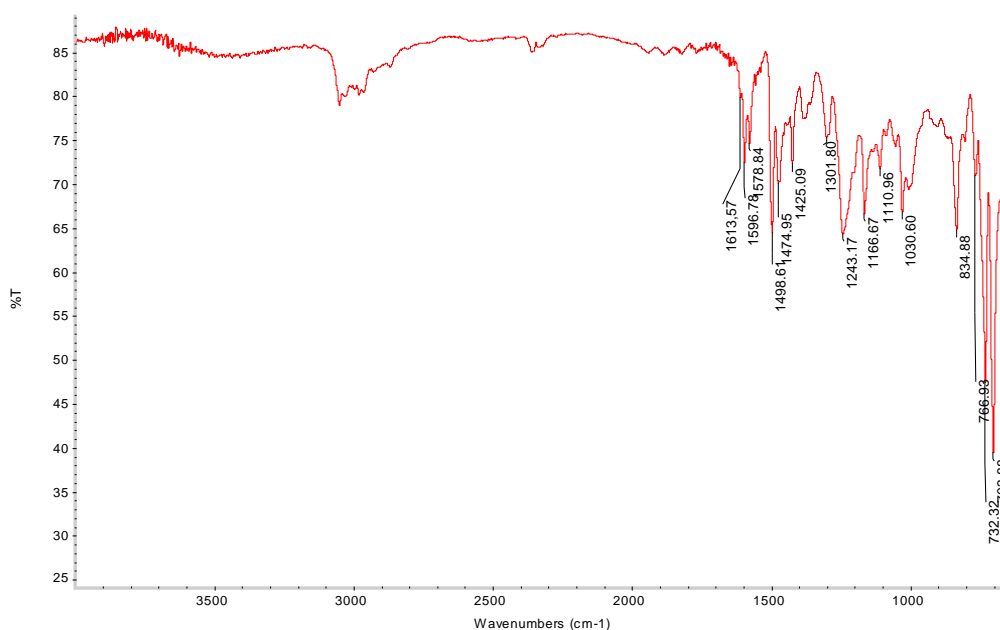
Figure 4-17: C5 before catalysis

After using the catalyst precursor in catalysis and recovering it, the IR spectrum showed significant differences as shown below:

Figure 4-18: C5 after catalysis

The absorbances around 2000 cm^{-1} dominates the spectrum. This is the region where Ru-H (2061 cm^{-1}) and Ru-CO (1950, 1994 and 2032 cm^{-1}) moieties normally occurs. The IR results is thus potential evidence how the catalyst precursor is converted to the active catalyst *in situ*.

85

Chapter 4: Evaluation of Rh(I) and Ru(II) Catalyst Precursors in the Hydroformylation of 1-Octene

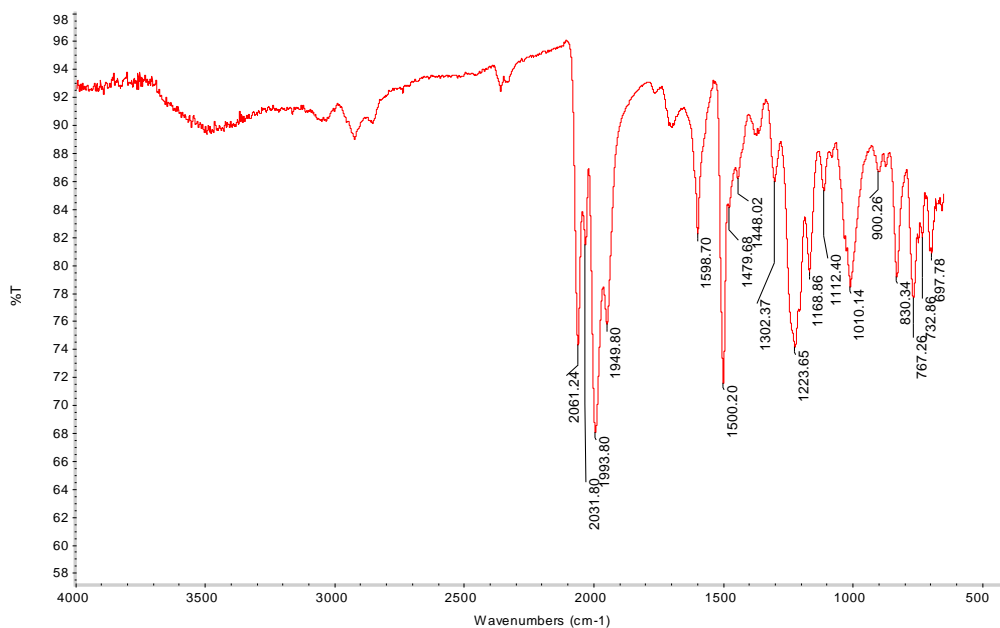Two of the analogous rhodium catalysts (**MC2** and **C4**) were tested under the same reaction conditions as the ruthenium catalyst in order to compare the activities of these two metals under more robust conditions.

Table 4-11: Chemo - and regioselectivity for the Rh(I) catalyst precursors[a]

Cat.	Time (h)	% Conv.	% Int. Octenes	% Octane	% Ald.	n:iso	TON[b]
MC2	2	96	5	2	92	1.46	192
MC2	8	100	0	1	99	1.34	200
C4	2	90	13	2	84	1.66	179
C4	8	100	0	1	99	1.38	200

[a]1-octene (3.8 mmol), 45 bar CO:H$_2$, 120 °C, 10 ml THF:Toluene (1:1), 0.5 mol % Rh(I)

[b]TON = (mol product/mol Rh)

Both **MC2** and **C4** registered conversion around 90 % after only two hours. Both the catalysts displays a slight selectivity to the linear aldehyde. The % internal octenes is low since it was converted to the branched aldehydes. Lastly, this confirms the high activity of rhodium in hydroformylation compared to the other metals.

4.3 Conclusion

In conclusion, five novel Rh(I) and five novel Ru(II) catalyst precursors were tested in the hydroformylation of 1-octene. The Rh(I) catalyst precursors displayed relatively high activities which is comparable to other systems in the literature. Owing to steric interactions, the linear aldehyde was the major product. The branched aldehydes largely resulted from the hydroformylation of internal octenes, as was confirmed when a separate reaction was performed using 2-octene as substrate. In this case, 2-methyloctanal was once again the major product which formed. The chemoselectivity towards aldehydes increased as the reaction time was extended due to the hydroformylation of the internal octenes that was initially formed. As such, the regioselectivity towards the branched aldehydes also increased.

In terms of the Ru(II) catalyst precursors, the bi-nuclear catalyst was more active than its mononuclear counterpart. However, both these catalysts were more active than the "heterogeneous" catalysts, **C3** and **C5**. **MC1** was the best performing Ru(II) catalyst registering full conversion of the substrate after 21 h. However, this was accompanied with poor regioselectivity. The other ruthenium catalysts displayed good regioselectivity towards the linear aldehyde, albeit at lower conversions and with poor chemoselectivity.

Lastly, the mononuclear complexes bearing the phenol group was more active than the mononuclear complexes bearing the benzyl ether. This was attributed to the weaker donating

effect of the phenol group. The Rh(I) and Ru(II) bi-nuclear catalysts were more active than their mononuclear counterparts due to the increased local concentration of metal ions. However, the activities of the tri- and tetra-nuclear complexes were governed largely by solubility of the complexes. Low solubility resulted in low activity.

4.4   Experimental Section

General Methods and Materials

All of the reagents and standards were purchased from either Merck or Sigma Aldrich and were used without further purification. Solvents were purchased from Merck or Kimix, and were purified by a Pure Solv^{TM} Micro solvent purifier equipped with activated alumina columns.

Syngas (CO:H$_2$, 1:1) was purchased from Afrox and used as is.

Instrumentation

Catalytic reactions were performed in a 250 ml Berghoff reactor equipped with a Teflon liner. Catalytic reactions were monitored using a Varian 3900 Gas Chromatograph containing a Cyclosil-β (30 m x 0.25 mm x 0.25 μm) column equipped with a FID detector. Temperature program: 80 °C (6 min hold), 100 °C (10 °C/min), 100 °C (10 min hold), 220 °C (20 °C/min), 220 °C (10 min hold), with total run time of 34 min. Helium was used as carrier gas at constant flow with a 1.1 ml/min flowrate. P-Xylene was used as the internal standard.

Catalytic Procedure and Analysis

The following procedure describes a representative example of a typical rhodium hydroformylation reaction and its analysis using GC-FID. All experiments were performed in duplicate:

The reactor was charged with 5 ml THF and the appropriate amount of the catalyst precursor to yield a mixture containing a total amount of 0.019 mmol of rhodium. The catalyst precursor was dissolved or suspended in THF, after which 5 ml toluene was added. 5.97 ml 1-octene (38 mmol) was added resulting in a Rh:substrate ratio of 1:2000. The reactor was purged with 30 bar syngas after which the reactor was pressurized up to the required pressure and time and the heating started. At the conclusion of the reaction, the reactor was cooled in an ice-water bath for 30 min. After quenching, the reaction mixture was filtered using a

syringe filter. 0.15 ml of the reaction mixture, 0.05 ml p-xylene and 0.8 ml THF:Toluene were transferred to a GC vial and submitted for analysis. Substrate conversion, product distributions and chemo – and regioselectivities were calculated relative to the internal standard.

The following procedure describes a representative example of a typical ruthenium hydroformylation reaction and its analysis using GC-FID:

The reactor was charged with 5 ml THF and the appropriate amount of the catalyst precursor to yield a mixture containing a total amount of 0.019 mmol of ruthenium. The catalyst precursor was dissolved or suspended in THF, after which 5 ml toluene was added. 0.597 ml 1-octene (3.80 mmol) was added resulting in a Ru:substrate ratio of 1:200. The reactor was purged with 30 bar syngas after which the reactor was pressurized up to the required pressure and time and the heating started. At the conclusion of the reaction, the reactor was cooled in an ice-water bath for 30 min. After quenching, the reaction mixture was filtered using a syringe filter. 0.95 ml of the reaction mixture and 0.05 ml p-xylene were transferred to a GC vial and submitted for analysis. Substrate conversion, product distributions and chemo – and regioselectivities were calculated relative to the internal standard.

4.5   References

1. G. T. Whiteker and C. J. Cobley, *Top. Organomet. Chem.*, 2012, **42**, 35-46.
2. J. G. da Silva, H. J. V. Barros, A. Balanta, A. Bolanos, M. L. Novoa, M. Reyes, R. Contreras, J. C. Bayon, E. V. Gusevskaya and E. N. dos Santos, *Appl Catal A: Gen*., 2007, **326**, 219-226.
3. C. Botteghi, C. Delogu, M. Marchetti, S. Paganelli and B. Sechi, *J Mol Catal A: Chem*., 1999, **143**, 311-323.
4. R. F. Heck and D. S. Breslow, *J. Am. Chem. Soc.*, 1961, **83**, 4023-4027.
5. M. Caporali, P. Frediani, A. Salvini and G. Laurenczy, *Inorg. Chim. Acta*, 2004, **357**, 4537-4543.
6. E. B. Hager, B. C. E. Makhubela and G. S. Smith, *Dalton Trans.*, 2012, **41**, 13927-13935.
7. B. E. Ali, *Catal. Commun.*, 2003, **4**, 621-626.
8. S. B. Khan and B. M. Bhanage, *Tetrahedron Lett.*, 2013, **54**, 5998-6001.
9. A. A. Dabbawala, R. V. Jasra and H. C. Bajaj, *Catal. Commun.*, 2011, **12**, 403-407.
10. B. C. E. Makhubela, A. M. Jardine, G. Westman and G. S. Smith, *Dalton Trans.*, 2012, **41**, 10715-10723.

11. M. Madalska, P. Lönnecke and E. Hey-Hawkins, *J Mol Catal A: Chem.*, 2014, **383-384**, 137-142.

12. N. C. Antonels, J. R. Moss and G. S. Smith, *J. Organomet. Chem.*, 2011, **696**, 2003-2007.

13. B. E. Hanson and M. E. Davis, *J. Chem. Educ.*, 1987, **64**, 928-930.

14. A. Aghmiz, A. Orejón, M. Diéguez, M. D. Miquel-Serrano, C. Claver, A. M. Masdeu-Bultó, D. Sinou and G. Laurenczy, *J Mol Catal A: Chem.*, 2003, **195**, 113-124.

15. T. Mizugaki, M. Ooe, K. Ebitani and K. Kaneda, *J. Mol. Catal. A: Chem.*, 1999, **145**, 329-333.

16. G. Smith, R. Chen and S. F. Mapolie, *J. Organomet. Chem.*, 2003, **673**, 111-115.

17. R. Chen, J. Bacsa and S. F. Mapolie, *Inorg. Chem. Commun.*, 2002, **5**, 724-726.

18. R. Chen and S. F. Mapolie, *J. Mol. Catal. A: Chem.*, 2003, **193**, 33-40.

19. R. C. Matthews, D. K. Howell, W. Peng, S. G. Train, W. D. Treleaven and G. G. Stanley, *Angew. Chem. Int. Ed. Engl.*, 1996**, 35***, 2253-2256.

20. A. Oukhrib, L. Bonnafoux, A. Panossian, S. Waifang, D. H. Nguyen, M. Urrutigoity, F. Colobert, M. Gouygou and F. R. Leroux, *Tetrahedron*, 2014, **70**, 1431-1436.

21. L. Maqeda, B. C. E. Makhubela and G. S. Smith, *Polyhedron*, 2015, **91**, 128-135.

22. S. Chen, Y. Wang, Y. Li, X. Zhao and Y. Liu, *Catal. Commun.*, 2014, **50**, 5-8.

23. J. Pospech, I. Fleischer, R. Franke, S. Buchholz and M. Beller, *Angew. Chem. Int. Ed.*, 2013, **52**, 2852-2872.

24. L. H. Slaugh and R. D. Mullineaux, *J. Organomet. Chem.*, 1968, **13**, 469-477.

25. J. K. MacDougall, M. C. Simpson, M. J. Green and D. J. Cole-Hamilton, *J. Chem. Soc., Dalton Trans.*, 1996, 1161-1172.

26. M. C. Simpson, A. W. S. Currie, J. M. Andersen, D. J. Cole-Hamilton and M. J. Green, *J. Chem. Soc., Dalton Trans.*, 1996, 1793-1800.

27. I. Wender, S. Metlin, S. Ergun, H. W. Sternberg and H. Greenfield, *J. Am. Chem. Soc.*, 1956, **78**, 5401-5405.

28. G. L. Karapinka and M. Orchin, *J. Org. Chem.*, 1961, **26**, 4187-4190.

29. V. L. Hughes and I. Kirshenbaum, *Ind. Eng. Chem.*, 1957, **49**, 1999-2003.

30. J. Ternel, J. Couturier, J. Dubois and J. Carpentier, *Adv. Synth. Catal.*, 2013, **355**, 3191-3204.

31. P. J. Thomas, A. T. Axtell, J. Klosin, W. Peng, C. L. Rand, T. P. Clark, C. R. Landis and K. A. Abboud, *Org Letters*, 2007, **9**, 2665-2668.

32. Z. Sun, Y. Wang, M. Niu, H. Yi, J. Jiang and Z. Jin, *Catal. Commun.*, 2012, **27**, 78-82.

33. S. Khan and B. M. Bhanage, *Catal. Commun.*, 2014, **46**, 109-112.

34. Y. Xu, Y. Wang, Y. Zeng, J. Jiang and Z. Jin, *Catal Lett.*, 2012, **142**, 914-919.

35. L. Oresmaa, M. A. Moreno, M. Jakonen, S. Suvanto and M. Haukka, *Appl. Catal., A*, 2009, **353**, 113-116.

36. J. Norinder, C. Rodrigues and A. Börner, *J. Mol. Catal. A: Chem.*, 2014, **391**, 139-143.

37. L. C. Matsinha, P. Malatji, A. T. Hutton, G. A. Venter, S. F. Mapolie and G. S. Smith, *Eur. J. Inorg. Chem.*, 2013, 4318-4328.

38. R. Malgas, S. F. Mapolie, S. O. Ojwach, G. S. Smith and J. Darkwa, *Catal. Commun.*, 2008, **9**, 1612-1617.

39. M. Haukka, L. Alvila and T. A. Pakkanen, *J. Mol. Catal. A: Chem.*, 1995, **102**, 79-92.

40. M. A. Moreno, M. Haukka, A. Turunen and T. A. Pakkanen *J. Mol. Catal. A: Chem.*, 2005, **240**, 7-15.

41. M. Kontkanen and M. Haukka, *Catal. Commun.*, 2012, **23**, 25-29.

Chapter 5 : Concluding remarks and Future Prospects

5.1 Concluding remarks

The main aim of this project was the development of mono- and multi-nuclear rhodium and ruthenium complexes and their application as catalyst precursors in the hydroformylation of 1-octene.

The synthesis of the ligands was a two-step process, initially involving a Schiff base condensation reaction between 2-pyridinecarboxaldehyde and p-aminophenol. The resulting hydroxy functionalized pyridine-imine underwent a nucleophilic substitution reaction with appropriate benzyl bromide derivatives to yield four novel iminopyridyl ligands. Characterization of these ligands were carried out using IR and NMR spectroscopy (^{1}H and ^{13}C), mass spectrometry, elemental analysis and melting point determinations.

Upon successful synthesis of the ligands (**L1**-**L4**), they were complexed to Rh(I) and Ru(II) metal precursors. The hydroxy functionalized pyridine-imine compound was also complexed to Rh(I) and Ru(II) metal precursors. The result was five Rh(I) (**MC2**, **C7**, **C8**, **C4** and **C6**) and five Ru(II) (**MC1**, **C1**-**C3** and **C5**) metal complexes. These complexes were then characterized using IR and NMR spectroscopy (^{1}H and ^{13}C), mass spectrometry, elemental analysis and melting point determinations. The metal ions coordinate to the imine and pyridyl moieties and as such changes in these moieties were monitored in order to confirm successful complexation. IR and NMR spectroscopy revealed the expected shifts. In the ESI-MS (positive mode), the molecular ions could be observed for all the Ru(II) complexes, however, for the Rh(I) complexes, the molecular ion was only observed for **MC2**, **C7** and **C8**. In the case of **C4** and **C6**, an ion corresponding to [Rh(COD)(MeCN)] was observed.

All the complexes were utilized as catalyst precursors in the hydroformylation of 1-octene. Relatively high activities were obtained using the rhodium complexes at 30 bar, 75 °C, 0.05 mol % and reaction times of 8 and 21 h. Solubility proved to be very important, since the bi-nuclear complex outperformed the tri-nuclear complex, with the latter having a lower solubility. When the ruthenium complexes were tested under the same conditions as the rhodium complexes, very low activity was observed. In terms of the chemoselectivity, all the catalysts were chemoselective towards aldehydes when tested over an 8 h reaction period, with increasing chemoselectivity with increasing reaction time. Linear regioselectivity was

Chapter 5: Concluding remarks and Future Prospects

also relatively high, however, it decreased with increasing reaction time. The influence of the pressure and temperature on the activity and selectivity were also investigated. It was found that a decrease in pressure led to a decrease in the activity, however, it led to an increase in the linear regioselectivity. Temperature had a profound effect on the rate of alkene isomerization and hydroformylation. The ruthenium complexes had to be tested under more stringent reaction conditions. These complexes also performed relatively well compared to other ruthenium complexes in the literature. However, isomerization was particularly high together with the linear regioselectivity. All of these catalysts exclusively produced aldehydes, with no significant hydrogenation of 1-octene to octane, and also no evidence of reduction of the aldehydes to alcohols. This latter result is particularly important for subsequent hydroaminomethylation experiments, discussed under the future prospects section.

5.2   Future Prospects

There are a number of aspects of this work that require further probing. Since we found that the activity of the mononuclear complexes are enhanced by the presence of a phenol group on one of the aromatic rings, various other substituents with different electronic properties should be investigated. This will hopefully lead to more active catalysts and thus shorter reaction times.

The low solubility of some of the dendritic complexes was a major issue impacting on the characterization and their application in catalysis, especially for the tri- and tetra-nuclear complexes. The solubility of the complexes can possibility be improved by using smaller counter-ions such as PF_6 and BF_4.

A 1:1 ratio of $CO:H_2$ was utilized during the hydroformylation experiments. This ratio can be varied in order to study the influence of this on the selectivity of the reaction. The selectivity towards the linear aldehyde could possibly be enhanced by using a higher CO concentration relative to H_2 since a higher CO partial pressure can suppress alkene isomerization. The linear regioselectivity can also possibly be improved by introducing phosphines into the ligand system. Thus, metal precursors of the type $[RhCl(PPh_3)_3]$ or $[RuCl_2(PPh_3)_3]$ can be used to prepare the dendritic catalyst precursors.

Furthermore, mechanistic investigations using HP-IR (High pressure Infrared) and HP-NMR (High pressure Nuclear Magnetic Resonance) spectroscopy could reveal information

regarding the species formed during the catalytic cycle. Since the activity of the mononuclear complexes (**MC2** vs **C7** and **MC1** vs **C1**) were quite different, it might suggest that the catalytically active species still have the diimine ligand intact.

Moreover, these complexes can also be investigated as catalyst precursors in the hydroaminomethylation of alkenes to amines. Hydroaminomethylation entails the initial hydroformylation of the alkene to an aldehyde. The aldehyde then undergoes a condensation reaction with an amine to form either an enamine or an imine intermediate. The catalyst then hydrogenates these intermediates to amines.